

Summer 1987

Cross-Shore Sediment Transport in Relation to Waves and Currents in a Groin Compartment

Hyo Jin Kang
Old Dominion University

Follow this and additional works at: https://digitalcommons.odu.edu/oeas_etds



Part of the [Oceanography Commons](#)

Recommended Citation

Kang, Hyo J.. "Cross-Shore Sediment Transport in Relation to Waves and Currents in a Groin Compartment" (1987). Doctor of Philosophy (PhD), Dissertation, Ocean & Earth Sciences, Old Dominion University, DOI: 10.25777/c8w2-6h05
https://digitalcommons.odu.edu/oeas_etds/132

This Dissertation is brought to you for free and open access by the Ocean & Earth Sciences at ODU Digital Commons. It has been accepted for inclusion in OES Theses and Dissertations by an authorized administrator of ODU Digital Commons. For more information, please contact digitalcommons@odu.edu.

CROSS-SHORE SEDIMENT TRANSPORT IN RELATION TO
WAVES AND CURRENTS IN A GROIN COMPARTMENT

by

Hyo Jin Kang

B.S. February 1973, Seoul National University, Seoul, Korea

M.S. February 1981, Seoul National University, Seoul, Korea

A Dissertation Submitted to the Faculty of
Old Dominion University in Partial Fulfillment of the
Requirements for the Degree of

DOCTOR OF PHILOSOPHY
OCEANOGRAPHY

OLD DOMINION UNIVERSITY
August, 1987

Approved by:

John C. Ludwick (Director)

ACKNOWLEDGEMENTS

I am deeply indebted and grateful to my advisor Dr. John C. Ludwick. He patiently guided me into the subject field of sediment transport in which I was a total stranger before I met him. Discussions with him have always been a pleasure to me and enlightened me on the matters with which I was stumbling along. His advice and support in the field and in the laboratory throughout the study were most essential to the completion of this study including the refinement of this dissertation. Most importantly, he taught me how to study science.

My gratitude is extended to Dr. Chester E. Grosch and Dr. George F. Oertel for their warm support and advice in the course of the study. Especially, the comment by Dr. Oertel at the beginning of the study was helpful for the design of this study. Dr. Grosch spent his precious time helping me through the numerical calculations.

Special thanks go to Mr. Donald W. Mathias of the City of Norfolk and Mr. James R. Melchor of the U.S. Army Corps of Engineers, Norfolk District Office. The electro-magnetic current meter for the study was provided by Mr. Melchor through his office. Mr. Mathias provided necessary information on the bench mark, the groins, and the beach-filling operation.

The labor-intensive field surveys could have never been successful without the help of my friends and fellow students, Joung W. Kim (now Ph.D.), Changho Moon, Young S. Kim, Cheolsoo Kim, Seungdo Kim, Seung H. Song, Dennis L. Lundberg (now Ph.D.), R. Neville Reynolds, and Tom Kovalchuck. Everybody voluntarily took part in the measurements of shoreline, bathymetry, and near-bottom currents at various

times. Dennis L. Lundberg and R. Neville Reynolds provided helpful opinions on the study, and they endured the mess I made in the laboratory which we shared for more than two years. Every assistance mentioned is greatly appreciated.

The crew of the R/V Linwood Holton, Robert Bray, Donald Padget, and Nelson Griffin, helped with the tidal current measurement. Capt. Robert Bray and John Keating operated the boat during the tripod test and grab sampling. Mr. James Dixson of NOAA kindly provided the tidal information at Sewells Point Tidal Station. Wind data were provided by the Naval Base in Norfolk, U.S. Navy. Dennis L. Lundberg delivered them back and forth. Construction of the tripod and the maintenance of the problematic equipments were done by Messers Thurman E. Gardner, Bobby Powell, and Bob Kirzzar of the Science Shop. Tremendous amount of data processing and plotting was possible with the help of the computer operators of the Computer Center. Messers Timothy Hendrickson and Paul Reynolds provided consultation about tape handling and Mr. Tad Guy helped to transfer the CMS file to the VAX minicomputer system. Everybody deserves sincere appreciation.

The encouragement of my Korean friends provided emotional relief to help finish my study in the U.S. They are presently at ODU; Joung W. Kim, Chelsoo Kim, Changho Moon, Hanjun Woo, and Young S. Kim, and formerly at ODU; Young W. Kwon, Ungmo Kim, Pil S. Park, Jong S. Byun, Seungdo Kim, and Seung H. Song. Especially, Joung W. Kim, who never failed to show his faith in friendship, has always been forthcoming and volunteered to help me at any time and at any place. The encouragement by him and his wife enabled me to overcome the frustration of my

gloomy days.

The financial and administrative support by the Department is also gratefully acknowledged. Special thanks go to the chairman Dr. William M. Dunstan, the present GPD Dr. George T. F. Wong, and the former GPD Dr. Ronald E. Johnson. Dr. Larry P. Atkinson kindly allowed me to use the computer terminal and the laser printer in his laboratory for word-processing of this dissertation.

I dedicate this work to my parents. Their love and devotion to me is far beyond description. My sister and brother also showed great affection and understanding consistently in spite of the slow progress in my study.

The study was funded by the Virginia Sea Grant College program, Project Number R/CP-1 granted to Dr. John C. Ludwick.

TABLE OF CONTENTS

LIST OF TABLES -----	vi
LIST OF FIGURES -----	vii
Chapter	
INTRODUCTION -----	1
WILLOUGHBY SPIT AND GROINS -----	4
EXPERIMENTAL DESIGN AND DATA COLLECTION -----	14
MODELS ON CROSS-SHORE SEDIMENT TRANSPORT -----	18
SEDIMENT TRANSPORT UNDER WAVES AND CURRENTS -----	23
Initiation of motion on a sloping bed -----	23
Sediment transport under waves -----	33
Sediment transport under combined waves and currents -----	37
SEDIMENT TRANSPORT BETWEEN TWO GROINS AT WILLOUGHBY SPIT -----	40
Asymmetry in the frequency distribution of wave orbital velocity -----	50
Sediment transport by irregular waves and currents -----	77
Evolution of bathymetry after the fill -----	99
SUMMARY AND CONCLUSIONS -----	114
FURTHER SUGGESTIONS -----	118
REFERENCES -----	119
APPENDIX -----	127

LIST OF TABLES

1. Characteristics of irregular wave-induced near bottom current -----	61
2. Cross-shore component of current measurement at 30 <i>cm</i> above bottom at Willoughby Spit (Ludwick, 1987) -----	63
3. Cross-shore component of oscillatory motion measured at Willoughby Spit (mean currents were removed from Table 2) -----	66
4. Magnitude asymmetry (S_m) and duration asymmetry (S_t) of RMS velocities of cross-shore component oscillatory motion at Willoughby Spit -----	69

LIST OF FIGURES

1. Index map of the study area -----	5
2. Distribution of the mean grain size in the test compartment before the fill -----	8
3. Typical size frequency distribution of the bottom sediment before the fill -----	9
4. Beach topography and shoreface bathymetry of the study area before the fill (August 11, 1983) -----	11
5. Typical size frequency distribution of the fill sediment -----	13
6. Coordinate system for the analysis of force acting on a grain on a sloping bed -----	25
7. Modified Shields diagram for the initiation of sediment movement on a horizontal bed (from Madsen and Grant, 1976) -----	29
8. Settling velocity of a spherical grain (from Madsen and Grant, 1976) -----	31
9. Change of shoreline with time before and after the fill. Dotted line is the distance of the mean low water shoreline from the line connecting the seaward end of the groins at the eastern 1/3, short dashed line is at the middle, and the long broken line is at the western 1/3 of the compartment. Thick solid line is the average of those three distances. Triangles denote the date when the bathymetric survey was done -----	42
10. Time-history of sediment volume in the test compartment. The shaded area gives the cumulation of values derived from the sequence of elevation maps. The dashed line is corrected time-history curve allowing for whether erosion at a point is in fill or pre-fill sediment -----	43
11. Bathymetric map before the fill (September 5, 1983) -----	44
12. Elevation difference between August 11 and September 5, 1983 -----	45
13. Pre-fill and post-fill shoreline change at the study area -----	47
14. Track of drogues during the flood -----	48
15. Track of drogues during the ebb -----	49

16. Schematic time-velocity curve of linear(a) and nonlinear(b) waves -----	51
17. Probability distribution of velocities for linear and nonlinear waves -----	52
18. Near-bottom current measurement at Willoughby Spit (for location see Fig. 21) -----	57
19. Time-velocity curve of the characteristic irregular waves near the bottom at the water depth of 2 m -----	58
20. Time-velocity curve of the characteristic irregular waves near the bottom at the water depth of 0.5 m -----	59
21. Location of the near-bottom current measurement -----	65
22. Horizontal component of oscillatory motion at Willoughby Spit (mean current was removed from Figure 19) -----	68
23. Skewness, magnitude asymmetry, and duration asymmetry of the characteristic irregular waves -----	73
24. Magnitude asymmetry and duration asymmetry of the measured oscillatory motion at Willoughby Spit -----	74
25. Change of sediment transport rate with depth by the characteristic irregular waves -----	78
26. Change of sediment transport rate due to the wave-current interaction (current direction = 0 degree) -----	83
27. Change of sediment transport rate due to the wave-current interaction (current direction = 180 degree) -----	84
28. Change of sediment transport rate due to the wave-current interaction (current direction = 90 degree) -----	86
29. Change of sediment transport rate due to the wave-current interaction (current direction = 270 degree) -----	87
30. Post-fill bathymetry approximately 1 month after the fill -----	90
31. Change of water depth with time after the fill due to the offshore loss of sediment calculated from the characteristic irregular waves -----	91

32. Change of sediment transport rate with time calculated from the characteristic irregular waves -----	94
33. Post-fill bathymetry approximately 1 year after the fill -----	95
34. Pre-fill bathymetry approximately 1 month before the fill -----	96
35. Cumulative volume loss from the compartment after the fill calculated from the characteristic irregular waves -----	98
36. Total offshore loss of sediment calculated by the model of Ludwick (1987) ---	100
37. Change of neutral depth due to the wave-current interaction (Current speed = 25 <i>cm/sec</i>) -----	103
38. Numerical calculation of the evolution of bottom profile for 1 year after the fill (west) -----	105
39. Numerical calculation of the evolution of bottom profile for 10 years after the fill (west) -----	107
40. Post-fill bathymetry approximately 3 months after the fill -----	109
41. Numerical calculation of the evolution of bottom profile for 1 year after the fill (east) -----	110
42. Numerical calculation of the evolution of bottom profile for 10 years after the fill (east) -----	111
43. Change of neutral depth due to the wave-current interaction (current speed = 5 <i>cm/sec</i>) -----	113

ABSTRACT

CROSS-SHORE SEDIMENT TRANSPORT IN RELATION TO WAVES AND CURRENTS IN A GROIN COMPARTMENT

Hyo Jin Kang
Old Dominion University, 1987
Director: Dr. John C. Ludwick

In nearshore areas waves are generally irregular, and the irregular wave-induced currents have different peak velocities (magnitude asymmetry) and durations (duration asymmetry) between forward and backward motions. These asymmetries may produce a net cross-shore sediment transport in one direction. The sediment transport mostly occurs as bedload where the waves are non-breaking.

Sediment transport on a sloping bed is also affected by gravity, and accordingly the Shields parameter should be re-evaluated for a grain on a sloping bed. It was also found that the affect of a steady current that interacts nonlinearly with the waves was important for the cross-shore sediment transport and for the nearshore bottom morphology.

Both the numerical calculation and the near-bottom current measurements at Willoughby Spit show stronger peak velocities of shorter duration in the offshore direction in shallow water. This trend reversed with greater depth. The peak velocities were found to be more important than the complete velocity distribution for the net cross-shore sediment transport rate under oscillatory flow. The rate of sediment transport decreased exponentially with increasing water depth.

The calculation of cross-shore sediment transport rate and the analysis of magnitude asymmetry showed the existence of the depth of a neutral line (convergence). At

depths shallower than the neutral depth sediment transport occurs in the offshore direction; the direction is onshore where the water depth is deeper than the neutral depth. Beach can reach a state of dynamical equilibrium by adjusting the water depth to the neutral depth corresponding to the local wave conditions.

At Willoughby Spit, the landwards shoreline retreat and the change of bathymetry after the beach-fill were accounted for by actions associated with the neutral depth. The change of the neutral depth as a result of wave-current interactions may very well explain the development of a characteristic trough and bar system within the groin compartment.

The bedload model of Madsen and Grant (1976), when incorporated with the irregular waves which were solved for by Biésel (1952), could reasonably well predict the overall bathymetric change after the fill at the study area.

INTRODUCTION

Sediment movement in nearshore areas is governed by the dynamics of waves and currents which are progressively modified by the varying water depths manifested in the shallow-water bathymetry. Asymmetry in the horizontal component of the oscillatory water motion is enhanced as the water depth becomes shallower, an affect which is most evident perhaps in the swash and backwash zone. If a steady current of any azimuth coexists with the waves, the sediment is easily carried to a new position by the resultant bottom shear stress of waves and currents. This movement of sediment, which is in the most general sense cross-shore, dominates erosion and accretion of sediment on a beach where: 1) the longshore current is weak; or 2) where the flux of longshore sediment is in a quasi-steady state.

The transport of sediment under waves and currents has been investigated by a number of scientists working on coastal and nearshore areas (Bagnold, 1963; Inman and Bagnold, 1963; Einstein, 1971; Madsen and Grant, 1976; Sleath, 1978, Bailard and Inman, 1981; Kobayashi, 1982). More generalized investigations have dealt with the dissipation of wave energy and the transport of momentum in nearshore areas in terms of time averaged radiation stress (*i.e.*, flux of momentum) (Longuet-Higgins and Stewart, 1960; 1964). Changes of boundary layer thickness and bottom shear stress by the nonlinear interaction of waves and currents have also been studied by several workers to solve the complex dynamics of sediment transport under waves and currents (Smith, 1977; Grant and Madsen, 1978 and 1979; Tanaka and Shuto, 1981; Christoffersen and Jonsson, 1985).

Wells (1967), evaluating the null-point hypothesis of Paulo Cornaglia (1889), explained cross-shore sediment movement in a model by analysing the skewness of the distribution of the horizontal component of wave orbital velocity. The acting irregular wave was comprised of a number of superimposed nonlinear wave trains. The relevant equations were developed earlier by Biésel (1952). Equilibrium beach slope and morphological changes in foreshore bathymetry have been modeled in terms of cross-shore sediment transport by calculating sediment response to the dynamics of waves (Bagnold, 1946; Inman and Bagnold, 1963; Inman and Bowen, 1963; Bailard and Inman, 1981; Holman and Bowen, 1982; Bowen and Huntly, 1984).

Cross-shore transport of sediment, which can be onshore or offshore, is one of the major mechanisms of sediment loss between groins which hinder the transport of sediment in the longshore direction. Transformation of incoming waves and a cell-like circulation pattern of a steady current between groins form a characteristic distribution of bottom drift velocity (Nagai and Kubo, 1958; Kemp, 1962; Kolp, 1970). Generation of rip currents along the groin walls is also expected due to the blocking and bending of longshore currents (Nagai and Kubo, 1958; Kemp, 1962; Curren and Chatham, 1977; Ludwick, 1987; Lundberg, 1987). The exact mechanism of sediment transport under waves and currents is still poorly understood in spite of many theoretical and empirical works published during the last two decades. The state of knowledge is even weaker for sites near or between coastal structures built to prevent beach erosion.

The present study examines the asymmetry of wave-induced near-bottom currents caused by the nonlinear interaction of waves. The distribution of near-bottom shear

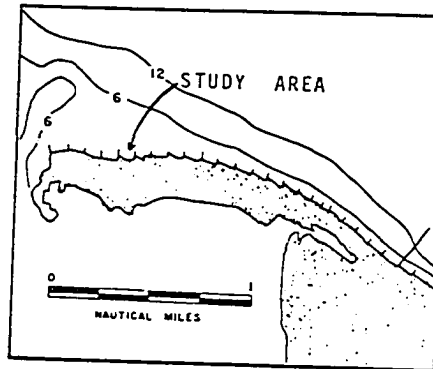
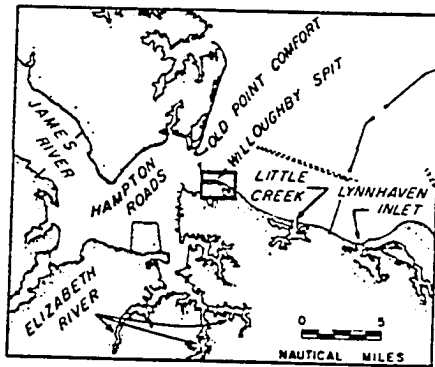
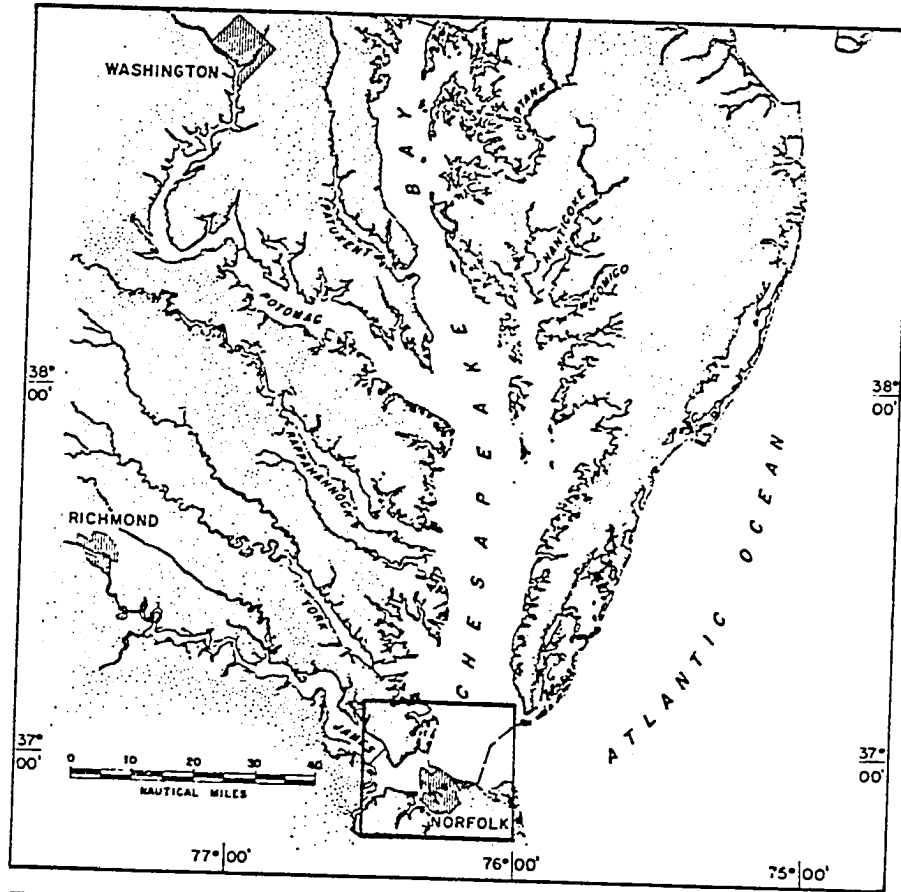
stress under nonlinear irregular waves and steady currents is evaluated to elucidate the causes of changes in beach and nearshore areas in both time and space. A sediment transport model (Madsen and Grant, 1976 and 1977) developed for linear waves is adapted in calculating the sediment transport rate under the irregular waves and currents. An example of numerical calculation of the cross-shore sediment transport rate using characteristic wave and current conditions is performed to explain the escape of sediment from a specific groin compartment. The direction of evolution of the bottom morphology to the point when the beach reaches a quasi-equilibrium state is predicted. Results are tested with actual field data including bathymetry, waves and currents, and shoreline changes before and after a sand-fill between two groins at Willoughby Spit, Virginia.

WILLOUGHBY SPIT AND GROINS

Willoughby Spit, a prominent feature of lower Chesapeake Bay, is elongated east-west, and lies at the western end of a beach system which is continuous from the mouth of the Chesapeake Bay, Virginia (Fig. 1). The spit is 3.2 *km* long and 135 to 535 *m* wide with an average elevation of approximately 2 *m*. Melchor (1970) reports the first recognition of the spit in the vicinity area map published in 1806. The spit did not appear in the map of 1800, which suggests a very rapid development and growth of the spit for 5 or 6 years initially. Before modification by works of man, the spit underwent narrowing in width and elongation in the direction of dominant transport due to both wave-induced and tidally-induced currents. In the long term, the east-west Bay shoreline showed a rapid shoreline retreat up to values of 180 *cm/yr* until the construction of groins to protect the beach from erosion (Brown et al., 1938) and an average shoreline retreat of about 30 *cm/yr* between 1852 and 1942 (Byrne and Anderson, 1977). Recently an erosion rate of about 7.6 *cm/yr* was reported for the western part of Willoughby Spit (Fleischer et al., 1977).

The tidal currents in this area are reversing, semi-diurnal, and of the standing-type tidal wave. Mean range is 72.6 *cm* and spring range is 94.5 *cm* (Harris, 1981). Superelevations of water level greater than 2.4, 1.8, and 1.2 *m* above mean sea level at Willoughby Spit by storm surge were estimated to have recurrence times of 71, 14, and 1.2 years, respectively (Ludwick, 1987). The tidal currents flow close inshore. Measurements at the seaward limit of a groin compartment show that the currents are flood dominant in speed and duration (Ludwick, 1987). Ludwick (1987) measured that

Figure 1. Index map of the study area



the average current speeds near the bed corrected to mean range were 27 *cm/sec* during the flood and 18 *cm/sec* during the ebb. Typical durations of flood and ebb near this area are 7 and 5.4 hours respectively (USACE, 1982; Ludwick, 1987).

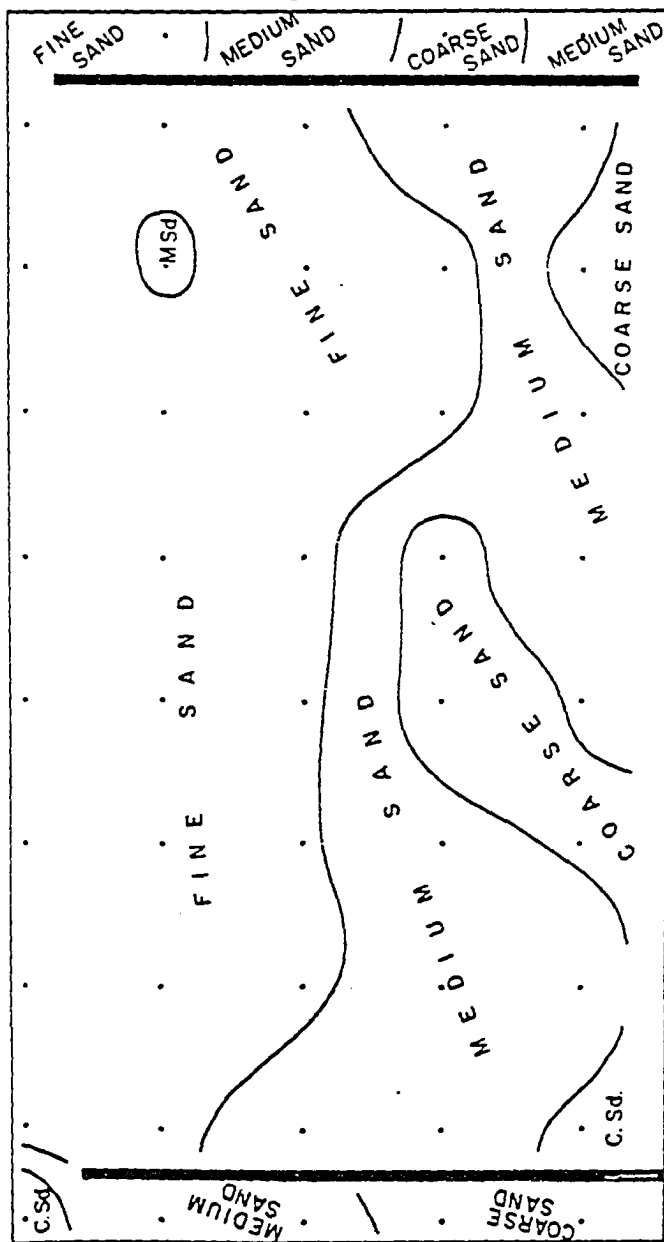
The beach onshore is characterized by low to medium wave energy which comes from the northern sector often at an angle of approximately 10 - 30 degrees to the coast. Long term wind frequencies in the area show that the NE component is dominant followed by SW and N while NW is minor (Brown et al., 1938; NWRP, 1964). The waves are usually less than 30 *cm* in height and correspondingly the surf zone is very limited usually less than 1 *m* in width; however, destructive wave attack and elevated water levels up to 1 *m* can be caused by storm winds coming from the NNE to E, and the surf zone then extends slightly beyond the ends of groins. Average height of waves in the area was reported to be about 15 *cm* (Fleischer et al., 1977; Ludwick, 1987). Ludwick (1987) identified five wave types by analysing 48 measured current spectra: 1) local wind chop less than 2 seconds in period; 2) wind waves over a bay fetch in the 2 to 5 seconds band; 3) Atlantic wind waves in the 5 to 12 seconds band; 4) surf beat in the 12 to 16 seconds; 5) edge waves with offshore modal numbers of 0 and 1 in bands from the 32.1 to 32.7 seconds and the 52.9 to 56.2 seconds respectively.

Westward longshore transport of sediment is dominant in the western part of Willoughby Spit (Fleischer et al., 1977, Ludwick et al.; 1987; Reynolds, 1987), and a well-designed groin system for the area is attractive as a beach protection method since the starvation of sediment downdrift, which is usually a major drawback of groins for

beach protection, is a desirable condition as regards the Hampton Roads navigational channel located at the end of the spit (Fig. 1). Bearing this in mind and based on the report by Brown et al. (1938), a field of 37 wooden impermeable groins were built along the 5.5 km reach of northern shoreline from the western tip of the spit in late 1930's, and 18 of them were rebuilt recently. They are straight and at right angles to the shoreline oriented approximately towards true north. The structures are approximately 79 to 100 m long and 152 m apart. Each groin has an inner level section at 180 cm above MLW, an outer level section at about 60 cm above MLW, and an intermediate inclined section approximately 23 m long. The groins, however, have not been so successful in keeping the beach from erosion due to a) sea level rise (Hicks, 1973), b) groin overwashing, c) offshore transfer of sediment by rip currents along the structures (Lundberg, 1987), and d) seaward transport by wave induced currents (Ludwick et al., 1987). The groins have substantially reduced the beach erosion rate however (Fleischer et al., 1977).

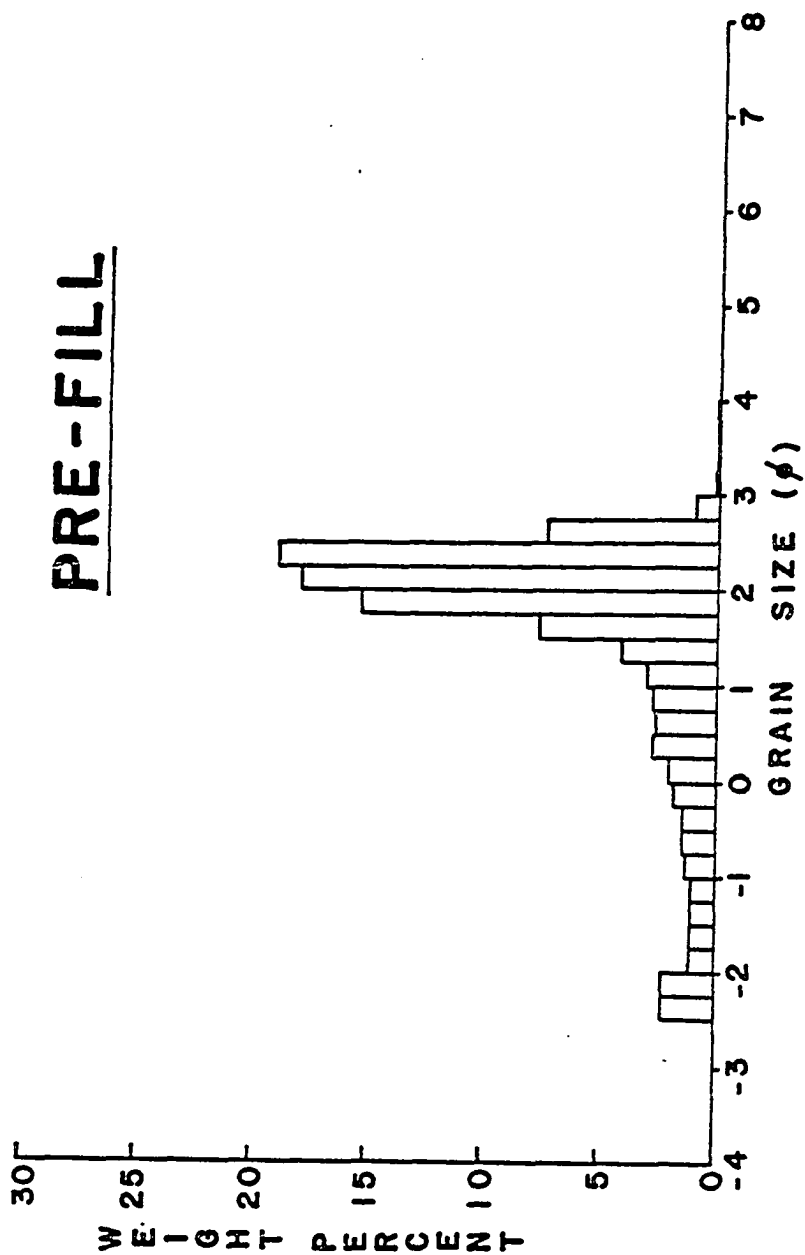
Before beach nourishment which took place during late August and September, 1984, the superficial sediments in the area were coarse (mean; 0.7 mm) to fine (mean; 0.2 mm) sands with a seaward fining trend (Fig. 2). Most modal diameters ranged from 0.13 to 0.25 mm and the averaged phi standard deviation value was 0.68 phi. Many samples were negatively skewed (Fig. 3) and contained small pebbles up to diameters as large as 6 mm along the shore. In plan, the elevations onshore on either side of a groin showed an accretional feature on the east side (upstream relative to the dominant longshore drift direction) and erosional feature on the west (leeside of the dominant

Figure 2. Distribution of the mean grain size in the test compartment
before the fill



M# (5/14/84)

Figure 3. Typical size frequency distribution of the bottom sediment before the fill

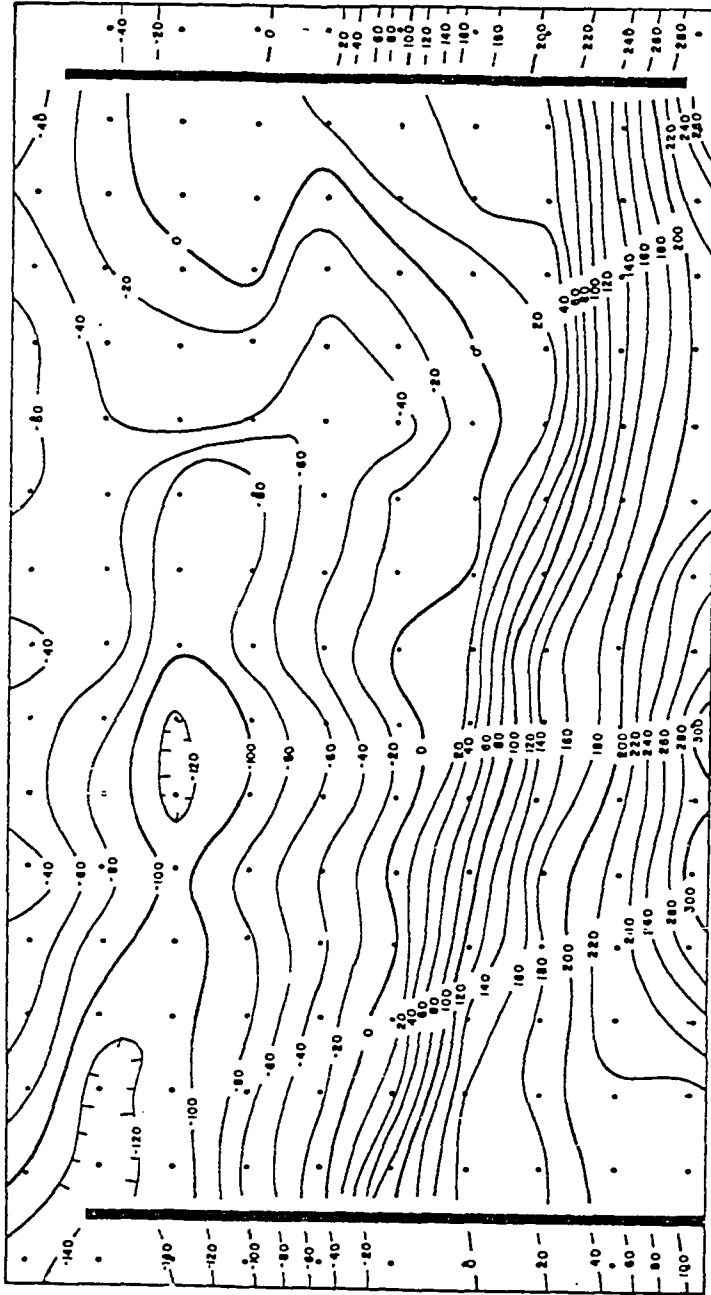


longshore drift direction) resulting in the typical saw-tooth shaped shoreline which groins produce under wave-induced longshore currents (Fig. 1). The accretion on east-side and erosion on west-side of a groin onshore resulted in elevation differences reaching up to 1.7 *m*.

According to bathymetric surveys in a compartment between two groins, the general shape of the bed was characterized by a comparatively steeply sloping foreshore which had a slope of approximately 5 degrees and a broad smooth seaward sloping shoreface. The slope of the shoreface varied between less than 1 degree at the eastern part and more than 3 degrees at the western part. A trough and bar system developed from the seaward end of western groin, the axis of which trended approximately WNW. Overall, the average slope of the compartment bed was about 2 degrees (Fig. 4). However, as shown in Figure 4, there is a narrow berm onshore with steeper foreshore and a gently sloping broad offshore portion in the eastern part of the compartment and vice versa at the western part. This general character of the bottom did not appear to change much with time, which may imply that the transport of sediment through the area had reached a condition of quasi-equilibrium.

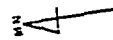
In late August through September, 1984, the beach was filled nearly up to the seaward end of the groins with borrow material from a nearby naval base dock construction site. An estimated volume of about 410,600 *m*³ sand mixed with gravel was pumped through pipeline to the shore from the western end of the spit up to about 3.9 *km* reach to the east. The fill surface was bulldozed to a plane dipping seawards to the groin ends at a slope of about 3 degrees. On the backshore, fill was formed into a

Figure 4. Beach topography and shoreface bathymetry of the study area before the fill (August 11, 1983)



8-11-83

ELEVATIONS IN CENTIMETERS



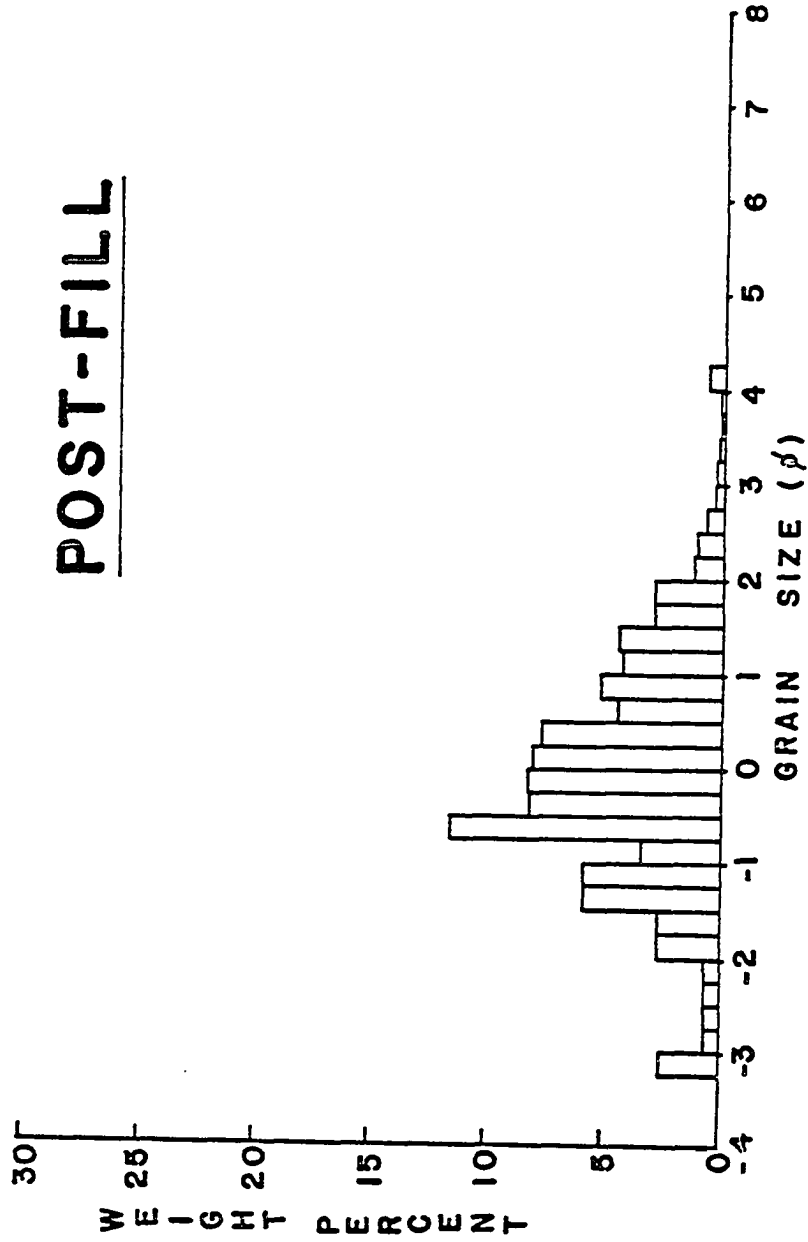
dune-like ridge with a top elevation of approximately 3.7 *m* above mean low water. The mean grain diameter of the fill material was 0.9 *mm* with poor sorting and negative skewness (Fig. 5). The fill material also contained broken shell fragments which comprised up to 50 percent of the larger size classes and 10 to 15 percent of the fine sand classes (Reynolds, 1987).

Immediately after the beach was filled, the shoreline was slightly concave seaward and the bottom was approximately flat. However the beach underwent an exponentially rapid erosion of bottom and retreat of the shoreline for the first one and a half months following the fill (Ludwick, 1987; Ludwick et al., 1987). A new spit has formed at the western tip of the Willoughby Spit comprised of the fill material, strongly suggesting the westward transport of sediment in spite of the intended blocking action of the structures along the beach (Ludwick et al., 1987; Reynolds, 1987).

After the rapid recession of the shoreline during the first one and a half months, the bathymetry of the study area formed a trough at the western side of the compartment and a deep area near the middle and eastern part of the compartment. The rates of change in shoreline and bathymetry became much slower than the initial rapid changes even though the mean low water shoreline at present still lies farther offshore than the pre-fill quasi-equilibrium shoreline.

Figure 5. Typical size frequency distribution of the fill sediment

POST-FILL



EXPERIMENTAL DESIGN AND DATA COLLECTION

The present study is devised to examine the validity and consequences of the presently most appropriate cross-shore sediment transport model developed by Madsen and Grant (1976) together with the wave asymmetry model of Wells (1967). This model which has been modified in the present work deals with bedload transport under waves and currents. It is the intent of the study to test the model with a set of long term field data gathered at a beach section between two groins. The model, if successful, is expected to depict the acting sedimentary process and to predict the evolution of bathymetric change between groins under waves and currents.

To establish a sediment transport model under waves and currents, the following physical factors which affect the force acting on a sand grain are considered: 1) grain diameter; 2) slope of the bottom; 3) asymmetry in the distribution of horizontal component of wave orbital velocity near bottom; 4) effect of steady current; and, 5) threshold bottom shear stress to set the grain in motion.

The following affects of the bounding groins will also be considered: 1) cell-like circulation between groins induced by action of the tidal currents; 2) distribution of bottom shear stress by the nonlinear interaction of wave-induced oscillatory currents and the tidally induced steady currents. The corresponding evolution of the bathymetry is obtained by numerical solutions of the relevant equations.

To test the model, an area between two groins located approximately 0.7 *km* east of the west end of Willoughby Spit was chosen (Fig. 1). A reference datum for elevations was established. The difference in elevation between the top of a post at the

study area and a bench mark which located approximately 100 *m* from the post was measured. The elevation of the top of the post was expressed relative to mean low water of 1959, since the elevation of the bench mark was known relative to mean low water of 1959 at the beginning of the present study. Later corrections due to recent surveys of National Geodetic Survey and consideration of the trend of mean sea level rise in lower Chesapeake Bay area showed that the mean low water of 1959 was approximately 30 *cm* below mean low water of the present time.

A survey grid, 10 *m* on a side, was comprised of fifteen lines, parallel to the trend of groins between the two groins, reaching slightly beyond the seaward end of groins and 10 lines normal to the trend of groins. Surveys of beach topography and shoreface bathymetry were made approximately monthly for 3 years beginning in August of 1983 using a plane table and alidade. The elevations of the starting points of each shore-normal line were determined relative to the reference datum. The plane table and alidade were then carried to each starting point, and the elevations of each survey station on the line were read using the alidade with respect to the elevation of the starting point by reading the elevation on a rod which was positioned by another person at predetermined points along the line. All readings were corrected to the reference datum for purposes of constructing a bathymetric contour map later. Elevation differences between consecutive surveys for each station were also calculated and contoured to show patterns of accretion and erosion.

To monitor the shoreline change after the fill, the position of the mean low water shoreline was determined by measuring sextant angles at points along the actual shore-

line at the time of mean low water. The distances of the mean low water shoreline from the line connecting the seaward ends of the two groins along profile lines positioned at $1/4$, $1/2$, and $3/4$ of the distance between the two groins were calculated later. Actual measurements of the shoreline location at mean low water were taken approximately two to three times a month after the date of fill in September, 1984. An intensive survey was made almost every day between May and September, 1986 to provide data on the short-term variability of the mean low water shoreline. Pre-fill shorelines, which did not change very much with time, were determined from the surveyed bathymetric maps.

Currents near the bottom were measured at 48 sites on different days both before and after the date of fill in conjunction with the work of Ludwick (1987). An electromagnetic current meter which measures x- and y-component of the currents together with the orientation of the meter was positioned 30 *cm* above the bed. A tripod designed to minimize the affect to the flow field was used to hold the current meter in position. An experiment typically consisted of moving the meter among a group of locations cyclically for 12 hours to cover a whole tidal cycle. Single sites were occupied for 12 minutes with readings of the components taken at intervals of 0.5 second. Data gathered were stored on a magnetic cassette tape at the site, and later transferred to disk on the main frame computer on campus for statistical analysis. Drogue bottles made neutrally buoyant were also tracked several times in the compartment. Use was made of both surface drifters and those at 50 *cm* below the surface.

Bottom sediments were collected at the site and particle sizes were analysed rou-

tinely at a sieve interval of one-quarter phi. Composition of the sediment was estimated by visual examination.

MODELS ON CROSS-SHORE SEDIMENT TRANSPORT

The distinction between bedload and suspended load is often ambiguous and always arbitrary. Einstein (1950, 1971) defined the bedload as the bed particles moving in the bed layer by rolling, sliding, and sometimes by jumping, and the particle weight is to a large part transmitted directly to the nonmoving bed. Above the bed layer the particles move in suspension, and therefore the weight of the particle is transmitted to the surrounding fluid rather than to the solid part of the bed. The thickness of the bed layer was suggested to be two grain diameters (Einstein, 1950). However, most workers prefer a thicker bed layer.

Accepting the above definition with a thicker bedload layer, however, a single mode of transport for a grain, especially in the field, is seldom maintained during the whole course of the transport. The dominance of transport mode is yet to be determined if one is to adopt a given model in the laboratory or field. Komar (1978) presented quantitative arguments that greatly favored the dominance of bedload transport alongshore within a turbulent surf zone. Other workers treated the sediment transport as a suspended load phenomenon within the surf zone (Wright et al., 1982) or as occurring under nonbreaking waves (Nielsen et al., 1978; Nielsen, 1979). Hattori (1982) suggested the dominance of bedload transport outside the surf zone and the dominance of suspended load within the surf zone based on field study at Orai Beach, Japan. However, even in the presence of bedforms and the generation of turbulence under waves (Nielsen, 1979), the sediment concentration in the water column is usually insignificant at more than about three ripple heights above the bed under non-

breaking waves (Sleath, 1984). Thus from the foregoing arguments the use of a bedload transport model seems to be most appropriate for the present study area.

Basically models that give the rate of sediment transport under wave motion are either theoretical (Bagnold, 1963; Einstein, 1971; Bailard and Inman, 1981; Bailard, 1981; Kobayashi, 1982) or are empirical and are then based on laboratory experiments or on other models (Madsen and Grant, 1976; Sleath, 1978; Shibayama and Horikawa, 1980; Vincent et al., 1981; Hallermeier, 1982). However, even at the present time, there is no single model which is broadly applicable to various conditions such as bed-form, grain characteristics, wave condition, etc. Existing theoretical models need calibration and modification for valid application (Abou Seida, 1965; Kachel and Sternberg, 1971; Bailard, 1982; Hardisty, 1983; Hardisty et al., 1984) and empirical models also have certain limitation of application within the condition in which each model was developed originally since the form of the models may vary at different conditions of the test.

Even though each model has its own range of applicability in which the model predicts the sediment transport rate better than the others do, the empirical model developed and tested by Madsen and Grant (1976, 1977) evaluated here as being the most broadly applicable (Sleath, 1978). This model tends to predict a somewhat higher transport rate than the actual rate or than is predicted by other models at high transport rates (Vincent et al., 1981 and 1983; Sleath, 1984). However, under moderate to low transport rate, the model was generally supported by the results obtained by other workers (Sleath, 1978; Vincent et al., 1981; Hallermeier, 1982; Shibayama and Hori-

kawa, 1980). Horikawa et al. (1982) also found better agreement between experiment and the original model of Madsen and Grant (1976) than the slightly modified model of Shibayama and Horikawa (1980) even at very high transport rate. Pattiaratchi and Collins (1985) tested 10 models including the model of Madsen and Grant (1976) using fluorescent sand tracer at an area of high tidal current and wave energy in northern Bristol Channel, UK. The study was conducted under what the authors term average conditions (wave period 7.5 sec, wave height 1.5 m), oceanic conditions (wave period 12.5 sec, wave height 2.3 m), and stormy conditions (wave period 12.5 sec, wave height, 3.2 m), and it was found that only the Madsen and Grant (1976) model and the model of Sternberg (1972), with some modification, predicted rates that are close to realistic estimations. Field experiments by Young et al. (1980) and Shibayama and Horikawa (1980) also support the general applicability of the model of Madsen and Grant (1976).

The direction of net sediment movement in the on-offshore direction is a major concern as regards beach accretion and erosion especially where sediment transport in longshore direction is minimal or has reached a quasi-steady state. The above models on the rate of sediment transport simply calculate the amount of sediment transported in the direction of flow applied to the bed. The models do not predict any net sediment transport when a simple sinusoidal wave theory is incorporated except for the models by Bailard and Inman (1981) and Kobayashi (1982) which have the parameters of bed slope and angle of repose.

Prediction of the direction of sediment transport, onshore or offshore, has been

attempted based on several mechanisms occurring in the beach and nearshore area. The parameters each model used are: 1) cross-shore component of surface wind (King and Williams, 1949; Seibold, 1963); 2) variation in the height of the highest tides (Shepard, 1950); 3) wave steepness (Dean, 1973; Hattori and Kawamata, 1980); 4) wave height (Aubrey, 1978; Hashimoto and Uda, 1979; Shepard, 1950; Short, 1978); 5) energy dissipation (Inman and Bagnold, 1963); 6) wave power (Short, 1978); 7) velocity asymmetry (Wells, 1967); and, 8) general sediment transport (Bailard and Inman, 1981; Bailard, 1981).

Seymour and King (1982) reviewed each model and tested the models using the data gathered during the National Sediment Transport Study (NSTS) experiment at Torrey Pines Beach, California. The result was discouraging in that none of the models could predict the change of the beach effectively. Seymour and Castel (1987) again tested some different practical models which can be represented in terms of a wave-sediment parameter (ratio between significant wave height and fall speed of the median sediment particle multiplied by characteristic period of incident waves) (Dean, 1973; Short, 1978; Hattori and Kawamata, 1980; Quick and Har, 1985; Sunamura and Hori-kawa, 1974). The models were evaluated by the data from Scripps Beach and Virginia Beach. The results from these tests were also not satisfactory.

The models developed by Inman and Bailard (1981), Bailard (1981), and Wells (1967) predict the direction of bedload transport. Models by Inman and Bailard (1981) and Bailard (1981) have the most sound physical analysis of sediment movement on a sloping bed under waves and currents. However, their models are based on the sedi-

ment transport model of Bagnold (1963) which required a calibration of some coefficients embodied in the model. Their models also do not consider the threshold of grain movement or grain characteristics explicitly. Field comparison of the models by Seymour and King (1982) and Bailard (1982) shows that the models are not very predictive in the field.

Wells (1967) derived a simple model for predicting the direction of bedload transport by analysing the distribution of the horizontal component of the wave orbital velocity near the bottom statistically. Even though the model failed to predict the direction of sediment transport in the field as shown by Seymour and King (1982), the model seems to shed some light on the problem of cross-shore sediment transport since the model adopts irregular waves whose equations are solved for by Biésel (1952). These waves are more likely in the nearshore region than the monochromatic sinusoidal waves used in other models. Skewness of the distribution, which is obtained from the model, evaluates the asymmetry of the distribution of the near bottom velocity, and has the same dimensions as the stream power $\tau_0 U$ which is the third power of the velocity. Therefore the parameter can be related conceptually to the rate of bedload transport with some modification.

The following chapter will examine the models of Madsen and Grant (1976) and Wells (1967) more in detail, and an effort is made to modify these models considering the local slope of the bed, nonlinear interaction of irregular waves and currents, and the threshold of grain movement with the goal of solving the sediment transport problem between two groins.

SEDIMENT TRANSPORT UNDER WAVES AND CURRENTS

The transport of bed material by water flowing over the bed is subject to the all complexities of the interaction between the fluid and the bed material. The rate and mode of transport is affected by fluid characteristics such as turbulence of the flow, fluid density, velocity of the flow, etc., and is also affected by sediment grain size, density of the grain, shape of the particles, etc.

To move a sediment grain on the bed, fluid flowing over the bed should exert force on the grain sufficient to overcome the resisting force due to gravity, friction between grains, and any effects due to sheltering of the grain in-amongst other grains. Bedforms, slope of the bed, and the interaction between steady and unsteady currents also affect the fluid force acting on the grain and thus the rate of sediment transport. In oscillatory flow, net transport of sediment may occur in one direction when there is an asymmetry in the distribution of the flow velocity in magnitude and duration.

- Initiation of motion on a sloping bed

Forces acting on a grain resting on the bottom under a steady flow are

$$\text{Drag force } (\vec{F}_D) : \vec{F}_D = C_D \frac{1}{2} \rho \vec{U} |\vec{U}| \frac{\pi}{4} d^2 \quad (1)$$

$$= C_1 \tau_o d^2 \quad (2)$$

$$\text{Lift force } (\vec{F}_L) : \vec{F}_L = C_L \frac{1}{2} \rho \vec{U} |\vec{U}| \frac{\pi}{4} d^2 \quad (3)$$

$$= C_2 \tau_o d^2 \quad (4)$$

$$\text{Gravity force } (\vec{F}_G) : \vec{F}_G = \frac{\pi}{6} (\rho_s - \rho) \vec{g} d^3 \quad (5)$$

$$= C_3(\rho_s - \rho) \vec{g} d^3 \quad (6)$$

where τ_o : boundary shear stress due to the flow acting on the bed grains

\vec{U} : velocity of the steady flow near the bottom

\vec{g} : acceleration of gravity

C_D : drag coefficient

C_L : lift coefficient

d : nominal diameter of the grain

ρ_s, ρ : density of grain and fluid respectively

C_1, C_2, C_3 : shape factors

Therefore the forces acting on a grain on a sloping bed under a current flowing at an arbitrary angle can be analysed into components on a rectangular coordinate system. The z-axis is normal to the bed positive upward, and the y-axis is parallel to the direction of bed slope positive onshore (Fig. 6).

$$\vec{F}_D = (F_{Dx}, F_{Dy}, 0) \quad (7)$$

$$\vec{F}_L = (0, 0, F_{Lz}) \quad (8)$$

$$\vec{F}_G = (0, F_{Gy}, F_{Gz}) \quad (9)$$

Further, the components can be expressed as following:

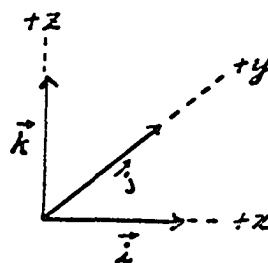
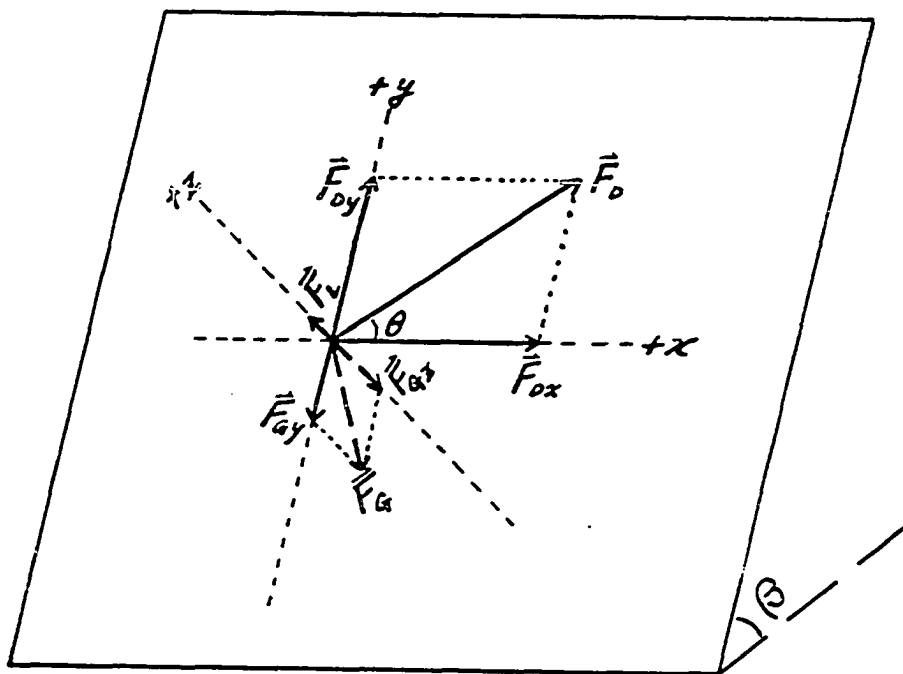
$$F_{Dx} = \vec{i} \cdot \vec{F}_D = |\vec{F}_D| \cos\theta \quad (10)$$

$$F_{Dy} = \vec{j} \cdot \vec{F}_D = |\vec{F}_D| \sin\theta \quad (11)$$

$$F_{Lz} = \vec{k} \cdot \vec{F}_L = |\vec{F}_L| \quad (12)$$

$$F_{Gy} = \vec{j} \cdot \vec{F}_G = -|\vec{F}_G| \sin\beta \quad (13)$$

Figure 6. Coordinate system for the analysis of force acting on a grain on a sloping bed



$$F_{Gz} = \vec{k} \cdot \vec{F}_G = -|\vec{F}_G| \cos\beta \quad (14)$$

where β : slope of the bed in degrees or radians taken to be positive for upslope
in onshore direction

θ : flow direction measured counterclockwise from positive x-axis.

$\vec{i}, \vec{j}, \vec{k}$: unit vector in x, y, and z direction, respectively.

Then, the total tangential force (\vec{F}_t), the direction in which grain movement occurs, becomes

$$\vec{F}_t = \vec{F}_D + \vec{j} F_{Gy} = (F_{Dx}, F_{Dy} + F_{Gy}, 0) \quad (15)$$

$$= C_1 \tau_a d^2 \quad (16)$$

where τ_a : apparent shear stress associated with the total tangential force
acting on the grain

τ_a can be determined by defining

$$\vec{j} F_{Gy} = C_1 \tau_G d^2 \quad (17)$$

$$\tau_o = (\tau_{ox}, \tau_{oy}, 0) \quad (18)$$

$$\tau_G = (0, \tau_{Gy}, 0) \quad (19)$$

$$\tau_a = (\tau_{ax}, \tau_{ay}, 0) = (\tau_{ox}, \tau_{oy} + \tau_{Gy}, 0) \quad (20)$$

where τ_G is the down slope component of stress due to the weight of the grain.

The boundary shear stress due to the motion of the fluid is given as

$$\tau_o = \frac{1}{2} \rho f \vec{U} |\vec{U}| \quad (21)$$

where f : friction factor

And, by equations (2) and (21)

$$C_1 = \frac{\pi C_D}{4 f} \quad (22)$$

Therefore , the downslope component of stress due to gravity can be re-written from equation (17) using equations (1), (5), (13) and (22) as

$$\tau_G = \vec{j} (C_1 d^2)^{-1} F_{Gy} = \vec{j} \left(-\frac{2}{3} \frac{f}{C_D} (\rho_s - \rho) |\vec{g}'| d \sin\beta \right) \quad (23)$$

Thus, the magnitude of the apparent shear stress is

$$|\tau_a| = \left\{ \left(\frac{1}{2} \rho f |\vec{U}|^2 \cos\theta \right)^2 + \left(\frac{1}{2} \rho f |\vec{U}|^2 \sin\theta - \frac{2}{3} \frac{f}{C_D} (\rho_s - \rho) |\vec{g}'| d \sin\beta \right)^2 \right\}^{1/2} \quad (24)$$

The drag coefficient for a spherical grain is given as

$$C_D = \frac{4}{3} |\vec{g}'| \frac{(\rho_s - \rho) d}{\rho w^2} \quad (25)$$

where, w : settling velocity of the grain

At the moment when the grain just starts to move, the tangential force equals the maximum frictional force, and thus we can write

$$\tan\phi = \frac{|\vec{F}_t|}{|\vec{F}_n|} \quad (26)$$

where \vec{F}_n : force acting on the grain normal to the bed

ϕ : internal frictional angle between grains (approximately the angle of repose)

On a horizontal ($\beta = 0$), flat bed, and neglecting the lift force,

$$\vec{F}_t = \vec{F}_D$$

$$\vec{F}_n = \vec{F}_G$$

and from equations (2), (6), and (26)

$$\tan\phi = \frac{|\vec{F}_D|}{|\vec{F}_G|} = \frac{C_1 |\tau_{oc}| d^2}{C_3 (\rho_s - \rho) |\vec{g}| d^3} = \frac{C_1}{C_3} \psi_{oc} \quad (27)$$

where τ_{oc} is the critical shear stress and ψ_{oc} is the critical Shields parameter defined as $\psi_{oc} = \frac{|\tau_{oc}|}{(\rho_s - \rho) |\vec{g}| d}$ which is that value required for movement of a characteristic grain under unidirectional steady flow on a horizontal and flat bed consisting of cohesionless and uniform grains (Shields, 1936).

For the initial motion of a grain on a sloping bed, also neglecting lift force,

$$\vec{F}_t = \vec{F}_D + \vec{j} F_{Gy}$$

$$\vec{F}_n = \vec{k} F_{Gz}$$

Thus,

$$\tan\phi = \frac{|\vec{F}_D + \vec{j} F_{Gy}|}{|\vec{k} F_{Gz}|} = \frac{C_1 |\tau_{ac}| d^2}{C_3 (\rho_s - \rho) |\vec{g}| d^3 \cos\beta} = \frac{C_1}{C_3} \frac{1}{\cos\beta} \Psi_{ac} \quad (28)$$

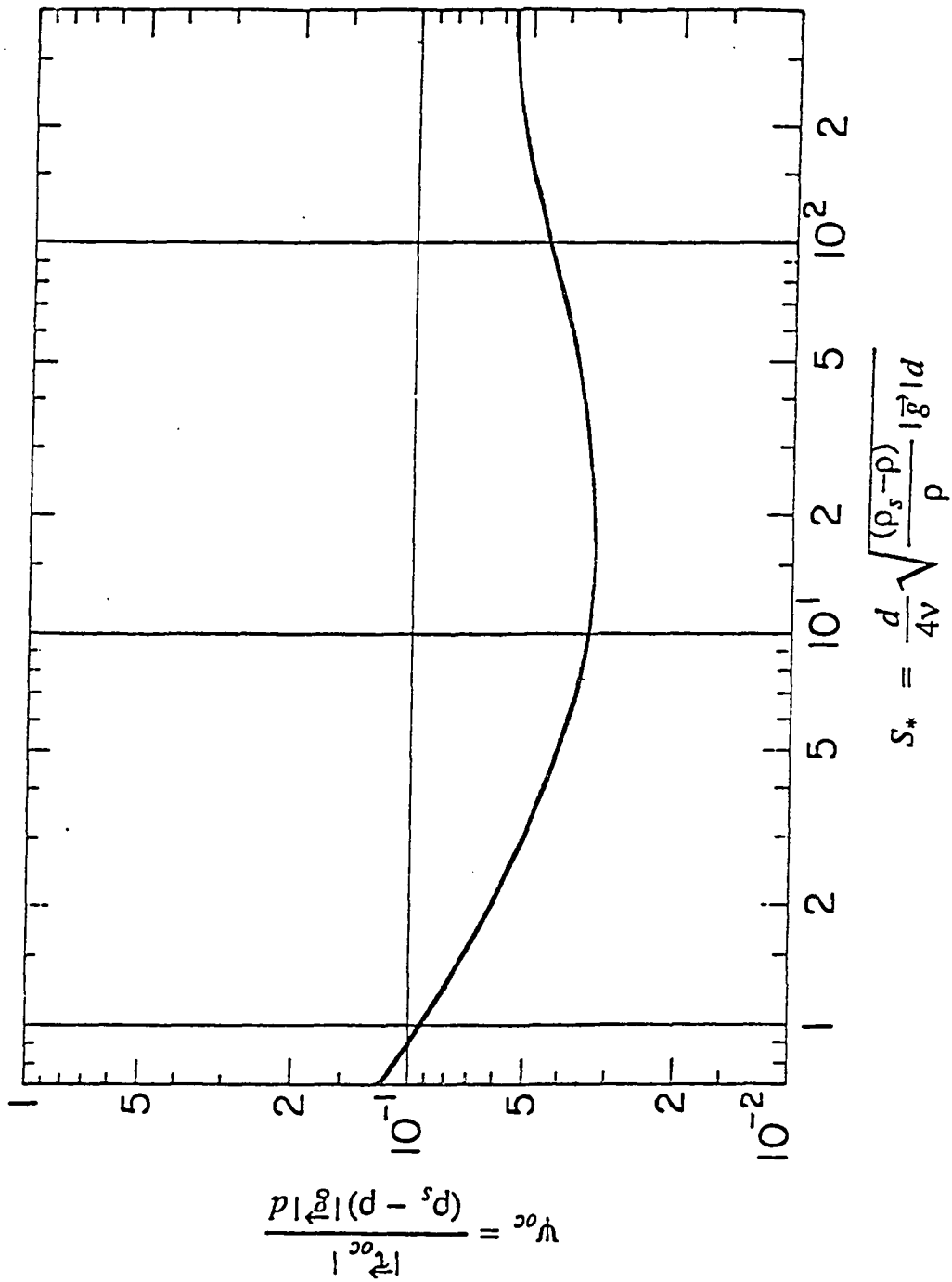
where, τ_{ac} is the apparent critical shear stress and Ψ_{ac} is the apparent critical Shields parameter defined as $\Psi_{ac} = \frac{|\tau_{ac}|}{(\rho_s - \rho) |\vec{g}| d}$ to move a grain on a sloping bed due to the combined effect of gravity and drag forces.

By equating equations (27) and (28),

$$\Psi_{ac} = \cos\beta \psi_{oc} \quad (29)$$

Now, Ψ_{ac} can be determined by choosing ψ_{oc} from the Shields diagram (Fig. 7)

Figure 7. Modified Shields diagram for the initiation of sediment movement on a horizontal bed (from Madsen and Grant, 1976)



modified in terms of a nondimensional parameter S_* which is only a function of sediment and grain properties.

$$S_* = \frac{d}{4\nu} \sqrt{\frac{(\rho_s - \rho)}{\rho} |\vec{g}| d} \quad (30)$$

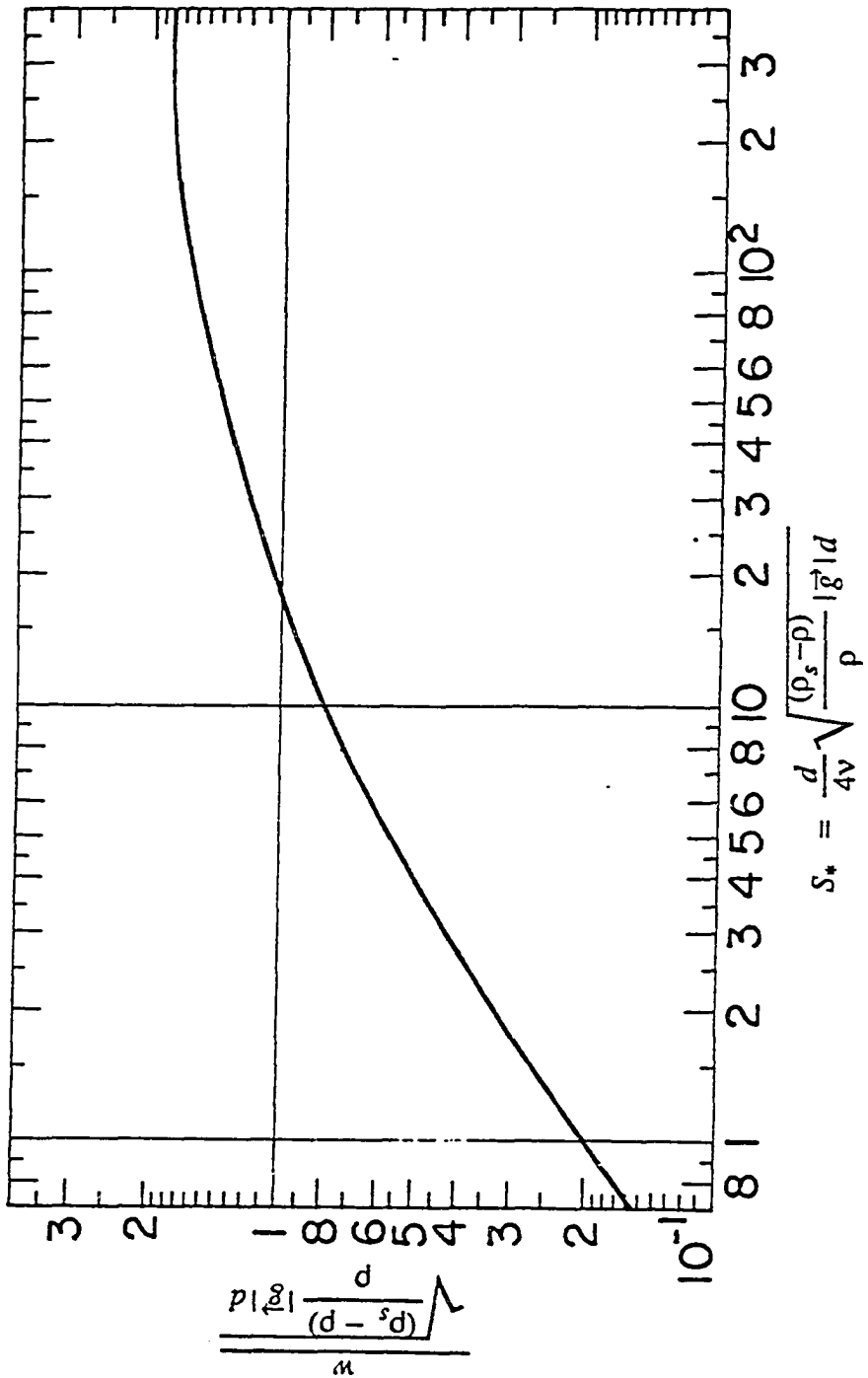
where, ν : kinematic viscosity of the fluid

Since the settling velocity of a grain is also a function of grain and fluid properties, the settling velocity can also be determined as a function of S_* when the fluid property is known (Fig. 8).

When the bed has no slope ($\beta = 0$), by equation (29), the apparent critical shear stress is identical to the critical shear stress on the horizontal bed given by Shields (1936). If the grain is only affected by the gravitational force ($\vec{U} = 0$), it can also be shown from equations (24), (27), and (29) that the slope of the bed must exceed the angle of repose for the mobilization of the grains to occur.

Initiation of motion on a sloping bed with a current at an arbitrary angle has been analysed by several workers (Lane, 1955; Brooks, 1963; Kobayashi, 1982). However, those works show the critical shear stress for the moving fluid relative to the grain instead of the critical shear stress for the total force acting on the grain including the slope component of the gravity. Moreover, it is necessary in these other works to evaluate the angle of repose to use the relationships. This property varies greatly according to packing and porosity (Conforth, 1973), particle size and shape (Lane, 1953; Simons and Albertson, 1960), and also with the composition of the sediment (Simons and Senturk, 1977). Equation (29) is advantageous in this regard since the

Figure 8. Settling velocity of a spherical grain (from Madsen and Grant, 1976)



$$S^* = \frac{d}{4v} \sqrt{\frac{(\rho_s - \rho)}{\rho}} |g| d$$

frictional angle is eliminated during the derivation of the relationship by adopting the apparent shear stress. It is also more consistent to calculate an apparent critical shear stress since movement of a grain is determined by the direction and magnitude of the total tangential force, including the contribution of gravity force (Bagnold, 1956; Fredsøe, 1974; Bailard and Inman, 1981), and not by those of the drag force alone.

In the analysis of the Shields criterion, earlier workers neglected the lift force (Shields, 1936; Lane, 1955; Brooks, 1963). However, the Shields curve, determined empirically for the initiation of motion of cohesionless grains, has been widely accepted, and more experimental data by other workers added to the curve later shows a good agreement (Yalin, 1977). Manze (1977) modified the Shields curve for the region of Reynolds number less than 1.0, where Shields (1936) extrapolated the curve without any data. However, in practice, the Shields curve holds for quartz grains larger than 0.1 mm in diameter in water at 20°C, which is most of the case in nature (Sleath, 1984).

Kobayashi (1982) developed a relationship between the critical Shields parameter for a grain on a sloping bed and on a horizontal bed by analysing the acting forces including the lift force. However, the critical Shields parameter on a horizontal bed only holds for a certain condition, and the relationship does not yield the proper slope of grain failure when there is no current due to the assumptions made and calibration of the coefficients in the Kobayashi analysis.

- Sediment transport under waves

The initiation of motion of a sediment particle under a steady current was examined in a section above by analysing the acting forces, in which case the entraining tangential force was the sum of the drag force and the slope component of the gravity force. Under an unsteady current, however, the inertia force (\vec{F}_I) due to the acceleration of the flow must be considered in addition to the drag force (\vec{F}_D) which changes with the velocity of the flow. To this end, the tangential force on a spherical grain induced by an unsteady current can be expressed by the Morison equation (Morison et al., 1950).

$$\begin{aligned}\vec{F}_{f_t} &= \vec{F}_D + \vec{F}_I \\ &= C_D \frac{1}{2} \rho \frac{\pi d^2}{4} \vec{U} |\vec{U}| + C_M \rho \frac{\pi d^3}{6} \frac{d\vec{U}}{dt}\end{aligned}\quad (31)$$

where C_M : inertia coefficient

\vec{F}_{f_t} : flow-induced tangential force

However, under an oscillatory current whose velocity can be written as

$$\vec{U} = \vec{U}_m \cos \sigma t \quad (32)$$

where \vec{U}_m : velocity amplitude at the bed

σ : angular frequency of the wave

The relative importance of inertia force (\vec{F}_I) compared to the drag force (\vec{F}_D) can be examined by comparing the maximum inertia force and the maximum drag force

$$\frac{|\vec{F}_I|_{\max}}{|\vec{F}_D|_{\max}} = \frac{4}{3} \frac{C_M}{C_D} \frac{1}{(A_o/d)} \quad (33)$$

where A_o : horizontal amplitude of water particle displacement ($|\vec{U}_m|/\sigma$)

In equation (33), the magnitudes of C_M and C_D are $O(1)$ (Dean and Dalrymple, 1984), and thus the ratio is mainly dependent upon the ratio between the water particle excursion amplitude (A_o) to the particle size (d). Therefore, equation (33) suggests that the relative importance of inertia force compared to the drag force is negligible since A_o is much greater than d for most of waves which are able to move grains on the bottom in shallow water.

Madsen and Grant (1976) examined the problem of the initiation of motion of grains on a bed under waves by evaluating a number of experiments done by other workers (Bagnold, 1946; Manohar, 1955; Vincent, 1958; Horikawa and Watanabe, 1967; Rance and Warren, 1968). The acting shear stress on the grains by waves was expressed in terms of maximum near bottom shear stress using the wave friction factor given by Jonsson (1966). The Shields parameter calculated from the maximum near bottom shear stress was plotted against the nondimensional parameter S , given in equation (30). The result showed that the Shields curve for the initiation of motion under steady current could also satisfactorily predict the initiation of particle motion under waves. This result was also confirmed by other workers (Madsen and Grant, 1975; Komar and Miller, 1975; Sleath, 1978).

By adopting the maximum bottom shear stress, Madsen and Grant (1976) found that the empirically established relationship suggested by Brown (1950) for the bed-load sediment transport rate under unidirectional steady current, so called the Einstein-Brown formula, could also be used for the sediment transport rate under oscillating

currents. Further assuming a short response time of the sediment to the time-varying forces associated with the oscillating flow, the instantaneous sediment transport rate could be written as

$$\Phi(t) = 40\psi_o^3(t) \quad (34)$$

in which $\Phi(t)$ is the instantaneous nondimensionalized sediment transport rate written as

$$\Phi(t) = \frac{q_s(t)}{wd} \quad (35)$$

where $q_s(t)$ is the instantaneous sediment transport rate in grain volume per unit time per unit path width of the flow, and $\psi_o(t)$ is the instantaneous Shields parameter at the bottom on a horizontal bed

$$\psi_o(t) = \frac{|\tau_o(t)|}{(\rho_s - \rho) |g| d} \quad (36)$$

Instantaneous bottom shear stress $\tau_o(t)$ can be obtained by rewriting equation (21) as

$$\tau_o(t) = \frac{1}{2} \rho f_w \vec{U}(t) |\vec{U}(t)| \quad (37)$$

where f_w is the bottom friction factor under waves given by Jonsson (1966), and $\vec{U}(t)$ is the instantaneous near-bottom velocity.

Madsen and Grant (1976) calculated the average sediment transport rate using equation (34) for a half period of a sinusoidal wave while the bottom shear stress exceeded the critical shear stress given by the Shields diagram. The result showed an excellent agreement with the experiments of Kalkanis (1964), Abou-Seida (1965), and

even with the data of Manohar (1955) by taking the bottom boundary roughness as the grain diameter. The experiments of Manohar (1955) were done under asymmetric motion of a plate carrying the sediment and in some of the experiments ripples were developed.

The average sediment transport rate ($\bar{\Phi}$) averaged over the forward pulse was found to be proportional to the cube of the maximum Shields parameter (ψ_{om}). The coefficient was determined semi-empirically by Madsen and Grant (1976) as

$$\bar{\Phi} = 12.5\psi_{om}^3 \quad (38)$$

where the maximum Shields parameter is defined as

$$\psi_{om} = \frac{|\tau_{om}|}{(\rho_s - \rho) |g| d} \quad (39)$$

and τ_{om} is the maximum shear stress exerted by the wave

$$\tau_{om} = \frac{1}{2} \rho f_w \vec{U}_m |\vec{U}_m| \quad (40)$$

and \vec{U}_m is the maximum near bed velocity.

The coefficient in equation (38) varies with the ratio of the maximum Shields parameter to the critical Shields parameter. When the ratio is 1.03 the coefficient is 4.3, and it increases as the ratio increases. However, the coefficient remains almost constant at 12.5 when the maximum Shields parameter exceeded more than twice the value of the critical Shields parameter (Madsen and Grant, 1976). Shibayama and Horikawa (1980) re-evaluated the duration of grain movement and calculated that the coefficient was 19 under a simple sinusoidal wave. Horikawa et al. (1982), however,

found a good agreement of the coefficient 12.5 with the result of their experiments.

- Sediment transport under combined waves and currents

The successful prediction of sediment transport rate under waves by a quasi-steady treatment of the problem suggests that the sediment transport rate under combined waves and currents may also be calculated by equation (34). In the use of equation (34) to calculate sediment transport rate under waves and currents, the wave friction factor f_w in equation (37) should be replaced by the wave-current friction factor f_{cw} such as

$$\tau_o(t) = \frac{1}{2} \rho f_{cw} \vec{U}(t) |\vec{U}(t)| \quad (41)$$

and the near bottom flow velocity is

$$\begin{aligned} \vec{U}(t) &= \vec{U}_c + \vec{U}_w(t) \\ &= (U_{cx} + U_{wx}(t), U_{cy} + U_{wy}(t)) \\ &= (U_x(t), U_y(t)) \end{aligned} \quad (42)$$

where \vec{U}_c is the velocity component due to the steady current and $\vec{U}_w(t)$ is the velocity component due to the unsteady wave, and the subscripts x and y denote the x - and y -component, respectively.

The resultant velocity $\vec{U}(t)$ in equation (42) is the vector sum of the horizontal component of wave orbital velocity and the steady current near the bottom. The wave velocity $\vec{U}_w(t)$ and the current velocity \vec{U}_c interact non-linearly to produce the resultant bottom shear stress as is seen in equation (41). The non-linear interaction between waves and currents alters the dynamics of wave and current motions, and thus the

friction factor under the combined waves and currents is different from that of waves or currents alone (Smith, 1977; Grant and Madsen, 1978; Tanaka and Shuto, 1981; Christoffersen and Jonsson, 1985).

The wave-current friction factor f_{cw} for a combined wave and current propagating at an arbitrary angle to each other on a rough bottom was investigated by Grant and Madsen (1978). The friction factor was found to be a function of several parameters

$$f_{cw} = F(k_b, A_o, U_c, U_m, \phi_c) \quad (43)$$

where k_b is the physical bottom roughness and ϕ_c is the angle between the direction of current and the direction of propagation of the wave. The exact solution of equation (43) involves Bessel functions which can be solved numerically. An iterative procedure is needed to solve for the parameters in equation (43), and a diagram was prepared by Grant and Madsen (1978) to facilitate the solution of f_{cw} using the parameters. A numerical example of the step-by-step procedure for practical use is given in Grant and Madsen (1978) in great detail.

Once the friction factor f_{cw} is determined, the shear stress by the combined waves and currents near the bottom can be calculated by equation (41). Assuming the friction factor f_{cw} is time-invariant and it can also be applied on a sloping bed, the sediment transport rate under waves and currents on a sloping bed can be calculated by rewriting equation (34) as

$$\Phi(t) = 40\Psi_a^3(t) \quad (44)$$

where $\Psi_a(t)$ is the instantaneous apparent Shields parameter

$$\Psi_a(t) = \frac{|\tau_a(t)|}{(\rho_s - \rho) |\bar{g}| d} \quad (45)$$

And the net sediment transport rate for a period T is

$$\bar{\Phi}_T = \frac{1}{T} \int_{T'} \Phi(t) dt \quad (46)$$

where T' is the period during which the apparent Shields parameter $\Psi_a(t)$ exceeded the apparent critical Shields parameter Ψ_{ac} during the total period T .

SEDIMENT TRANSPORT BETWEEN TWO GROINS AT WILLOUGHBY SPIT

Groins may be used as an effective means of coastal protection where the coastal erosion is mainly caused by longshore transport of beach material. However, as Bruun (1972) adequately pointed out, groins may fail or be less effective in achieving the goal of beach protection if the material on the beach is also continuously lost offshore.

Balsillie and Bruno (1972) reviewed most of the published works done to date and Tomlinson (1980) also summarized the works on groins mainly focusing on the design effectiveness in practice. Many of the works done in the laboratory or in the field dealt with shoreline change in the presence of groins in relation to the rate of longshore sediment transport. Models of shoreline evolution were mostly based either on the one-line theory of Pelnard-Considere (1956) or on the two-line theory of Bakker (1968) and Bakker et al. (1970), which simply evaluate shoreline retreat or advance according to the input and output of longshore sediment transport at any place regardless of the detailed dynamics of sediment transport beyond the limit of effective longshore sediment transport.

The transport of sediment cross-shore between groins has not been studied intensively even though some laboratory experiments show the offshore transfer of sediment from the model beach near the bed or near the groin wall via rip current (Nagai and Kubo, 1958; Kemp, 1962; Hulsbergen et al., 1976). Nagai and Kubo (1958) observed an offshore transport of bedload material while suspended material was being carried onshore between groins.

Steady currents acting beyond but near the ends of groins in system generate a characteristic cell circulation pattern within the groin compartment, which is clearly seen in the experiments of Kemp (1962) and Kolp (1970). Therefore, for a better understanding of the phenomenon of sediment transport, a more detailed examination of flow dynamics and the response of bed material is needed beyond a simple consideration of longshore sediment transport. The foregoing applies especially where the development of the longshore current is minimal. Hulsbergen et al. (1976) also suggested that the two-line theory of shoreline evolution by Bakker (1968) was not enough to account for the bathymetric change caused by complex combination of waves and current.

At Willoughby Spit, the shoreline had attained a quasi-equilibrium state dynamically before the artificial fill was placed. The north shoreline of the feature did not show a significant change (Fig. 9) and the volume of sand in a surveyed compartment between two groins remained almost constant during the one year period of survey before the fill (Fig. 10). Figures 4 and 11 are the bathymetric maps on August 11, 1983 and September 5, 1983, respectively, and Figure 12 is the map of elevation difference involving comparison of the two bathymetric maps referred to above. These diagrams also suggest that the overall bottom morphology did not change very much with time even though some sediment was continuously moving over both groins.

After fill placement, the new shoreline underwent a rapid recession for two months and the volume of sand between the two groins continuously decreased. After the initial rapid retreat of the shoreline the rate of recession became slower and the

Figure 9. Change of shoreline with time before and after the fill. Dotted line is the distance of the mean low water shoreline from the line connecting the seaward end of the groins at the eastern 1/3, short dashed line is at the middle, and the long broken line is at the western 1/3 of the compartment. Thick solid line is the average of those three distances. Triangles denote the date when the bathymetric survey was done.

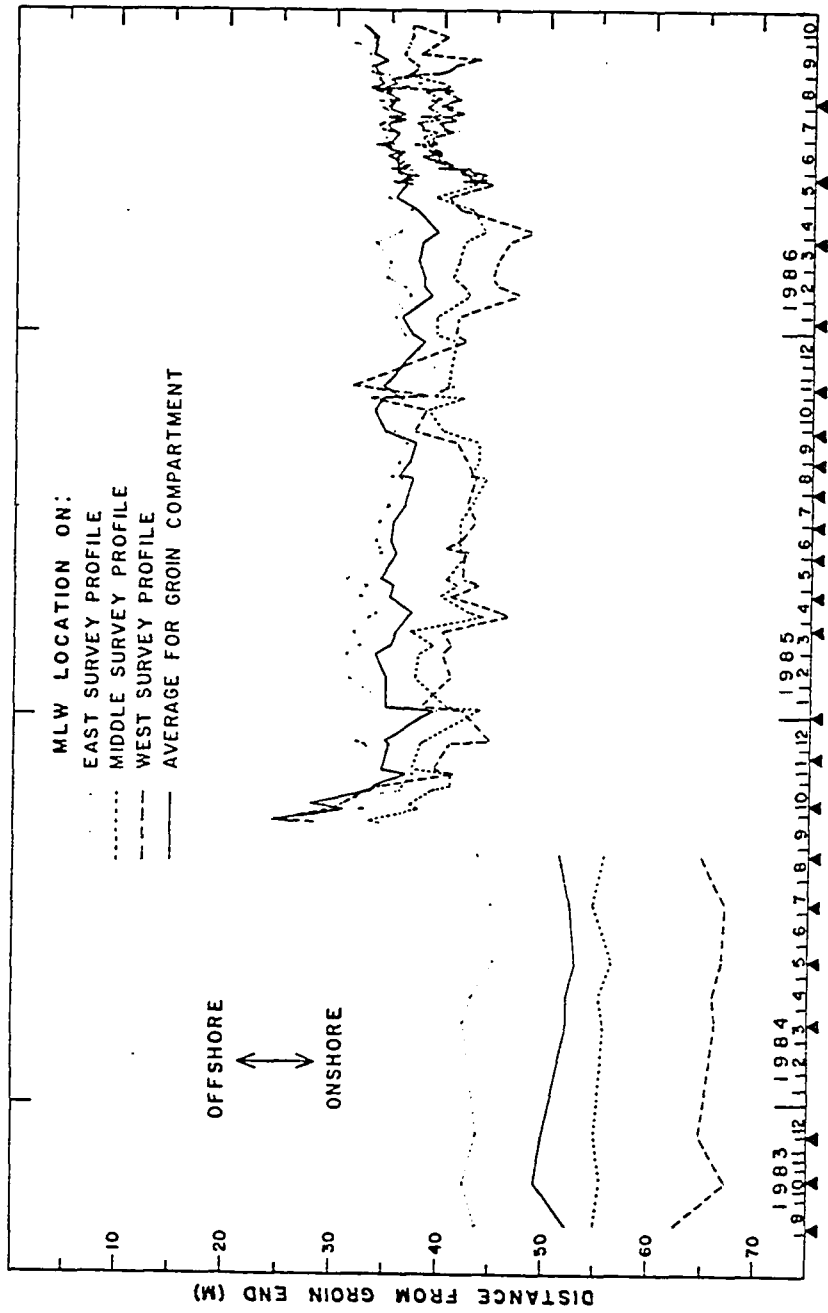


Figure 10. Time-history of sediment volume in the test compartment. The shaded area gives the cumulation of values derived from the sequence of elevation maps. The dashed line is corrected time-history curve allowing for whether erosion at a point is in fill or pre-fill sediment

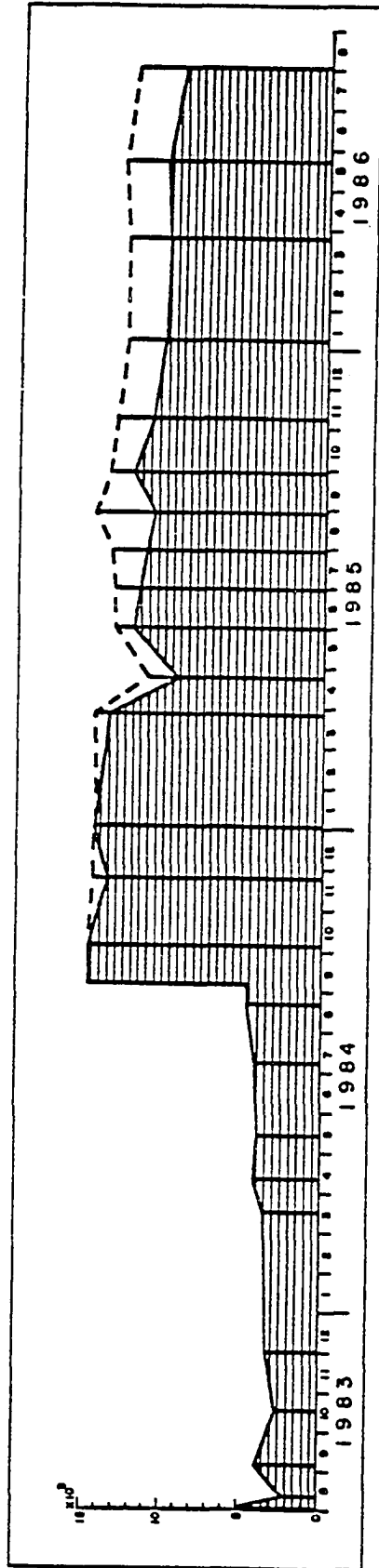
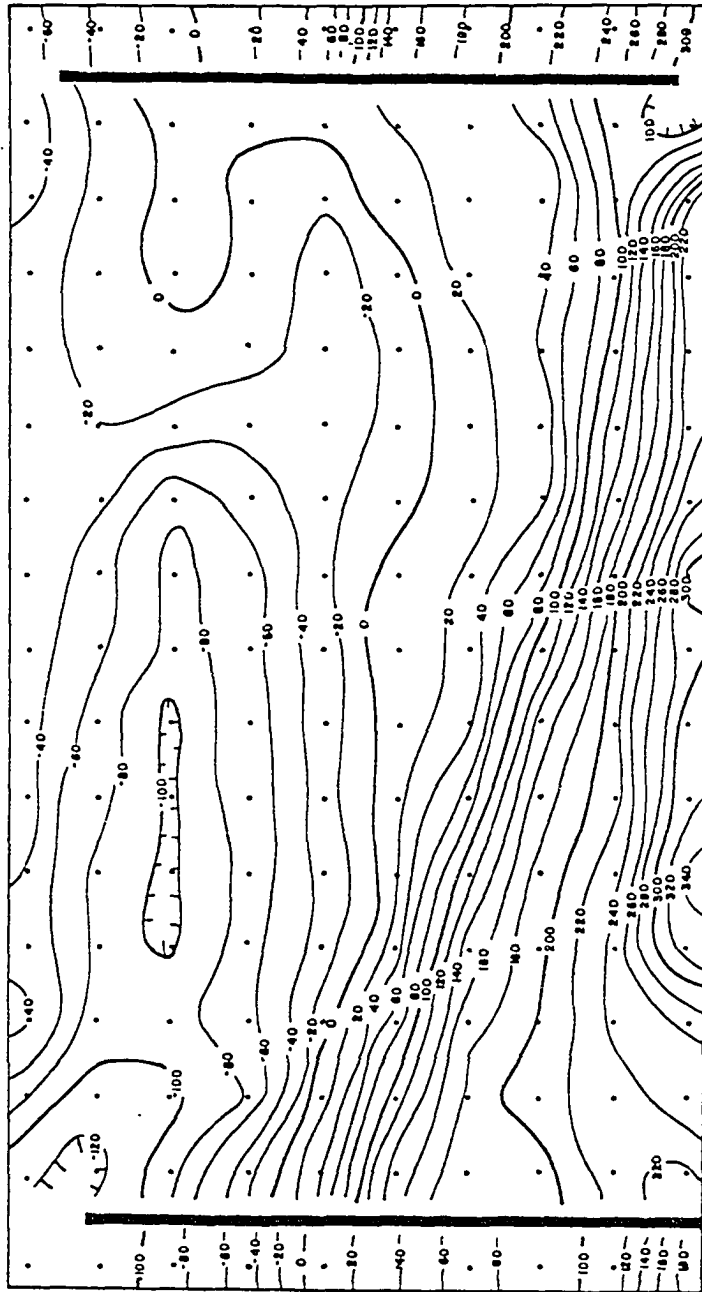


Figure 11. Bathymetric map before the fill (September 5, 1983)

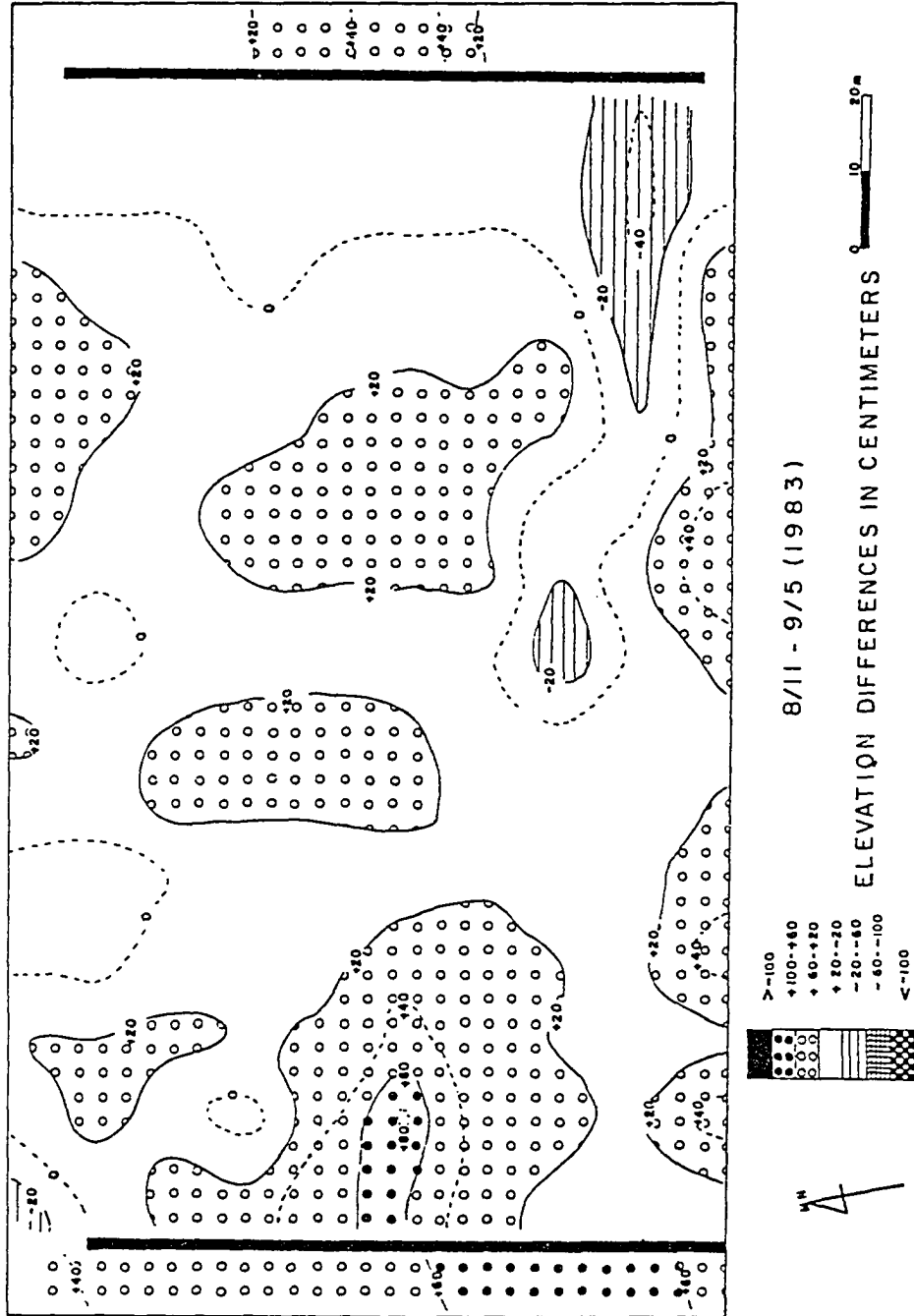


9 - 5 - 83

ELEVATIONS IN CENTIMETERS



Figure 12. Elevation difference between August 11 and September 5, 1983

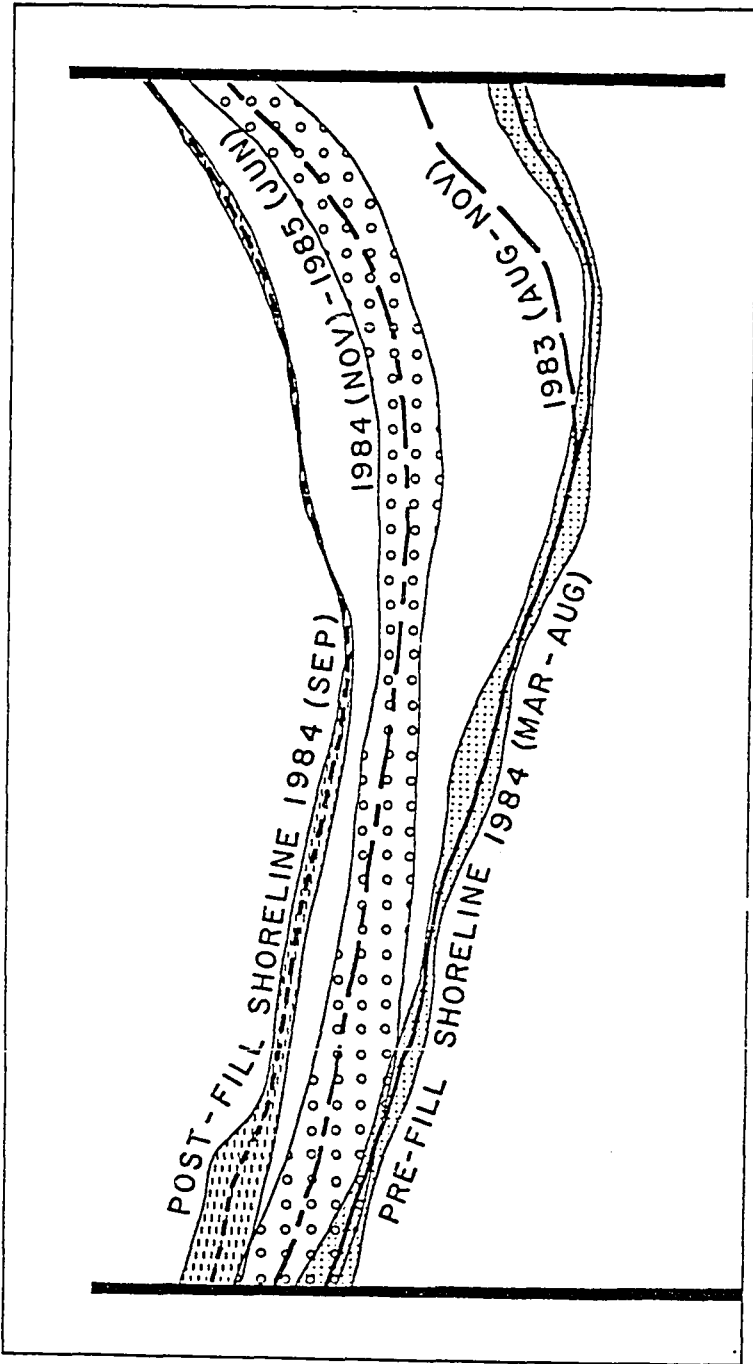


mean position of the shoreline stayed almost constant (Fig. 9). During this interval, the volume of sediment in the test compartment decreased (Fig. 10) and the shoreline began to develop the characteristic saw-tooth shape similar to that before fill placement (Fig. 13).

Ludwick et al. (1987) presented a model showing an exponential change of volume of sediment along the beach at Willoughby Spit after the fill. Based on the calculation of volume of sand between the two groins and at the newly developing spit at the end of the Willoughby Spit (Reynolds, 1987) two main routes of sediment transport by different mechanism were presented: 1) Belt 1 processes account for the longshore transport of sand near the shoreline by groin overwash mechanism or by sediment movement along the shore within a compartment; and, 2) Belt 2 processes are dominated by asymmetrical shore-parallel tidal currents. It was suggested that sediment from Belt 1 can be transferred to Belt 2 area by the actions of rip currents acting near groin walls and by the asymmetry of the distribution of wave orbital velocity near the bottom (Ludwick, 1987; Ludwick et al., 1987; Lundberg, 1987). Sediment thus entrained in Belt 2 is considered lost to the groin system.

The evolution of bottom morphology between the two groins seems to be caused by the complexity of flow pattern resulting from the interaction of the cell circulation caused by tidal currents beyond the groin ends and the wave induced unsteady current near the bed. Preliminary drogoue experiments at surface and 50 cm below the surface suggest a complex circulation pattern between the two groins (Figs. 14 and 15).

Figure 13. Pre-fill and post-fill shoreline change at the study area



MLW SHORELINE CHANGES

Figure 14. Track of drogues during the flood

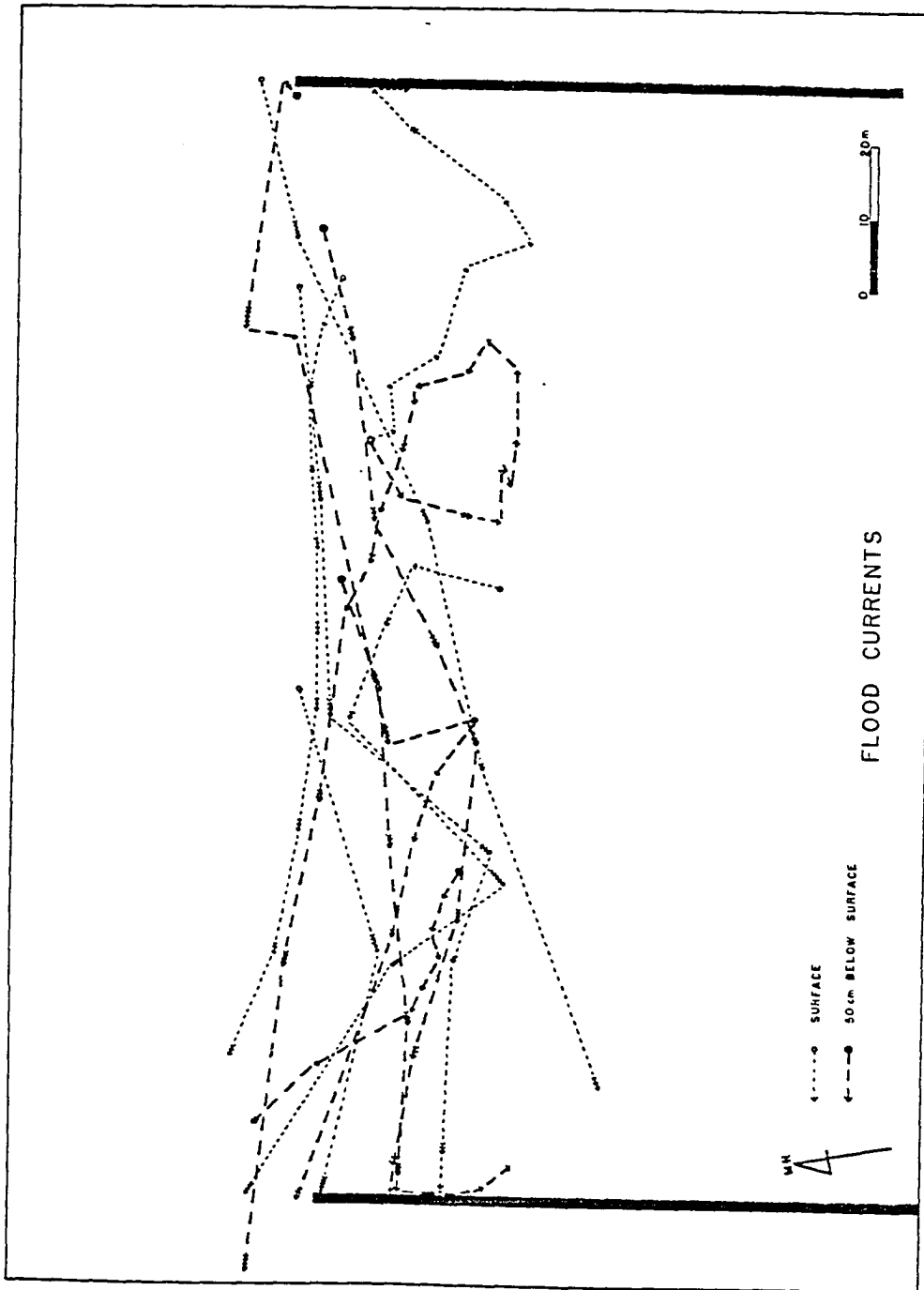
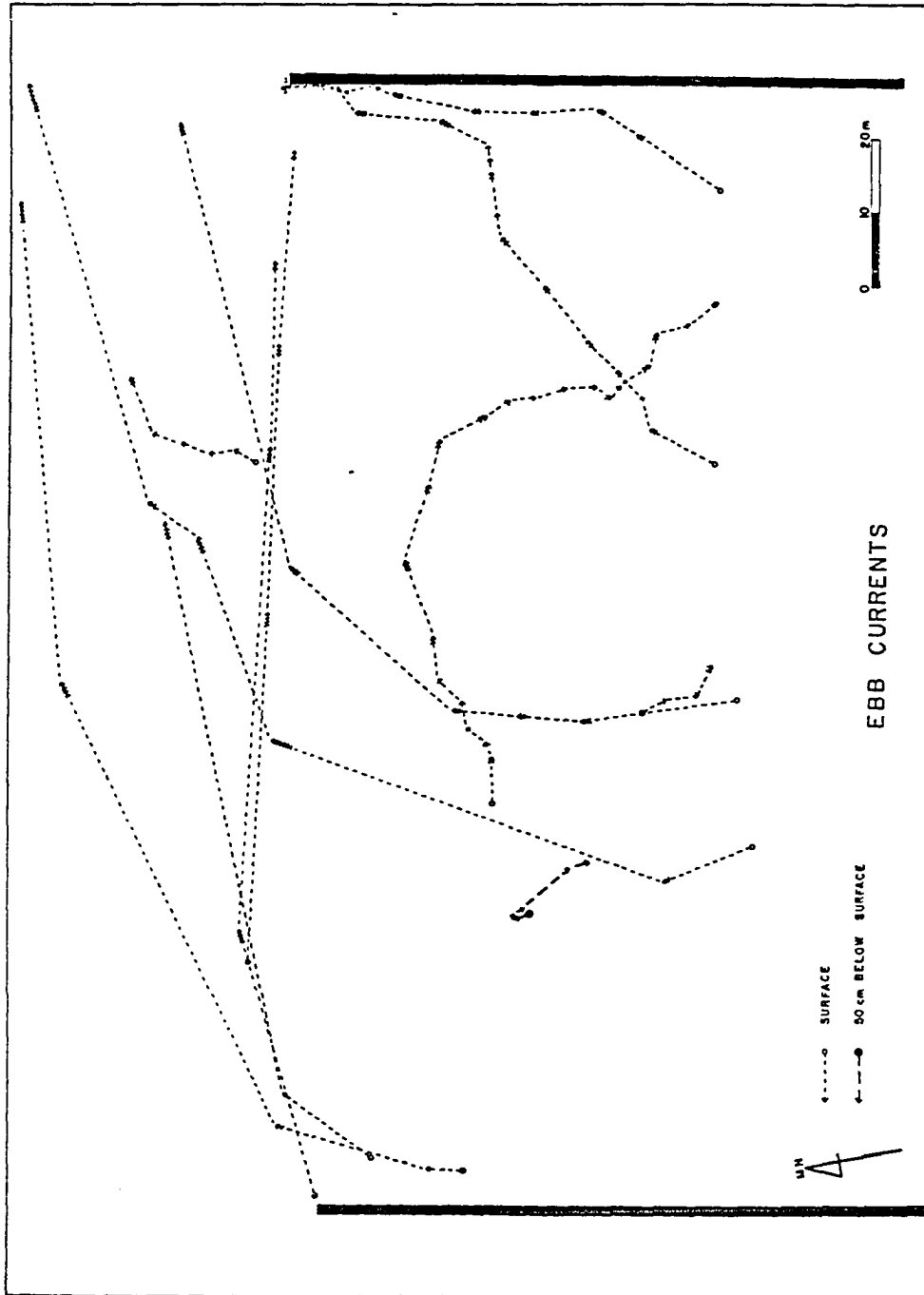


Figure 15. Track of drogues during the ebb



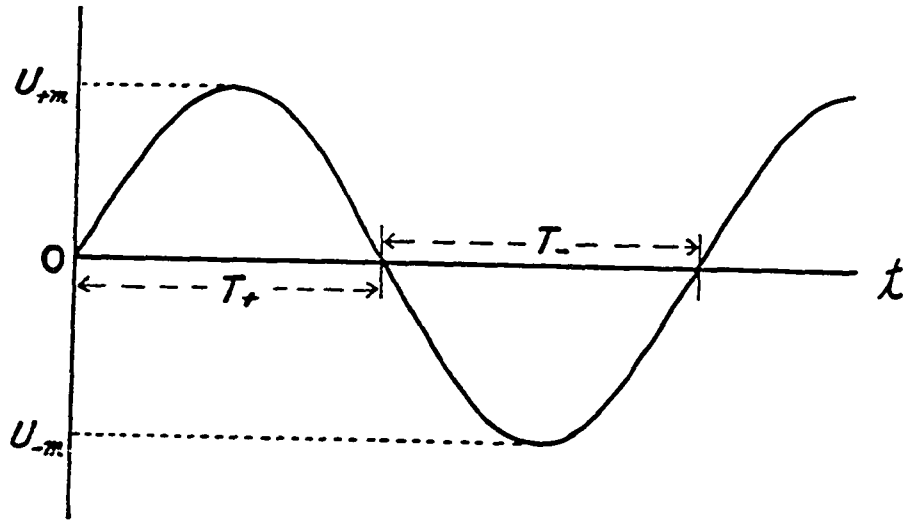
- Asymmetry in the frequency distribution of wave orbital velocity

Under sinusoidal oscillatory waves no net movement of water particle occurs near the bed. The frequency distribution of the velocities of the water particle under a linear wave shows a symmetrical distribution curve around the origin at zero, i.e., an equal frequency of occurrence for forward and backward velocities of same magnitude. However, under a nonlinear wave, the frequency distribution of velocities is not symmetrical with respect to the origin and instead is skewed towards one direction. For example under a 2nd order Stokes wave there are more occurrences of high velocities forward and low velocities backward than under a linear wave. In the case when there are N nonlinear waves coexisting, this nonlinear effect makes the probability distribution of ensemble averages skewed away from the normal distribution which is the case for the linear waves (Kinsman, 1965). Figure 16 shows the schematic velocity-versus-time curve of a linear wave and a nonlinear wave, and Figure 17 illustrates the probability distribution of velocities for the linear and nonlinear waves.

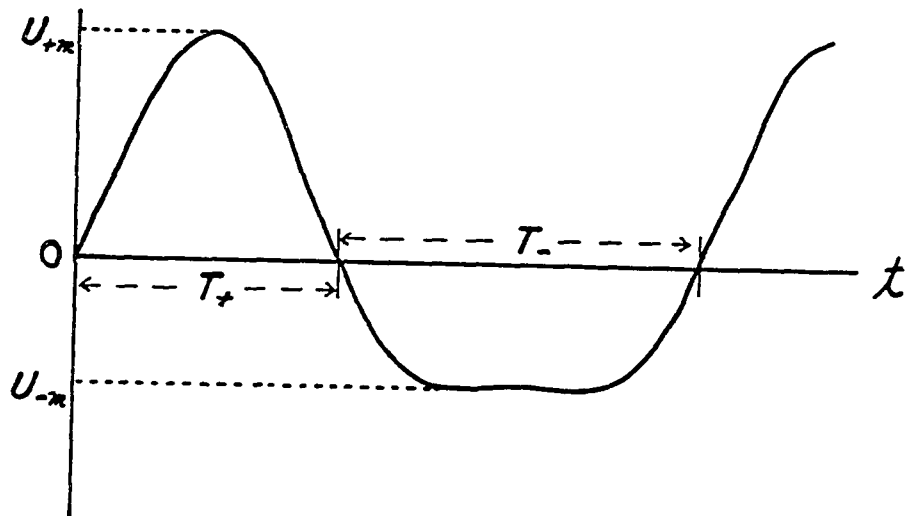
The sediment transport rate calculated from equation (46) is greatly affected by the asymmetrical distribution of near bottom velocities because it is a function of the 6th power of velocity and the frequency (duration) of the velocity. With a symmetrical velocity distribution no net transport of sediment is expected if the bed is horizontal ($\beta=0$). On the other hand, under an oscillatory current with an asymmetrical velocity distribution, a net transport of sediment in one direction may take place on a horizontal bed even without a net water particle movement.

The asymmetry of the frequency distribution of wave-induced currents results

Figure 16. Schematic time-velocity curve of linear(a) and nonlinear(b) waves

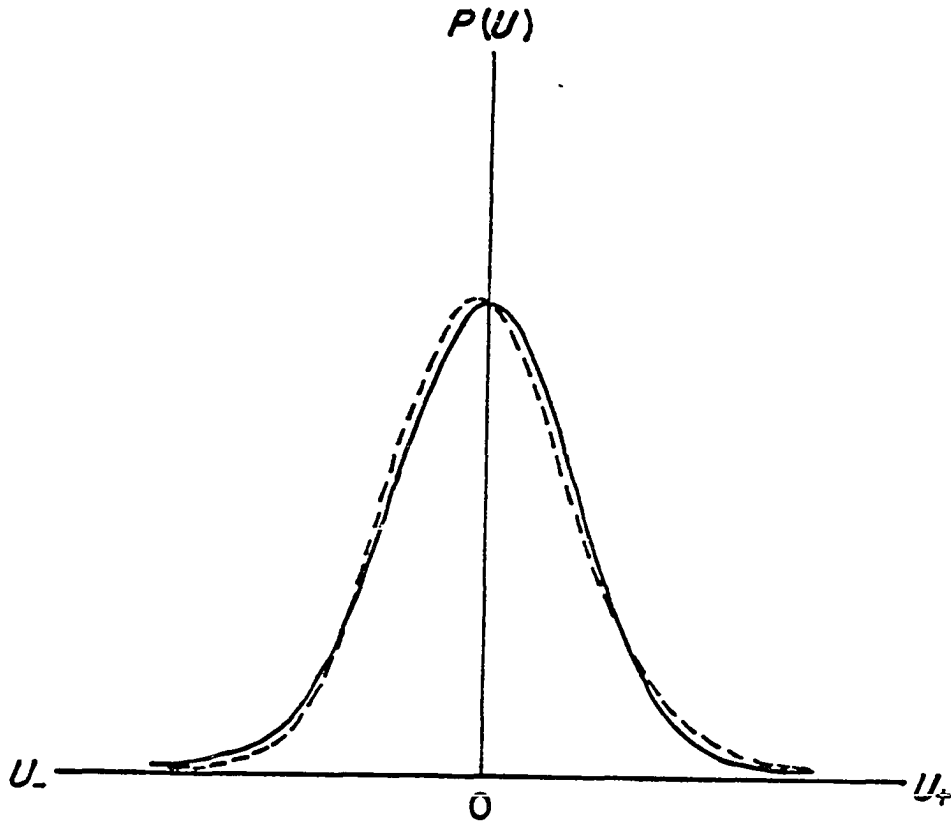


(a)



(b)

Figure 17. Probability distribution of velocities for linear and nonlinear waves



from the asymmetrical shape of velocity-versus-time curve (Fig. 16) which can be caused in nature by bedforms, shoaling of waves, superposition of waves with different frequencies and amplitudes etc. The asymmetrical shape of the velocity-versus-time curve can be conveniently described by the velocity magnitude asymmetry (S_m), the ratio of maximum forward and backward velocities, and by the velocity duration asymmetry (S_t), the ratio of the durations for forward and backward velocities.

$$S_m = \frac{U_{+m}}{U_{-m}} \quad (47)$$

$$S_t = \frac{T_+}{T_-} \quad (48)$$

where U_{+m} : maximum forward velocity magnitude

U_{-m} : maximum backward velocity magnitude

T_+ : duration of forward velocity

T_- : duration of backward velocity

Most sediment transport studies made under waves either in the laboratory or in the field have dealt with a simple monochromatic sinusoidal wave which does not produce asymmetry in the distribution of velocity. However, in reality, a simple linear wave seldom occurs especially in shallow water regions, and the measurements of wave orbital velocity in nearshore regions generally manifest a skewed frequency distribution of velocities rather than a normal distribution (Kinsman, 1965; Huntley and Bowen, 1975; Greenwood and Sherman, 1984; Bowen and Doering, 1984; Ludwick, 1987). The asymmetry of the velocity distribution is enhanced when a multiplicity of nonlinear waves interact. The interaction causes a harmonic distortion of the primary

waves by all the possible sum and difference frequencies of the primary waves (Phillips, 1977).

The nonlinear interaction of a finite number N of 2nd order waves was solved for by Biésel (1952). Under the nonlinearly interacting waves the horizontal component of wave orbital velocity was shown to be

$$u = \sum_{i=1}^N (A_i \cos \theta_i + B_i \cos 2\theta_i) + \sum_{i=1}^N \sum_{j=1}^{i-1} \left\{ S_{ij} \cos(\theta_i + \theta_j) + D_{ij} \cos(\theta_i - \theta_j) \right\} \quad (49)$$

where, $\theta_i = (k_i x - \sigma_i t)$, and the wave number $k_i = \frac{2\pi}{L_i}$, the angular frequency $\sigma_i = \frac{2\pi}{T_i}$, in which L_i and T_i are the length and the period of each monochromatic wave train respectively. The coefficients A_i, B_i, S_{ij} , and D_{ij} are given in Appendix 1, and the dispersion relation of each wave train is given as

$$\sigma_i^2 = g k_i \tanh k_i h \quad (50)$$

where g is the magnitude of acceleration of gravity and h is the water depth.

Wells (1967) evaluated the change in a quantity he termed the "skewness (β)" of the velocity distribution defined as

$$\beta = \frac{\mu_3}{(\mu_2)^{3/2}} \quad (51)$$

where μ_3 : third moment of the velocity distribution about the origin

μ_2 : second moment of the velocity distribution about the origin

The skewness was calculated for the velocity distribution at the bottom for different combinations of frequencies of incident waves with a change of water depth using

equation (49). The results showed that the sign of the skewness changed from negative (*i.e.*, more occurrence of high velocities and less occurrence of low velocities in the offshore direction than in the onshore direction) to positive (*i.e.*, same pattern but in opposite directions) as the irregular waves approached the shore moving from deep water to shallow water. The negative skewness in deeper water corresponds to the offshore movement of bottom sediment, and the positive skewness in shallower water corresponds to the onshore movement of bottom sediment. Further, the existence of a neutral line where the skewness becomes zero and thus no movement of sediment cross-shore occurs, was also suggested.

The simple model of cross-shore sediment transport by Wells (1967) considered neither the effects of sediment characteristics nor the slope of the bed. The model qualitatively predicted the direction of sediment movement based on the sign of the skewness of the near-bottom distribution of the velocity, which is solely dependent upon the wave characteristics and the water depth. Thus the model does not seem to be broad enough in scope to account for the on-offshore movement of sediment on a sloping beach. Neither does the model fully account for the neutral line as originally hypothesized by Cornaglia (1889), who observed that a certain sediment positioned on the bed would be carried onshore by waves if the particle was landwards of the neutral line and offshore if the particle was seawards of the neutral line, and, furthermore that the depth of the neutral line varied greatly with the slope of bottom, specific weight of the sediment, and the size of sediment.

At Willoughby Spit before the beach-fill was placed, the distribution of mean

grain size of the bottom sediment showed a trend of changing grain size in the cross-shore direction in the surveyed compartment between two groins (Fig. 2). This trend suggests a dynamical equilibrium of the beach and the existence of a neutral line corresponding to the characteristics of sediment and the condition of the waves and currents of the beach.

Ludwick (1987) analysed the near-bottom currents measured at 48 sites between the two groins before and after the fill. Most of the records show an asymmetrical distribution of velocity vectors in that the strongest offshore-directed vectors exceed the strongest onshore-directed vectors. The root mean square velocity amplitude of the records was about 20 *cm/sec* (Fig. 18).

Based on measurements and analyses of near bottom currents by Ludwick (1987), the following wave periods and heights were selected in the present study to be the characteristic normal wave conditions at the study area : $T_1 = 3.75$ sec, $T_2 = 5$ sec; $H_1 = 10$ cm, $H_2 = 10$ cm. The local wind chop of less than 2 seconds in period and the standing edge waves in the bands from 32.1 to 32.7 seconds and 52.9 to 56.2 seconds which oscillate parallel to the shoreline were assumed to be insignificant for cross-shore sediment transport.

Figures 19 and 20 shows the near-bottom time versus velocity curves for water depths of 2 m and 0.5 m, respectively, generated by equation (49). Transformation of the time-velocity curve is clearly depicted as the waves approach the shore. At the depth of 2 m (Fig. 19) the velocity fluctuates with a root mean square amplitude of approximately 9 *cm/sec*. The maximum amplitude in the forward direction is about 19

Figure 18. Near-bottom current measurement at Willoughby Spit
(for location see Fig. 21)

WAV26
(MEAN CURRENT NOT REMOVED)

TRUE NORTH

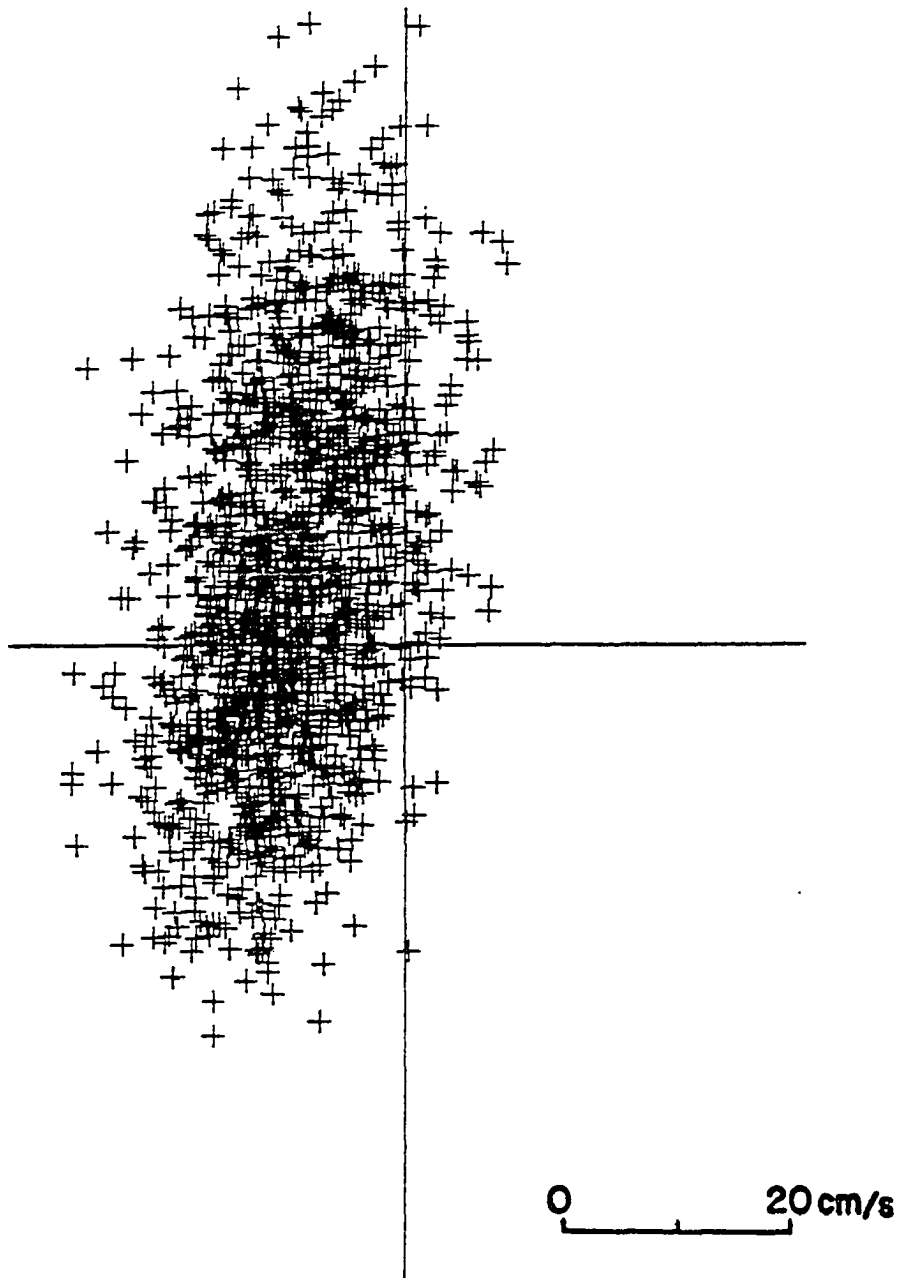


Figure 19. Time-velocity curve of the characteristic irregular waves near the bottom at the water depth of 2 *m*

HORIZONTAL COMPONENT OF WAVE ORBITAL VELOCITY AT BOTTOM
($T_1 = 3.5$ SEC, $T_2 = 5$ SEC, $H_1 = 10$ CM, $H_2 = 10$ CM, $D = 2.0$ M)

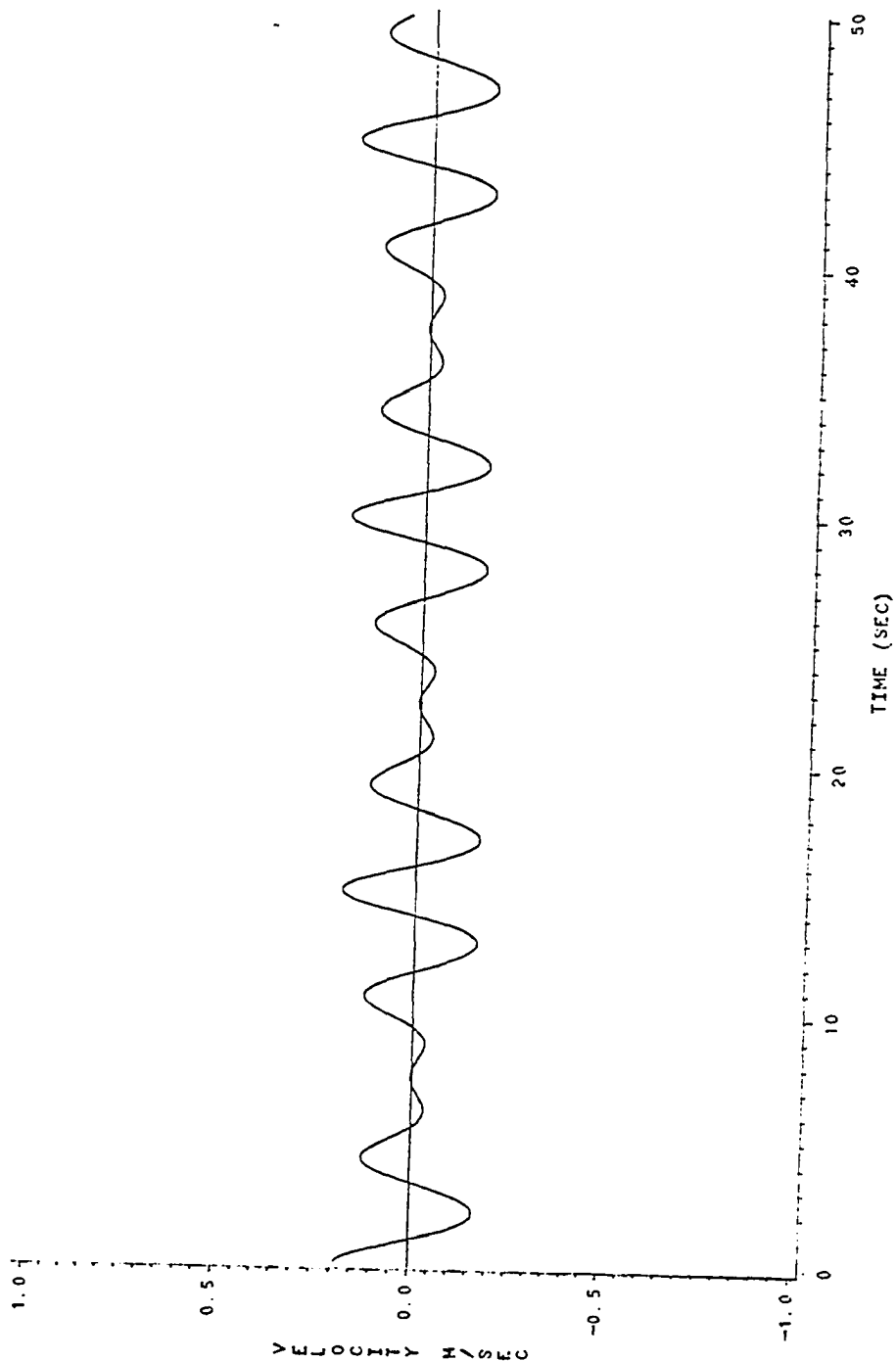
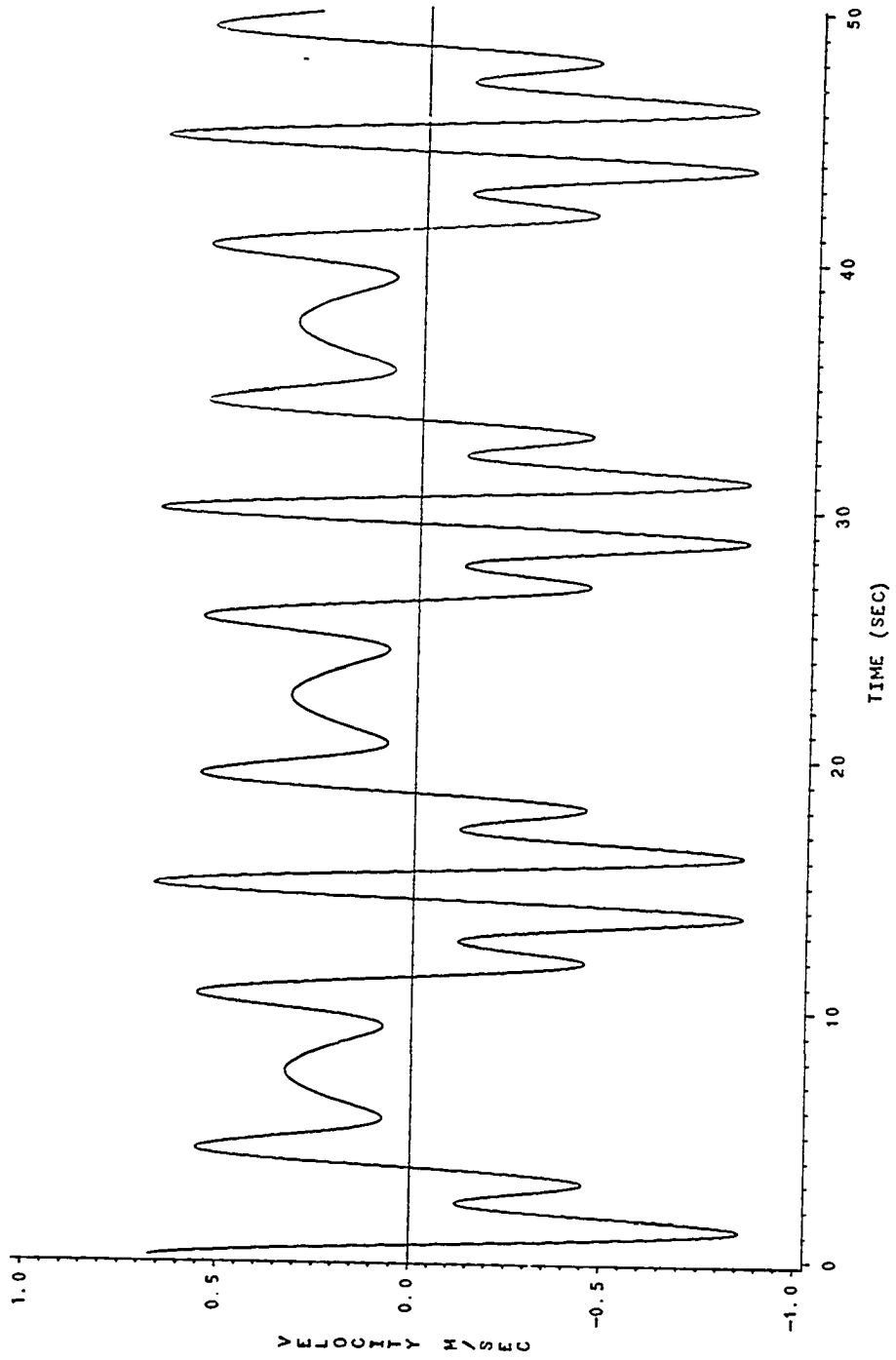


Figure 20. Time-velocity curve of the characteristic irregular waves near the bottom at the water depth of 0.5 *m*

HORIZONTAL COMPONENT OF WAVE ORBITAL VELOCITY AT BOTTOM

(T1 = 3.75 SEC, T2 = 5 SEC, H1 = 10 CM, H2 = 10 CM D = 0.5 M)



cm/sec and in the backward direction is about 17 *cm/sec*. The durations for forward and backward motions are about 6.8 seconds and 8.2 seconds respectively during the 15 second period which is the period of the composite irregular waves. As the waves approach the shallower depth of 0.5 *m* (Fig. 20) the velocity magnitude is greatly amplified up to a root mean square amplitude of about 39 *cm/sec*. Both magnitude and duration asymmetry are enhanced in that the strong backward peaks reach up to 86 *cm/sec* with a shorter duration of about 6.2 seconds as compared to the maximum forward peak velocity of about 67 *cm/sec* with a longer duration of about 8.8 seconds for the same period of 15 seconds.

Table 1 shows the change of the irregular wave-induced current at the the bottom with the change of water depth from 2 *m* to 0.5 *m*. Overall increase in root mean square values of velocity amplitude as well as the asymmetry in magnitudes and durations for forward and backward motions is seen as the water depth decreases. The maximum values for the forward direction are greater than those for the backward direction at depths deeper than 0.7 *m*. The root mean square values of peak velocities for forward motion is also greater than those for backward motion at the depths deeper than 0.7 *m*. However, at depths shallower than 0.7 *m*, the root mean square values of peaks show that a stronger backward current of shorter duration is generally coupled with a weaker forward current of longer duration.

The numerical calculation shown in Table 1 suggests that even mild irregular waves develop appreciable velocities that are large enough to move sediment at the bottom in shallow water. The observation that the backward peak velocities are

Table 1. Characteristics of irregular wave-induced near-bottom current.
 ($T_1 = 3.75 \text{ sec}$, $T_2 = 5 \text{ sec}$, $H_1 = 10 \text{ cm}$, $H_2 = 10 \text{ cm}$)

Depth (m)	Max (m/s)	Min (m/s)	RMS (m/s)	(+)Dur (sec)	(-)Dur (sec)	(+Peak) _{rms} (m/s)	(-Peak) _{rms} (m/s)
0.5	0.67	-0.85	0.39	8.78	6.22	0.48	0.56
0.6	0.53	-0.56	0.28	9.02	5.98	0.37	0.39
0.7	0.45	-0.41	0.23	9.24	5.76	0.30	0.30
0.8	0.39	-0.32	0.19	8.28	6.72	0.31	0.22
0.9	0.35	-0.27	0.17	7.90	7.10	0.27	0.19
1.0	0.32	-0.25	0.15	7.70	7.30	0.25	0.18
1.1	0.29	-0.23	0.14	7.56	7.44	0.23	0.17
1.2	0.28	-0.22	0.13	7.46	7.54	0.21	0.16
1.3	0.26	-0.21	0.13	7.38	7.62	0.20	0.15
1.4	0.24	-0.20	0.12	7.30	7.70	0.19	0.15
1.5	0.23	-0.20	0.12	7.22	7.78	0.18	0.14
1.6	0.22	-0.19	0.11	7.14	7.86	0.17	0.14
1.7	0.21	-0.18	0.11	7.08	7.92	0.16	0.13
1.8	0.20	-0.18	0.10	6.98	8.02	0.15	0.13
1.9	0.20	-0.17	0.10	6.90	8.10	0.15	0.12
2.0	0.19	-0.17	0.09	6.76	8.24	0.14	0.12

stronger than the forward peak velocities in shallow depths is consistent with the measurements of Ludwick (1987) in the field (Table 2). Table 2 shows the cross-shore component of current measurements which were measured at 30 *cm* above the bottom at the study area (Fig. 21). Ludwick (1987) also reported that a typical velocity amplitude of the wave-induced currents for a corresponding monochromatic wave would be approximately 15 *cm/sec* at the bottom in water 1.11 *m* deep, which suggests that most of the wave records were taken generally under milder wave conditions than the wave conditions presented in Table 1. However, It is clearly seen that most of the records show stronger offshore maximum values than the onshore maximum values.

When the vector mean was removed from the field records to examine the effect of oscillatory motion, 31 of 48 records show stronger offshore maximum velocities than onshore maximum velocities (Table 3, Fig. 22). The magnitude and duration asymmetries calculated by the root mean square values of onshore and offshore peaks also show that most of the currents have stronger offshore peaks with shorter offshore durations than the onshore peaks and durations (Table 4). The velocity magnitude asymmetry (S_m), and duration asymmetry (S_t) were obtained by rewriting equations (47) and (48) so as to correspond with the the convention that the sign of the forward motion is positive (+) and that the sign of the backward motion is negative (-)

$$S_m = \frac{(U_{+m})_{rms}}{(U_{-m})_{rms}} - 1 \quad (52)$$

$$S_t = \frac{T_+}{T_-} - 1 \quad (53)$$

Table 2. Cross-shore component of current measurement at 30 *cm* above bottom at Willoughby Spit (Ludwick, 1987).

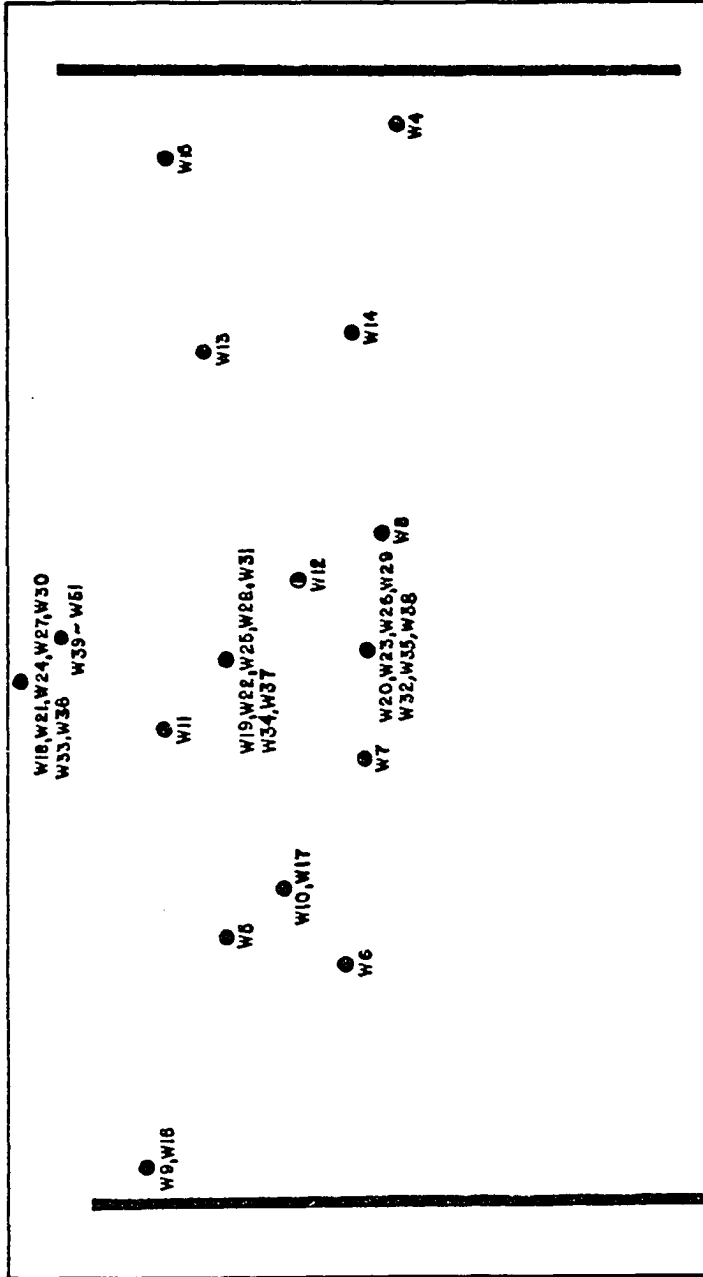
Record No.	Date	Water Depth (m)	Max (m/s)	Min (m/s)	RMS (m/s)
4	9-28-83	0.85	0.38	-0.30	0.13
5	3-22-84	1.42	0.20	-0.09	0.07
6	4-19-84	1.27	0.14	-0.14	0.04
7	4-19-84	1.19	0.11	-0.10	0.03
8	4-19-84	1.12	0.13	-0.17	0.05
9	5-10-84	1.32	0.09	-0.14	0.04
10	5-10-84	0.90	0.11	-0.31	0.05
11	5-10-84	1.13	0.12	-0.11	0.04
12	5-10-84	0.60	0.15	-0.23	0.06
13	5-10-84	0.63	0.18	-0.19	0.06
14	5-10-84	0.58	0.14	-0.21	0.07
15	5-10-84	0.50	0.33	-0.39	0.11
16	5-10-84	1.85	0.07	-0.13	0.04
17	5-10-84	1.45	0.10	-0.12	0.04
18	6-19-84	0.70	0.17	-0.28	0.08
19	6-19-84	1.35	0.12	-0.19	0.06
20	6-19-84	0.55	0.33	-0.40	0.11
21	6-19-84	0.75	0.27	-0.37	0.11
22	6-19-84	1.50	0.16	-0.23	0.08
23	6-19-84	0.60	0.41	-0.45	0.15
24	6-19-84	0.95	0.23	-0.33	0.10
25	6-19-84	1.65	0.19	-0.24	0.07
26	6-19-84	0.85	0.34	-0.54	0.18
27	6-19-84	2.00	0.29	-0.34	0.10
28	6-19-84	2.00	0.12	-0.17	0.05
29	6-19-84	1.05	0.20	-0.33	0.09
30	6-19-84	1.20	0.15	-0.20	0.06
31	6-19-84	1.75	0.23	-0.15	0.05
32	6-19-84	0.80	0.21	-0.28	0.08
33	6-19-84	1.00	0.16	-0.18	0.05
34	6-19-84	1.50	0.12	-0.11	0.04
35	6-19-84	0.60	0.23	-0.32	0.09
36	6-19-84	0.75	0.16	-0.21	0.07
37	6-19-84	1.35	0.10	-0.12	0.04

Continued

Table 2. Continued

38	6-19-84	0.55	0.24	-0.33	0.09
39	11-29-84	0.90	0.10	-0.21	0.05
40	11-29-84	0.90	0.15	-0.18	0.06
41	11-29-84	1.00	0.16	-0.14	0.05
42	11-29-84	1.00	0.19	-0.15	0.06
43	11-29-84	1.00	0.15	-0.19	0.05
44	11-29-84	1.10	0.18	-0.15	0.05
45	11-29-84	1.25	0.19	-0.09	0.07
46	11-29-84	1.35	0.15	-0.15	0.05
47	11-29-84	1.40	0.19	-0.14	0.06
48	11-29-84	1.30	0.14	-0.19	0.06
49	11-29-84	1.20	0.18	-0.18	0.06
50	11-29-84	1.05	0.18	-0.15	0.05
51	11-29-84	0.85	0.16	-0.17	0.05

Figure 21. Location of the near-bottom current measurement



E-M CURRENT METER STATIONS



Table 3. Cross-shore component of oscillatory motion measured at Willoughby Spit (mean currents were removed from Table 2).

Record No.	Date	Water Depth (m)	Max (m/s)	Min (m/s)	RMS (m/s)
4	9-28-83	0.85	0.34	-0.35	0.12
5	3-22-84	1.42	0.14	-0.15	0.04
6	4-19-84	1.27	0.14	-0.14	0.04
7	4-19-84	1.19	0.11	-0.10	0.03
8	4-19-84	1.12	0.14	-0.16	0.05
9	5-10-84	1.32	0.10	-0.13	0.03
10	5-10-84	0.90	0.13	-0.28	0.05
11	5-10-84	1.13	0.12	-0.12	0.04
12	5-10-84	0.60	0.16	-0.22	0.05
13	5-10-84	0.63	0.19	-0.18	0.06
14	5-10-84	0.58	0.16	-0.18	0.06
15	5-10-84	0.50	0.37	-0.35	0.10
16	5-10-84	1.85	0.08	-0.11	0.03
17	5-10-84	1.45	0.11	-0.12	0.04
18	6-19-84	0.70	0.18	-0.27	0.08
19	6-19-84	1.35	0.14	-0.17	0.05
20	6-19-84	0.55	0.35	-0.38	0.11
21	6-19-84	0.75	0.27	-0.37	0.11
22	6-19-84	1.50	0.18	-0.22	0.08
23	6-19-84	0.60	0.42	-0.44	0.15
24	6-19-84	0.95	0.24	-0.32	0.10
25	6-19-84	1.65	0.20	-0.23	0.07
26	6-19-84	0.85	0.40	-0.48	0.16
27	6-19-84	2.00	0.29	-0.35	0.10
28	6-19-84	2.00	0.13	-0.17	0.05
29	6-19-84	1.05	0.22	-0.31	0.09
30	6-19-84	1.20	0.16	-0.19	0.06
31	6-19-84	1.75	0.23	-0.14	0.05
32	6-19-84	0.80	0.23	-0.26	0.08
33	6-19-84	1.00	0.17	-0.17	0.05
34	6-19-84	1.50	0.11	-0.11	0.04
35	6-19-84	0.60	0.25	-0.31	0.08
36	6-19-84	0.75	0.19	-0.18	0.07
37	6-19-84	1.35	0.10	-0.12	0.04

Continued

Table 3. Continued

38	6-19-84	0.55	0.25	-0.32	0.09
39	11-29-84	0.90	0.12	-0.18	0.05
40	11-29-84	0.90	0.16	-0.16	0.05
41	11-29-84	1.00	0.16	-0.14	0.05
42	11-29-84	1.00	0.17	-0.17	0.06
43	11-29-84	1.00	0.16	-0.18	0.05
44	11-29-84	1.10	0.17	-0.15	0.05
45	11-29-84	1.25	0.14	-0.14	0.05
46	11-29-84	1.35	0.14	-0.16	0.04
47	11-29-84	1.40	0.18	-0.16	0.05
48	11-29-84	1.30	0.16	-0.17	0.06
49	11-29-84	1.20	0.19	-0.17	0.06
50	11-29-84	1.05	0.20	-0.14	0.05
51	11-29-84	0.85	0.16	-0.17	0.05

Figure 22. Horizontal component of oscillatory motion at Willoughby Spit
(mean current was removed from Figure 19)

WAV26
(MEAN CURRENT REMOVED)

TRUE NORTH

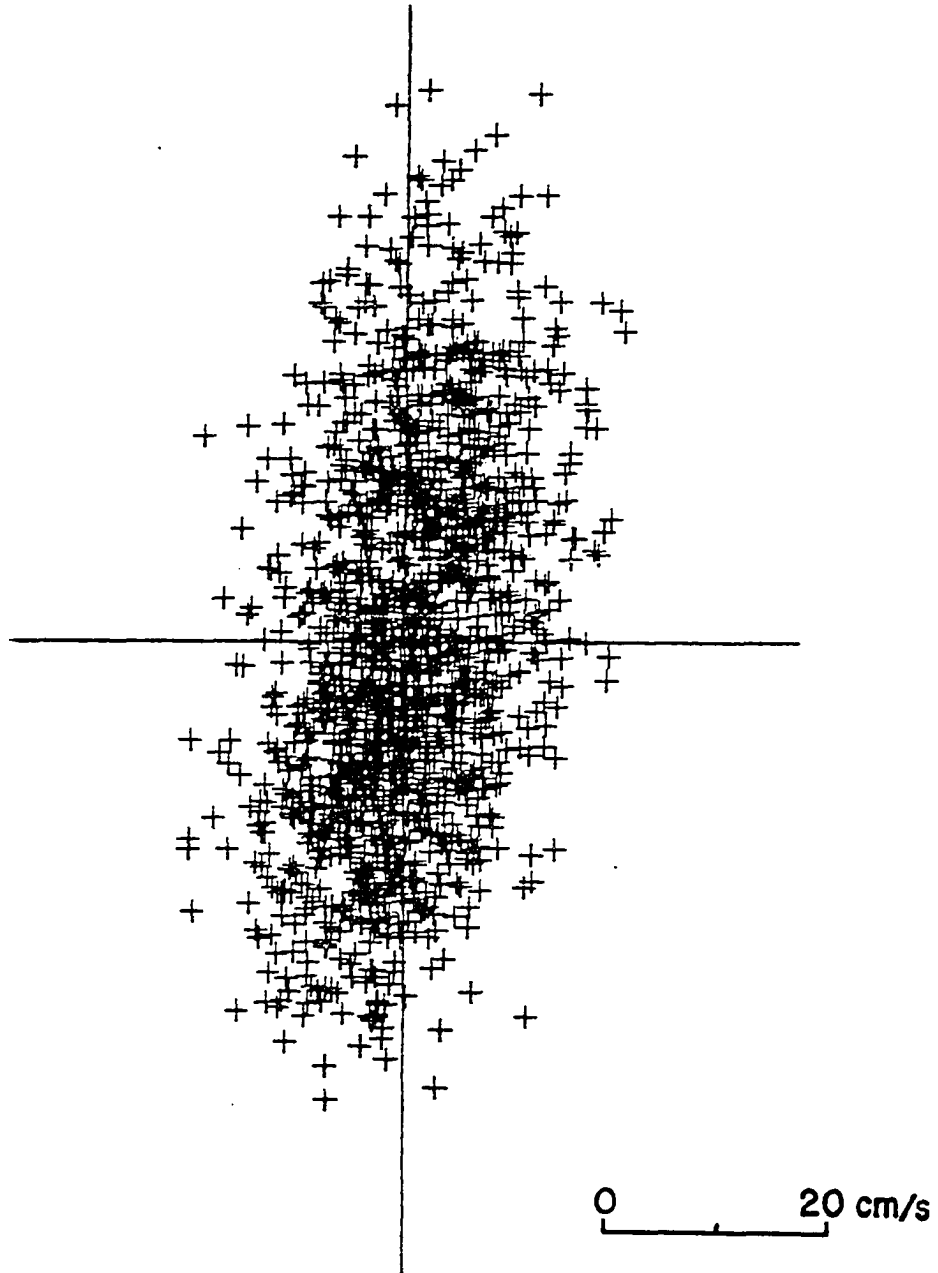


Table 4. Magnitude asymmetry (S_m) and duration asymmetry (S_t) of RMS velocities of cross-shore component oscillatory motion at Willoughby Spit.

Record No.	Date	Water Depth (m)	(+Peak) _{rms} (m/s)	(-Peak) _{rms} (m/s)	S_m	S_t
4	9-28-83	0.85	0.14	0.14	0.03	0.00
5	3-22-84	1.42	0.05	0.05	-0.03	0.01
6	4-19-84	1.27	0.05	0.05	-0.02	-0.01
7	4-19-84	1.19	0.04	0.04	0.03	0.01
8	4-19-84	1.12	0.06	0.05	0.02	-0.04
9	5-10-84	1.32	0.04	0.04	-0.08	0.02
10	5-10-84	0.90	0.06	0.06	-0.08	0.03
11	5-10-84	1.13	0.05	0.05	-0.02	0.00
12	5-10-84	0.60	0.07	0.07	-0.07	0.05
13	5-10-84	0.63	0.08	0.07	0.11	-0.07
14	5-10-84	0.58	0.08	0.08	0.02	-0.01
15	5-10-84	0.50	0.12	0.13	-0.01	0.06
16	5-10-84	1.85	0.04	0.04	-0.06	0.04
17	5-10-84	1.45	0.05	0.05	-0.06	0.04
18	6-19-84	0.70	0.09	0.10	-0.09	0.10
19	6-19-84	1.35	0.07	0.07	-0.08	0.08
20	6-19-84	0.55	0.13	0.13	-0.01	0.04
21	6-19-84	0.75	0.13	0.14	-0.03	0.03
22	6-19-84	1.50	0.09	0.11	-0.14	0.11
23	6-19-84	0.60	0.17	0.18	-0.05	0.01
24	6-19-84	0.95	0.13	0.13	-0.06	0.07
25	6-19-84	1.65	0.09	0.10	-0.07	0.04
26	6-19-84	0.85	0.19	0.22	-0.11	0.11
27	6-19-84	2.00	0.12	0.12	-0.06	0.05
28	6-19-84	2.00	0.05	0.06	-0.09	0.09
29	6-19-84	1.05	0.10	0.11	-0.09	0.08
30	6-19-84	1.20	0.08	0.07	0.03	-0.02
31	6-19-84	1.75	0.06	0.05	0.15	-0.08
32	6-19-84	0.80	0.09	0.10	-0.10	0.09
33	6-19-84	1.00	0.06	0.06	-0.02	0.01
34	6-19-84	1.50	0.04	0.04	-0.03	0.00
35	6-19-84	0.60	0.10	0.09	0.01	-0.03
36	6-19-84	0.75	0.07	0.08	-0.07	0.08
37	6-19-84	1.35	0.04	0.04	-0.03	0.05

Continued

Table 4. Continued

38	6-19-84	0.55	0.11	0.11	-0.05	0.05
39	11-29-84	0.90	0.06	0.06	0.01	-0.04
40	11-29-84	0.90	0.06	0.07	-0.06	0.04
41	11-29-84	1.00	0.06	0.06	0.02	-0.03
42	11-29-84	1.00	0.06	0.07	-0.09	0.09
43	11-29-84	1.00	0.06	0.06	0.04	-0.04
44	11-29-84	1.10	0.06	0.06	-0.04	0.03
45	11-29-84	1.25	0.05	0.06	-0.05	0.09
46	11-29-84	1.35	0.05	0.05	-0.10	0.09
47	11-29-84	1.40	0.06	0.06	0.01	0.02
48	11-29-84	1.30	0.06	0.06	-0.01	0.01
49	11-29-84	1.20	0.07	0.07	0.08	-0.06
50	11-29-84	1.05	0.06	0.06	0.10	-0.08
51	11-29-84	0.85	0.06	0.06	0.07	0.00

where $(U_{+m})_{rms}$: root mean square forward peak velocity

$(U_{-m})_{rms}$: root mean square backward peak velocity

T_+ : duration of forward velocity

T_- : duration of backward velocity

The occurrence of stronger offshore peak velocities implies an offshore movement of bottom sediment in the very shallow water region if the average sediment transport rate is calculated in terms of peak velocity such as is done in equation (38). This finding is contrary to that of Wells (1967) who predicted an onshore movement of sediment in shallow depths based on his analysis of skewness of the near bottom velocity distribution.

The significance of peak velocities in the calculation of sediment transport rate is emphasized when flow velocity is raised to the 6th power rather than to the 3rd power which was done by Wells (1967) in his evaluation in terms of skewness. Moreover, when the size distribution of the bed material is narrow, what is important in the evaluation of sediment transport is the velocity distribution above the threshold velocity rather than the entire velocity distribution. Therefore the sediment threshold velocity minimizes the affect of low velocities and enhances the importance of high velocities. .

The observation that at greater depths the forward peak velocities are stronger than the backward peak velocities also suggests that some onshore movement of bottom sediment from the deeper water may occur if the wave-induced current is strong enough to move the sediment. Therefore, from the results of the present study there

may be a neutral line towards which sediment is carried both from the shore region and from the offshore area. This type of neutral line (convergence) would take the place of the neutral line (divergence) computed by Wells (1967) from his skewness measure. At his neutral line, sediment is carried either towards the shoreline or the offshore.

Figure 23 shows the skewness (β) calculated using equation (51), the velocity magnitude asymmetry (S_m), and duration asymmetry (S_t) for the same waves using equations (52) and (53). In the diagram it is seen that the skewness (β) is always positive at depths less than 1.4 m and thus is predictive of a continuous onshore movement of sediment within this shallow region and offshore movement of sediment at depths deeper than 1.4 m. On the other hand the magnitude asymmetry (S_m) and duration asymmetry (S_t) show a change of sign at the depths of 0.7 m and 1.1 m respectively. The sign of magnitude asymmetry is negative in the region shallower than 0.7 m and the magnitudes of the peak velocities in this region are strong enough to move the sediment. Therefore, contrary to the prediction by Wells (1967), an offshore movement of sediment is expected in the region shallower than approximately 0.7 m. At depths greater than 0.7 m the sign of magnitude asymmetry is positive suggesting an onshore movement of sediment if the near bottom current is strong enough to move the sediment.

When the measured asymmetries of magnitude and duration (Table 4) are plotted with respect to the water depth (Fig. 24), it is seen that most of the magnitude asymmetry is negative and most of the duration asymmetry is positive. However, although it

Figure 23. Skewness, magnitude asymmetry, and duration asymmetry of the characteristic irregular waves

SKEWNESS(---), MAG ASYMMETRY(---), DUR ASYMMETRY(---)
(T1 = 3.75 SEC, T2 = 5 SEC, H1 = 10 CM, H2 = 10 CM)

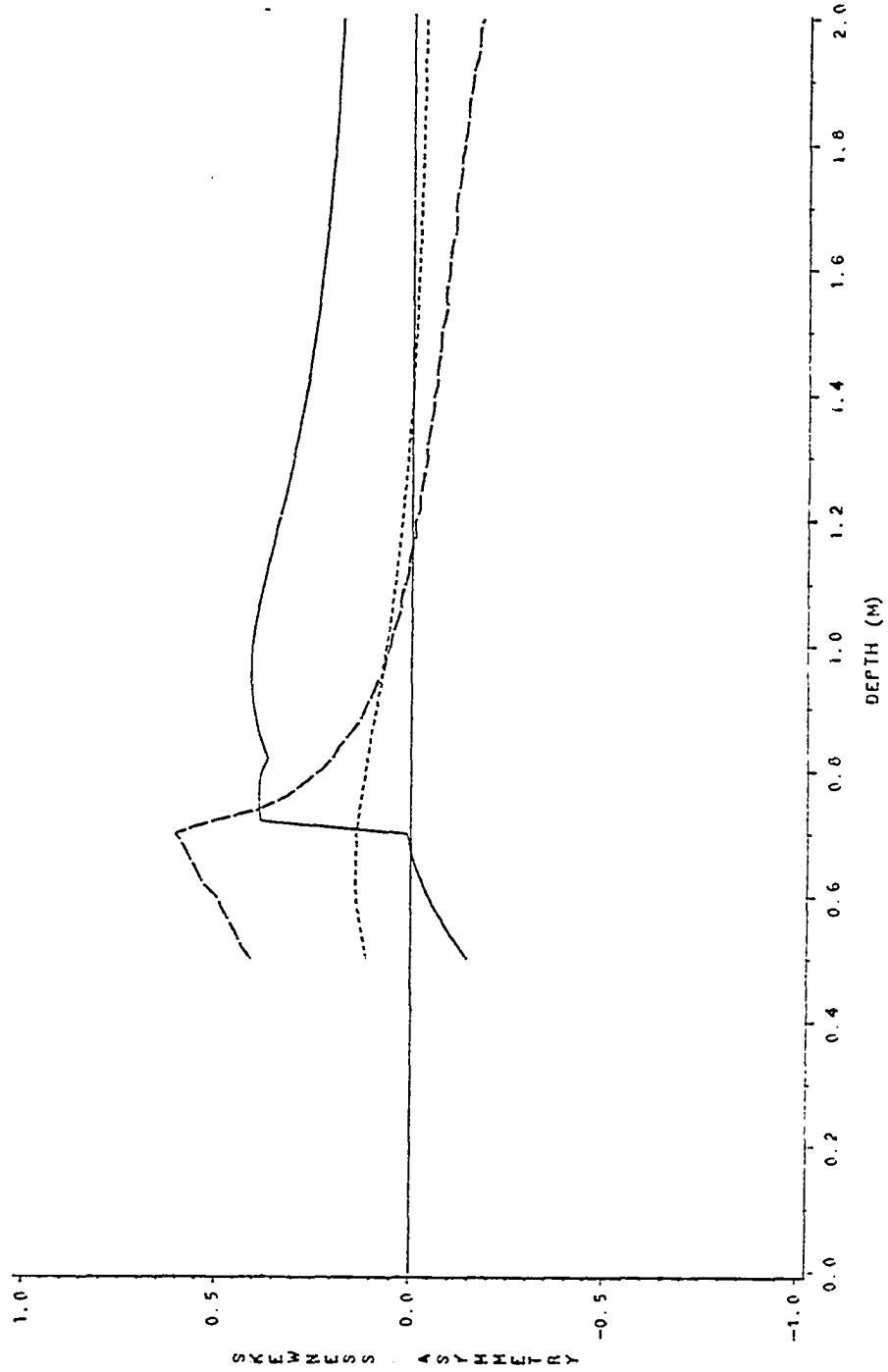
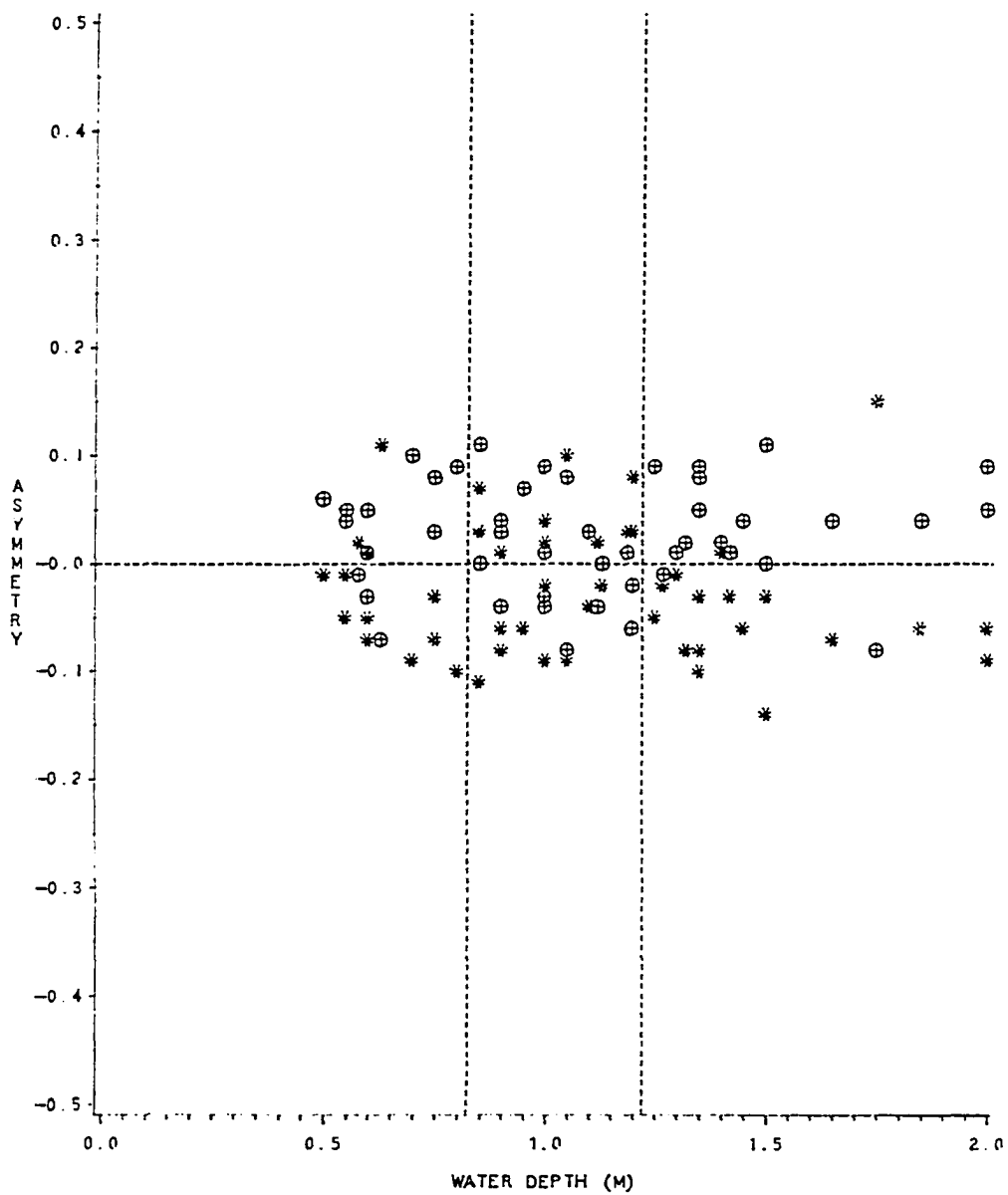


Figure 24. Magnitude asymmetry and duration asymmetry of the measured oscillatory motion at Willoughby Spit

Sm(*) AND St(⊕) WITH DEPTH AT WILLOUGHBY SPIT



is difficult to compare these specific observations to the calculated results shown in Figure 24, at water depths less than approximately 0.8 *m* most of the magnitude asymmetries are negative with positive duration asymmetries. At the depths greater than 0.8 *m* more positive magnitude asymmetries and negative duration asymmetries appear until the depth of about 1.2 *m*. The magnitude asymmetries again become mostly negative when the water depth is greater than 1.2 *m*.

Results of the actual measurement of wave-induced current near the bottom illustrate that in a very shallow region there are stronger peaks of shorter duration in the offshore direction, and that the asymmetries change with water depth for a given set of wave characteristics. The discrepancy between observation and numerical calculation is that the negative magnitude asymmetry occurs at depths greater than 0.7 *m* for the present study. This seems to be caused by the different wave conditions for each wave record taken, *e.g.*, such as smaller waves and more complexity of wave periods than the wave conditions used for the numerical calculation.

Since sediment transport rate is affected not only by the magnitude but also by the duration of the current in onshore or offshore direction, the duration asymmetry can also alter the depth of the neutral line and thus the direction of net sediment transport at any locality. Therefore, for an exact deduction of neutral line location and the direction of net sediment transport associated with it on both sides, a calculation of actual sediment transport rate needs be done. Such a calculation is affected by sediment characteristics, threshold velocity, and local slope of the bottom as well as by flow conditions. However, if the wave-induced peak velocities are sufficient to move

the sediment, the magnitude asymmetry is the most important factor determining the direction of net sediment transport since the sediment transport rate is a function of approximately 6th power of the velocity magnitude for the present study. Moreover the importance of the peak velocities is signified by the fact that the threshold velocity for bedload reduces the affect of the low velocities to the movement of sediment under an oscillatory flow.

Even with energetics models in which the sediment transport rate is a function of the 3rd power of velocity, for example in the bedload models of Bailard and Inman (1981) or Bagnold (1963), the peak velocities also seem to be more important than the whole distribution of velocities for an unsteady motion which fluctuates about zero velocity. Originally the model of Bagnold (1963) was developed for a unidirectional steady current which was assumed to be substantially above the threshold velocity of the bed material. However, for the application of the energetics model to unsteady flow conditions especially for wave-induced oscillatory currents, the threshold velocity for the movement of sediment should be applied to the instantaneous velocities that are relevant. Therefore, under oscillatory flow conditions, high velocities or peak velocities play a more important role in moving sediment than do the low velocities.

Wave conditions in shallow water on beaches are often irregular and quite unpredictable. The wave characteristics can only be deduced by a statistical means. Before recourse to an elaborate statistical analysis of wave records and the calculation of sediment transport rate it is suggested that analysis of onshore and offshore peaks can provide information about the direction of sediment transport. The root mean

square values are an appropriate representation of the varying peaks and are readily calculable either numerically or graphically. Rasmussen and Fredsøe (1981) also found that root mean square values of the irregular wave heights were more closely related to the sediment transport rate than were the mean or maximum one third value of the wave heights.

- Sediment transport by irregular waves and currents

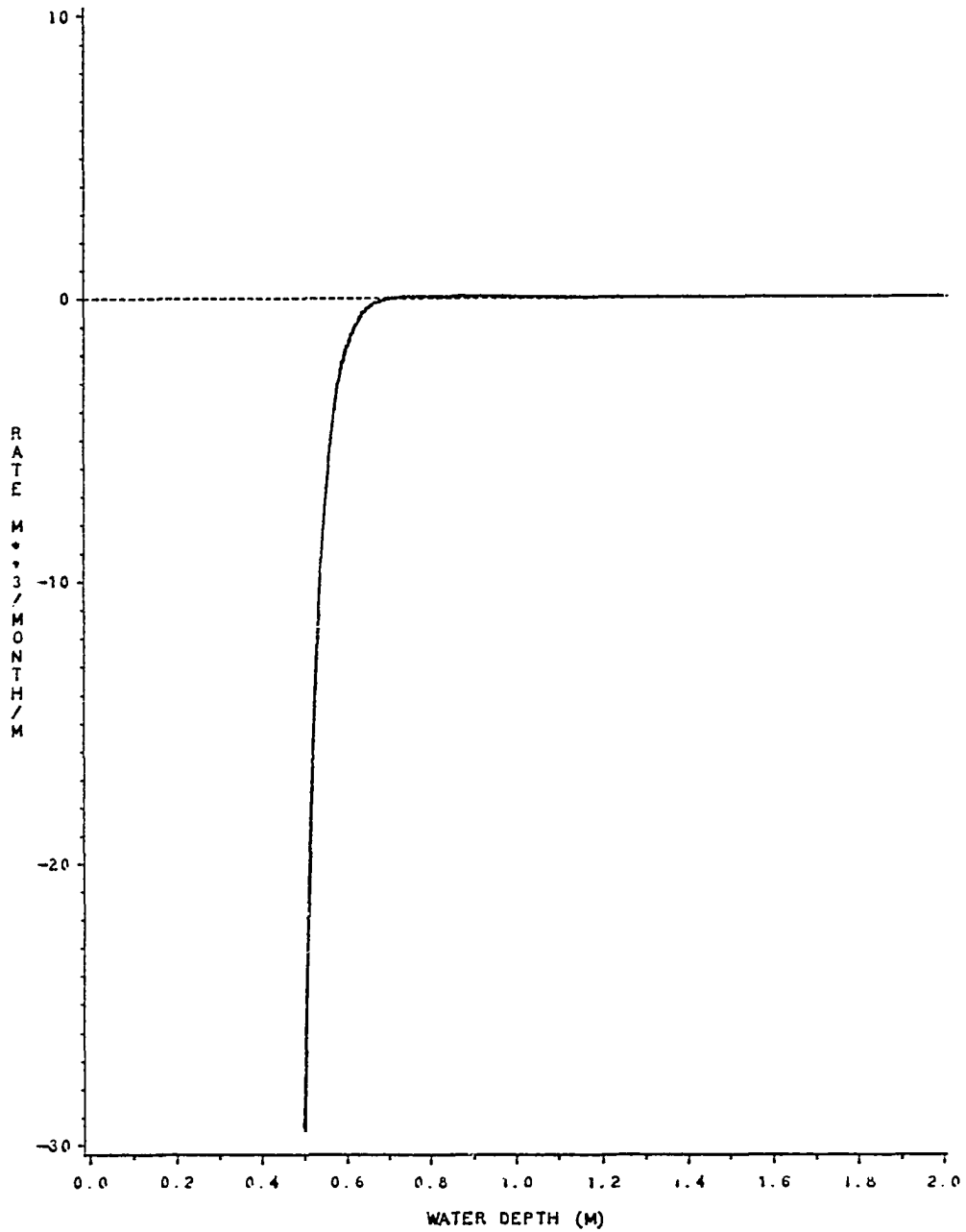
The irregular waves that produce the asymmetries in magnitude and duration shown in the previous section may result in a net sediment transport in one direction either onshore or offshore in a beach area. If a steady current is superimposed on the waves, the sediment transport is greatly affected by the combined waves and current. Together with the flow characteristics, the local slope of the bed and the grain characteristics of the area should also be considered in calculating the actual sediment transport rate.

Figure 25 shows the change of net cross-shore sediment transport rate with depth by the same waves discussed in the previous section. The sediment transport rate was calculated by equation (46) for quartz grains 1.0 *mm* in diameter on a horizontal bed. Waves were assumed to be approaching from 80 degrees with respect to the positive x-direction (see Figure 6 for coordinate system) which makes an angle between the wave crests and the shoreline of about 10 degrees, open to the west, for the study area. The wave friction factor f_w was chosen to be 0.015 and the critical Shields parameter ψ_{oc} was chosen to be 0.035.

Figure 25. Change of sediment transport rate with depth by the characteristic irregular waves

SEDIMENT TRANSPORT RATE WITH DEPTH

(T1 = 3.75 SEC. T2 = 5 SEC. H1 = 10 CM. H2 = 10 CM)
(SLOPE = 0 DEG. CURRENT = 0 CM/SEC. ALPA = 10 DEG)



It is seen that the rate of sediment transport decreases exponentially with increases in water depth and that the direction of transport is offshore within the shallow region up to the depth of about 0.7 *m*, which is approximately the depth where the sign of magnitude asymmetry S_m changed (Fig. 23). There is a small amount of onshore sediment transport between the depths of 0.7 *m* and 1.2 *m*. The wave-induced current at bottom is not strong enough to move sediment at depths deeper than 1.2 *m*.

The calculation of actual sediment transport rate also shows the existence of a neutral line (convergence) which was implied by the analysis of magnitude asymmetry in the previous section. In the region shallower than the depth of neutral line the direction of net sediment transport is offshore and vice versa.

At a submerged beach area, which is bounded by the shoreline on the landside, the direction of net sediment transport is as important as the amount of sediment transport rate because the direction directly determines the gain or loss of sediment to the beach. The net offshore sediment transport at the depths less than the depth of neutral line suggests that the inshore submerged beach loses sediment, which may result in either shoreline retreat or increasing water depth until the shallow area reaches the depth of neutral line. If the beach area near the shoreline became deeper than the depth of neutral line by some incidental temporary erosion, the submerged inshore beach would gain sediment by the net onshore movement of sediment which may manifest itself by either shoreline advance or filling of the submerged inshore beach until the water depth again attains the depth of neutral line.

The existence of a neutral line (convergence) implies that a beach can reach a

condition of dynamical equilibrium even after a chaotic perturbation of the bottom caused by an event such as a storm or an artificial fill. To achieve an equilibrium condition, the beach must have a tendency to reach stability corresponding to some local specified wave conditions. Under the convergent neutral line concept, a beach can reach the stable condition by moving sediment either offshore or onshore until the beach reaches the depth of the neutral line.

The well-known observed cyclic change of beach profile as adjustment is made to seasonal changes in wave conditions, *i.e.*, the development of the so-called swell-storm profile or the summer-winter profile, also seems to support the concept of neutral line (convergence). During the stormy weather following a calm swell season, the neutral depth may increase and thus sediment is carried offshore resulting in the deepening of the inshore area. When the calm swell season is back, the neutral depth decreases and thus the sediment is carried onshore to restore the previous shallow swell profile. This cyclic change of beach profile by the movement of sediment either onshore or offshore corresponding to the seasonal wave conditions is only possible by the adjustment of beach profile to the local wave conditions under the concept of convergent neutral line.

On the other hand, under a neutral line (divergence) such as suggested by Wells (1967), at depths shallower than the depth of neutral line the direction of net sediment transport is onshore and vice versa. Therefore, if a submerged beach section initially at equilibrium is filled with sediment so that the water becomes shallower than the neutral depth, the shoreline should advance seaward due to the onshore movement of the filled sediment while the water depth seaward away from the shoreline becomes deeper

until the beach reaches the depth of neutral line. For this instance the total filled sediment is preserved within the inshore beach area unless the sediment there is lost by longshore transport or by passing farther landwards through the shoreline, However, quite contrarily, the submerged beach section in the present study area at Willoughby Spit was losing sediment offshore and the shoreline was retreating landwards after the placement of artificial fill on the beach.

Further, under conditions of an assumed neutral line (divergence), if the same beach section lost sediment by a temporary disturbance to become deeper than the neutral depth for the normal wave conditions of the area, the beach would continuously lose sediment and/or the shoreline would retreat landwards until the water depth increased so much that the waves could not move the sediment at the bottom when the normal wave condition of the area recovered. Therefore a submerged beach, under the concept of a neutral line (divergence), can hardly be restored to the same equilibrium condition as before if the wave condition changes temporarily from normal wave conditions of the area.

When a steady current is superimposed on waves, the steady current not only changes the bottom friction factor but also affects the direction and amount of net sediment transport. According to the angle between the direction of the steady current and the wave propagation, the steady current either enhances or reduces the net sediment transport rate and thus changes the depth of the neutral line and the depth of no sediment motion from those that were developed under wave action alone. The wave-current friction factor f_{cw} can be determined from the diagram given by Grant and

Madsen (1978). For the present study the f_{cw} was approximately 0.01 when the angle between the axes of current and wave propagation was less than 60 degrees. When the angle is between 60 degrees and 90 degrees, the friction factor f_{cw} was interpolated between 0.01 and 0.012.

Figure 26 shows the change of sediment transport rate with depth when a steady current of 25 *cm/sec* flowing parallel to the shoreline (0 degrees with respect to positive x-direction) was superimposed on the same wave and sediment conditions stated above. The wave-current friction factor f_{cw} was calculated to be approximately 0.0113. It is seen that the steady current enhanced the onshore component of sediment transport rate and reduced the offshore component of sediment transport rate, and thus the depth of the neutral line was moved to a shallower depth at about 0.6 *m* and the sediment was still moving onshore even at the depth of about 2 *m*.

When the same steady current is flowing in opposite direction (negative x-direction), the steady current has an affect of increasing the offshore component of sediment transport rate and decreasing the onshore component of sediment transport rate compared to the steady current flowing in positive x-direction. Therefore, even though the amount of net offshore sediment transport rate was also reduced in shallow depths compared to the case of waves alone, the sediment was always carried offshore simply by reversing the direction of the same steady current. The combined waves and current moved sediment offshore up to the depth of about 2.3 *m* at which depth the near bottom current was not strong enough to move the sediment (Fig. 27).

If a steady current with strength sufficient to overcome the asymmetry of the

Figure 26. Change of sediment transport rate due to the wave-current interaction
(current direction = 0 degree)

SEDIMENT TRANSPORT RATE WITH DEPTH

(T1 = 3.75 SEC, T2 = 5 SEC, H1 = 10 CM, H2 = 10 CM)
(SLOPE = 0 DEG, CURRENT = 25 CM/SEC, 000 DEG, ALPHA = 10 DEG)

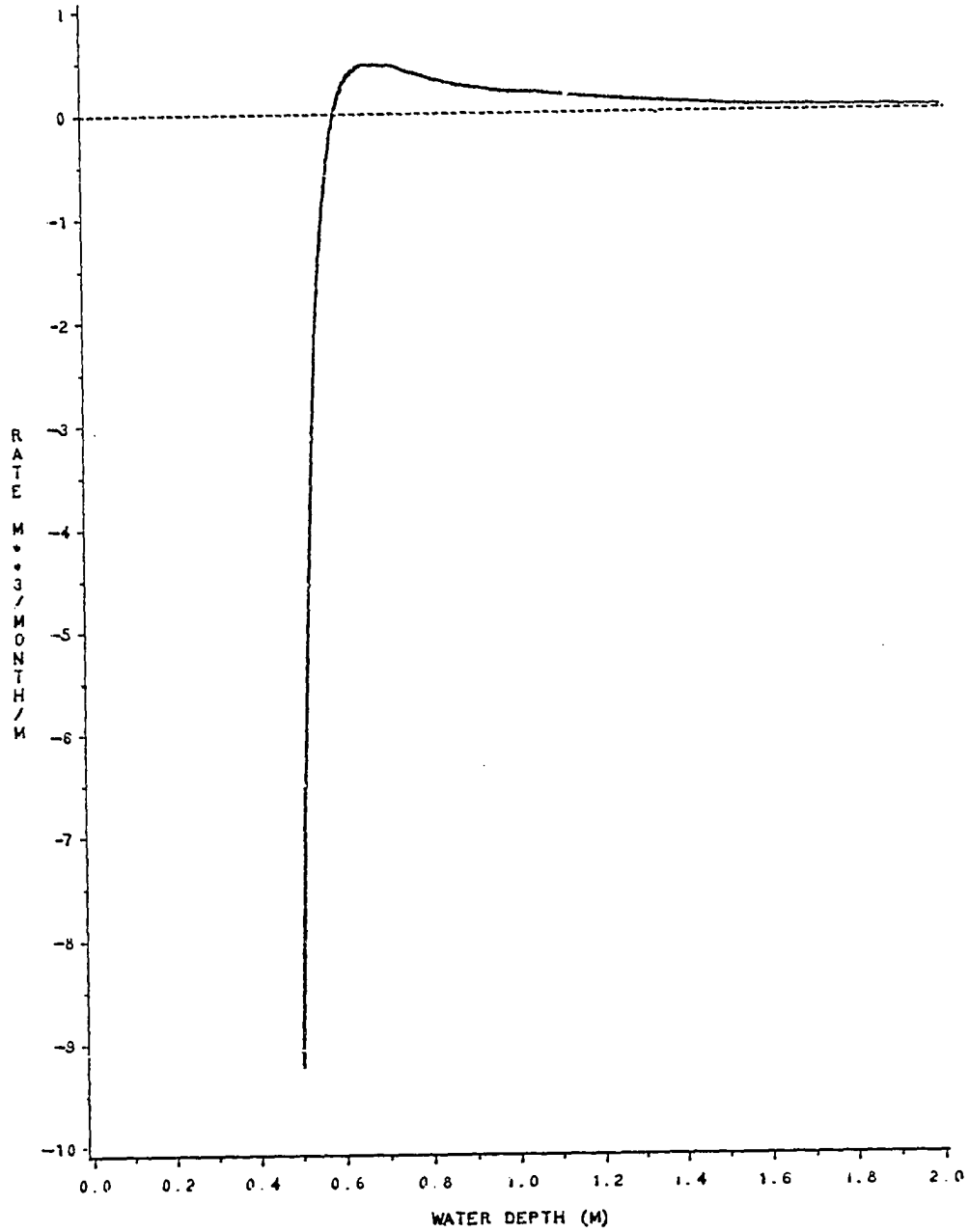
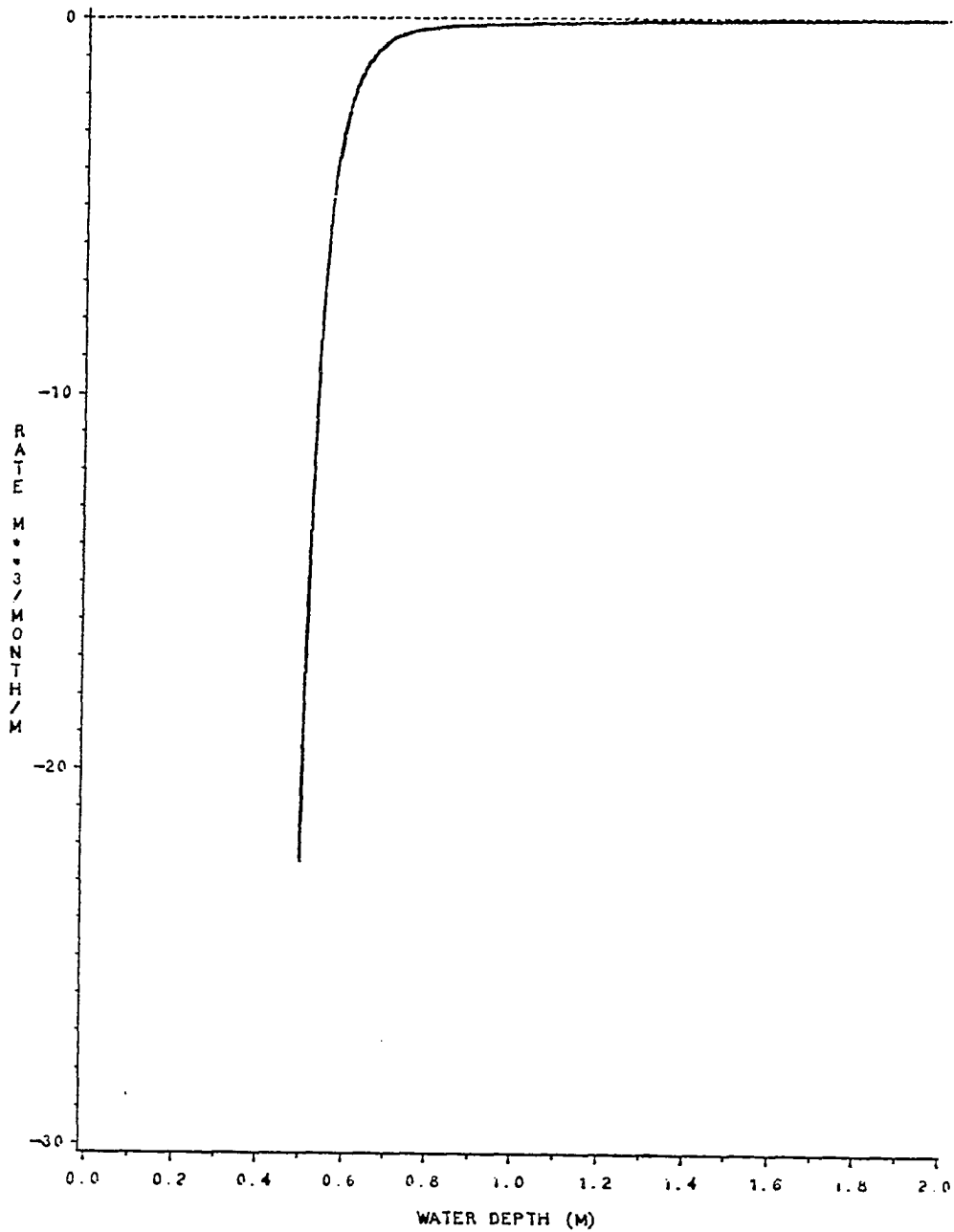


Figure 27. Change of sediment transport rate due to the wave-current interaction
(current direction = 180 degree)

SEDIMENT TRANSPORT RATE WITH DEPTH

(T1 = 3.75 SEC, T2 = 5 SEC, H1 = 10 CM, H2 = 10 CM)
(SLOPE = 0 DEG, CURRENT=25 CM/SEC, 180 DEG, ALFA=10 DEG)



wave-induced currents is flowing onshore (positive y-direction) or offshore (negative y-direction), the direction of net cross-shore sediment transport would obviously be either onshore or offshore following the direction of the steady current (Figs. 28 and 29).

The above numerical calculations show that a beach can gain or lose sediment without any significant change of longshore sediment transport rate. However, if sediment is not supplied or lost indefinitely through the shoreline, the beach will finally achieve equilibrium state by adjusting to the local wave conditions to reach the corresponding neutral depth or the depth of no sediment motion.

The foregoing arguments on the changes of shoreline and water depth is based on the assumptions that sediment does not pass through the shoreline and that the direction of sediment transport is directly related to the gain or loss of sediment at the submerged beach area. However, if sediment is continuously supplied from the shore to the submerged inshore area, deepening of the submerged area may not occur by the offshore movement of sediment alone. If sediment is continuously lost at the shoreline by longshore current, the water depth may not become shallower even when the sediment is transported onshore. At such an area local gradient of sediment transport rate can determine the gain or loss of sediment at the area.

Ludwick (1987) developed a model for predicting the life of filled sand in a system of groins along the Chesapeake Bay side beach of Willoughby Spit, Virginia. In the model, the loss of sand from a groin compartment was accounted for by two distinct processes: 1) Belt 1 processes which transfer the sediment by groin-top overwash-

Figure 28. Change of sediment transport rate due to the wave-current interaction
(current direction = 90 degree)

SEDIMENT TRANSPORT RATE WITH DEPTH

(T1 = 3.15 SEC, T2 = 5 SEC, H1 = 10 CM, H2 = 10 CM)
(SLOPE = 0 DEG, CURRENT = 25 CM/SEC, 90 DEG, ALPHA = 10 DEG)

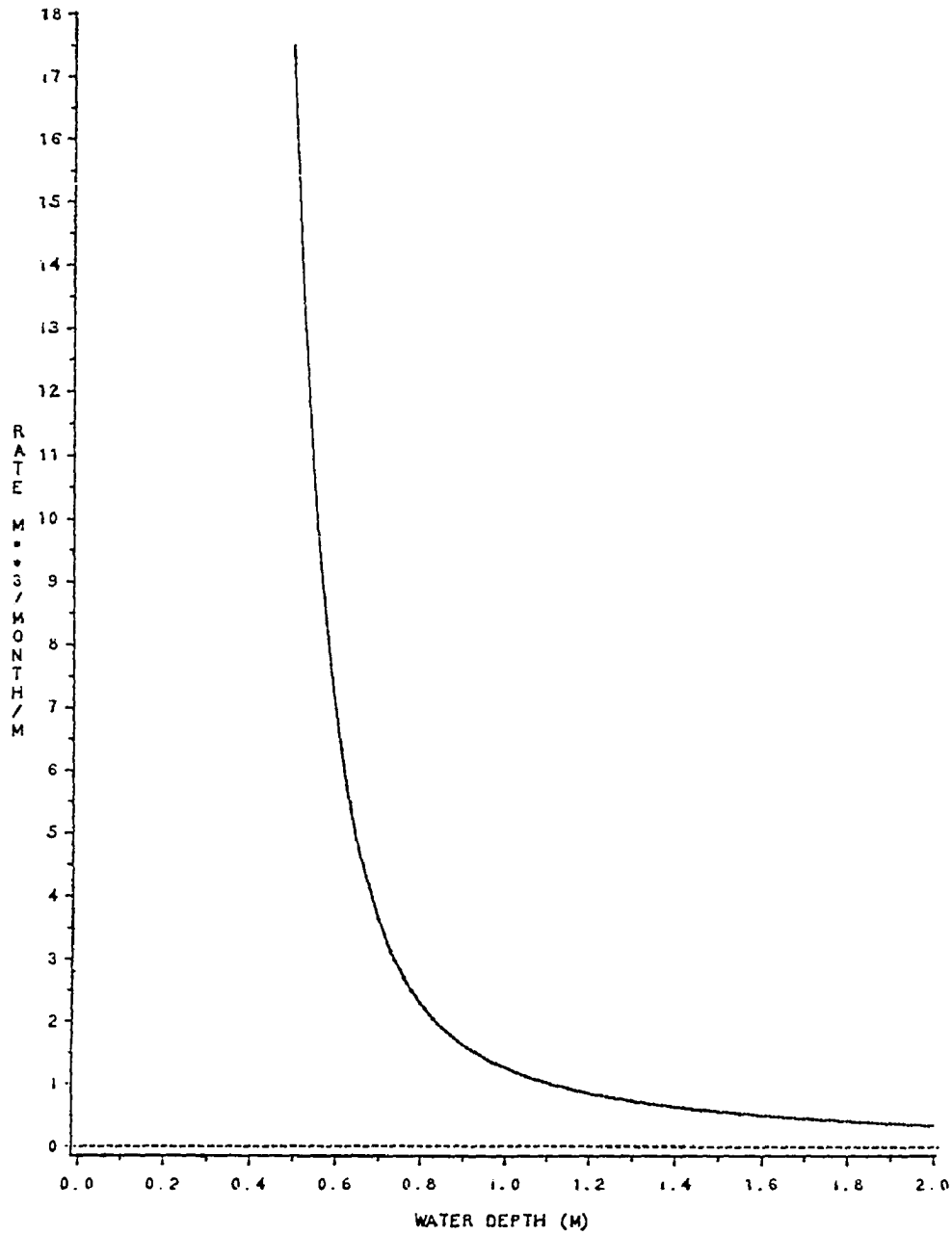
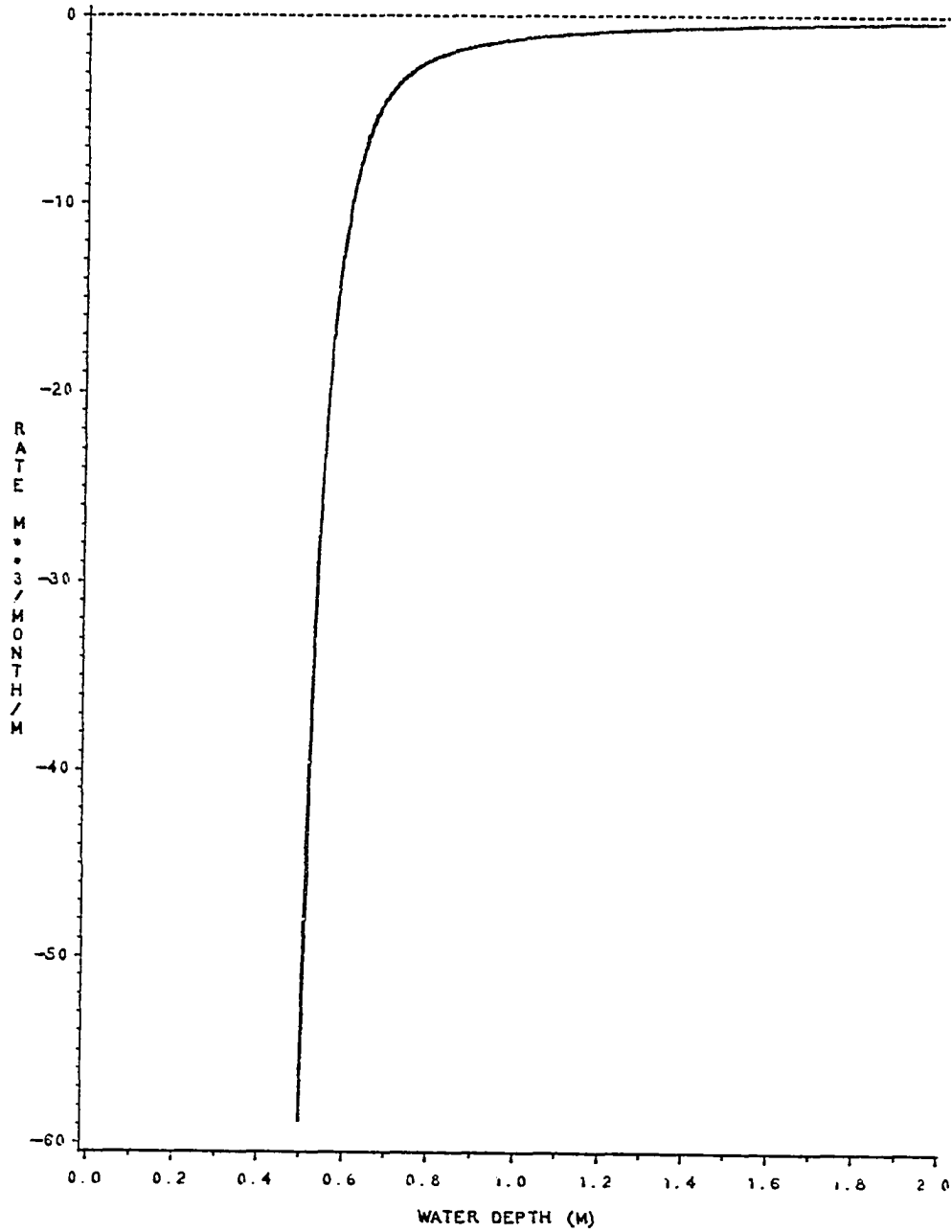


Figure 29. Change of sediment transport rate due to the wave-current interaction
(current direction = 270 degree)

SEDIMENT TRANSPORT RATE WITH DEPTH

(T1 = 3.75 SEC, T2 = 5 SEC, H1 = 10 CM, H2 = 10 CM)
(SLOPE = 0 DEG, CURRENT=25 CM/SEC, 270 DEG, ALPA=10 DEG)



ing along the shoreline finally contributing to the growth of a new spit at the western end of Willoughby Spit; and 2) Belt 2 processes which involve the action of tidal currents that flow shore-parallel and close to the seaward end of the groins. For introduction of sediment from Belt 1 into Belt 2, it was suggested that the offshore movement of sediment occurs by the action of rip currents acting along the groin wall fed by longshore currents along the shoreline and by the asymmetry of the wave orbital motion near the bottom within the shallow region between the Belt 1 area and Belt 2 area. The model was based on long term field measurements before and after the beach fill.

Ludwick (1987) model assumed that the time averaged rate of sediment overwashing in the longshore direction along the shoreline and the rate of loss of sand from the beach to the offshore direction decreased exponentially with the decrease of the volume of the fill-sediment retained within the groin compartment. The rate constants for the longshore overwashing and the offshore loss were determined based on the change of volume of the new spit growing at the western end of Willoughby Spit and the change of sediment volume with time at the study area. (Fig. 10).

In the model offshore loss of sediment included both the loss by rip currents and the loss by wave asymmetry, and the rate of offshore loss was a function of total volume of filled sediment remaining within the groin compartment. Since the rip currents along the wall of the groins are fed by the longshore currents along the shoreline (Lundberg, 1987) and the offshore loss of sediment caused by the asymmetry of wave-induced near bottom currents may result in shoreline retreat together with erosion

of the bottom, it seems to be hard to separate the regions of volume lost attributable to each different mechanism of sediment loss.

In the present study, the sediment loss by rip currents is not examined and the sediment loss by asymmetry of wave-induced near bottom currents was only considered at water depths deeper than 0.5 *m* assuming that the Belt 1 processes and feeder longshore currents to the rip currents were the dominant processes at depths shallower than 0.5 *m*. A bathymetric survey done approximately 1 month after the fill took place shows that the submerged portion of the groin compartment was filled to an average water depth of approximately 0.5 *m* MSL with a slope of less than 1 degree (Fig. 30). It also shows that the fill of the submerged portion reached to a distance of about 50 *m* from the shoreline.

Ludwick (1987) found that waves in the study were refracted as they approached the shoreline. For the dominant waves the angle between shoreline and wave crests were approximately 5 to 10 degrees open to the west. Therefore, in the present investigation for the calculation of sediment transport rate at the study area, it was assumed that the waves were approaching 80 degrees with respect to positive x-direction and that the sediment was comprised of mostly quartz grains of 1.0 *mm* in diameter which was approximately the mean diameter of the fill material.

Further assuming that only the cross-shore component of sediment transport is responsible for the loss or gain of sediment for the submerged area within the compartment and that no sediment is supplied from the shore, Figure 31 shows the change of average depth of the submerged area with time due to the offshore loss of sediment

Figure 30. Post-fill bathymetry approximately 1 month after the fill

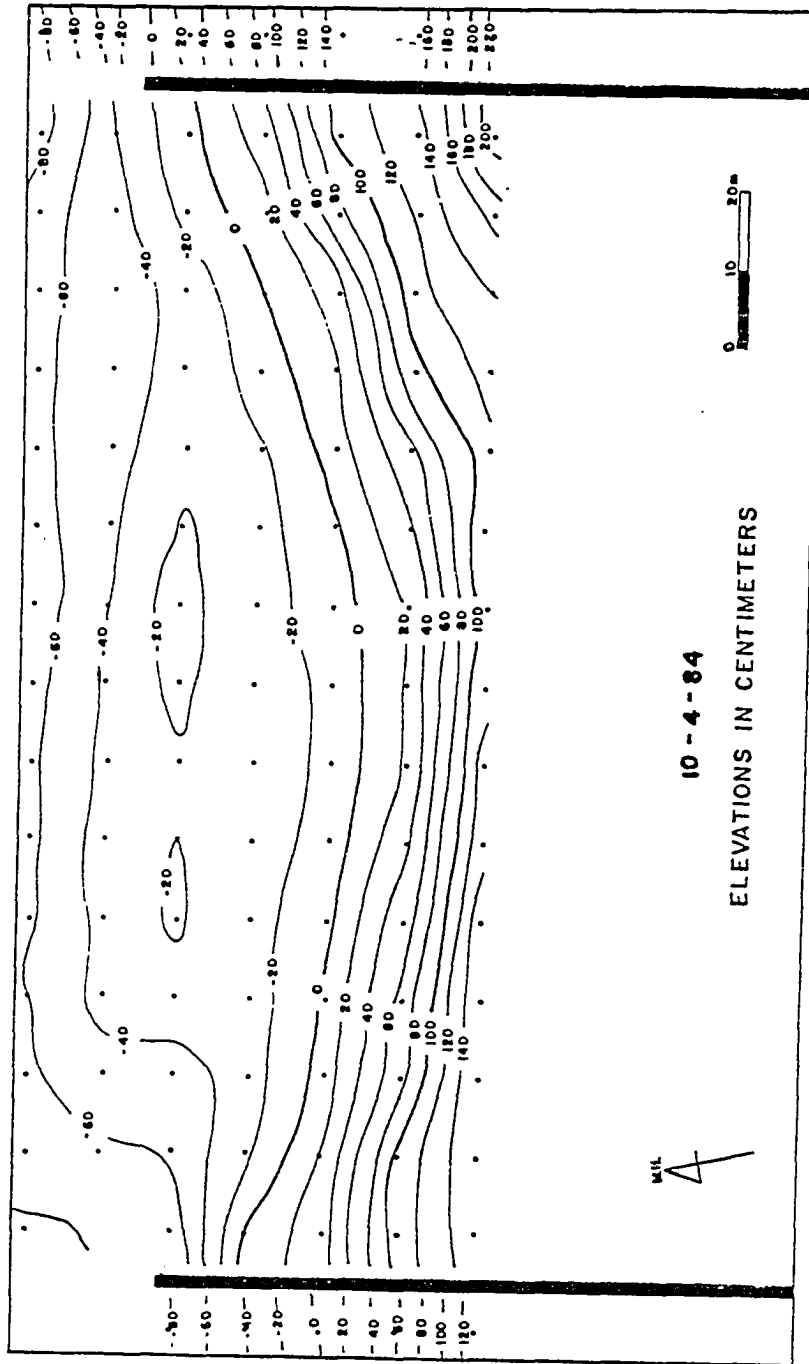
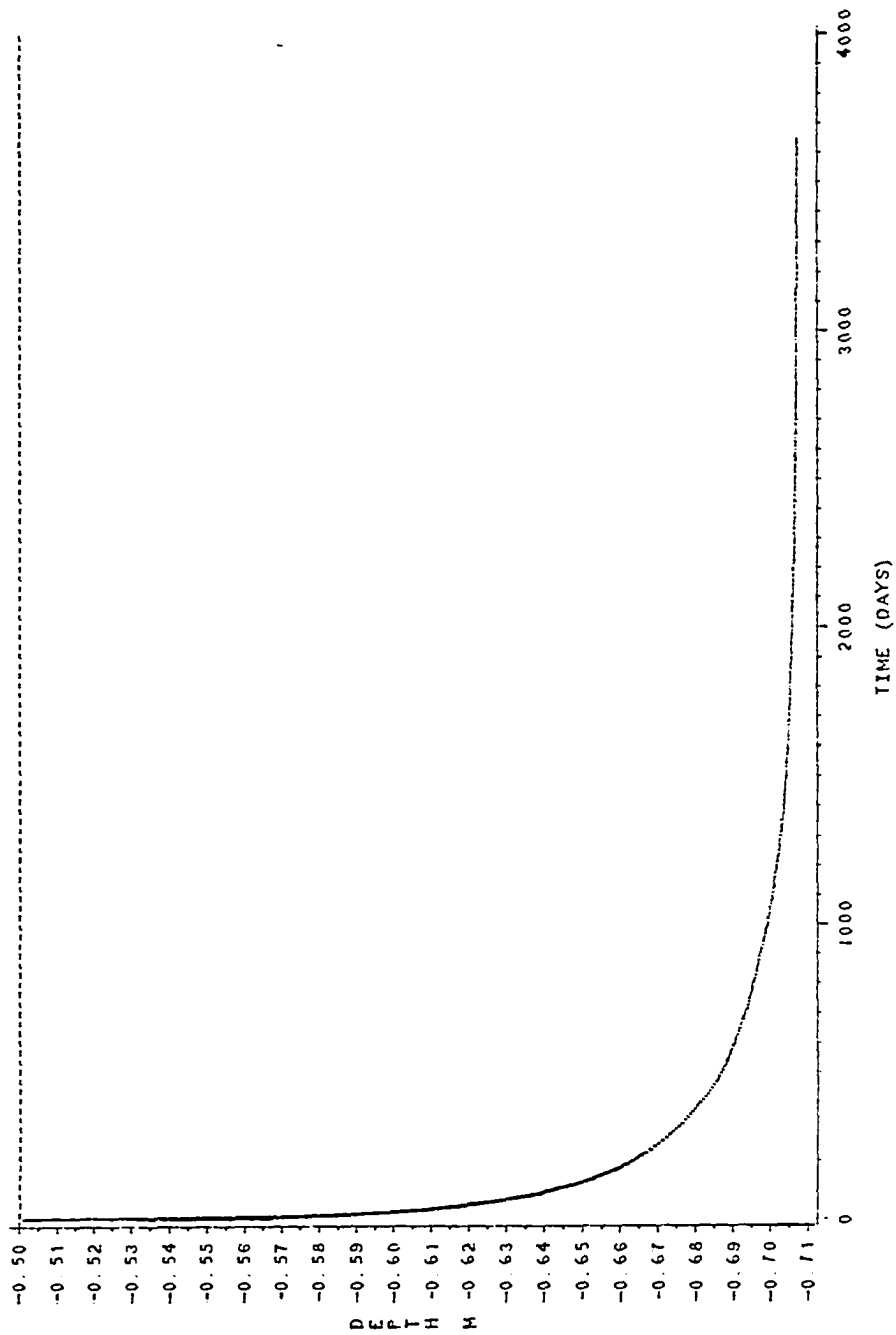


Figure 31. Change of water depth with time after the fill due to the offshore loss of sediment calculated from the characteristic irregular waves

DEPTH CHANGE WITH TIME



from the beach. Figure 31 was constructed such that sediment transport rate at the initial average depth of 0.5 *m* was calculated and the volume change with the calculated rate for 1 day period was used to adjust the depth after the 1 day period. New transport rate was calculated again at the adjusted depth for another 1 day period and the depth was adjusted again and so on. The average depth change for the 1 day period was obtained by dividing the volume change by the distance of the submerged area from the shoreline which was assumed to be approximately 50 *m*. It was also assumed in the calculation that the sediment within the compartment was always redistributed and thus the bed was flat.

It is seen from Figure 31 that the average water depth of the compartment initially assumed to be filled up to the depth of 0.5 *m* increases rapidly for the first 1 to 1.5 years. That is because the direction of sediment transport was offshore since the water depth was shallower than the neutral depth for the wave conditions used in the present study and thus the sediment was considered to be lost from the compartment. The initial rapid change is due to the large amount of sediment transport at shallow depth. As the water depth becomes deeper the rate of sediment transport decreases exponentially with the increasing depth (Fig. 25). Therefore the deepening becomes slower after the initial rapid deepening for the 1 to 1.5 years until the depth change becomes negligible after about 6 to 7 years to reach the neutral depth which is approximately 0.7 *m*.

Since the calculated onshore-offshore rate of sediment transport decreases exponentially with increasing depth, the rate of offshore sediment transport decreases

abruptly as the water depth increases with time. Figure 32 shows the change of sediment transport rate with time according to the change of water depth shown in Figure 31. The transport rate dropped from $0.98 \text{ m}^3/\text{day}/\text{m}$ to about less than $0.01 \text{ m}^3/\text{day}/\text{m}$ within the first year after the assumed fill up to 0.5 m deep. Figures 31 and 32 implies that most significant offshore loss of sediment under the submerged area within the compartment took place during the first 1 to 2 years even though the compartment was continuously losing sediment until it reached the neutral depth at which no net cross-shore transport of sediment occurs.

The rapid deepening of the submerged area for the initial 1 year period was seen in the bathymetric map taken approximately 1 year after the fill (Fig. 33). Figure 33 shows that the submerged area, except for small-scale morphologic features, has almost reached the average depth of the pre-fill bathymetric map surveyed just before the fill (Fig. 34) which is about 0.7 m represented as the -40 cm contour on the map.

As Ludwick (1987) pointed out, in spite of the fact that the fill material through the entire shoreline reach is lost from the system by longshore overwashing and that the rate constant of offshore transport is much smaller than the rate constant of longshore transport (approximately 1 to 11), the offshore loss would be significant initially at a mid-reach compartment of the groin system because the local gradient of groin-top overwashing is small shortly after the fill. Therefore the rapid recession followed by stabilization of the shoreline during the initial 2 months after the fill (Fig. 9) also seems to be attributable to the rapid decrease in the rate of offshore loss. Since then the shoreline became almost stable because the offshore loss of sediment was not

Figure 32. Change of sediment transport rate with time calculated from the characteristic irregular waves

SEDIMENT TRANSPORT RATE WITH TIME

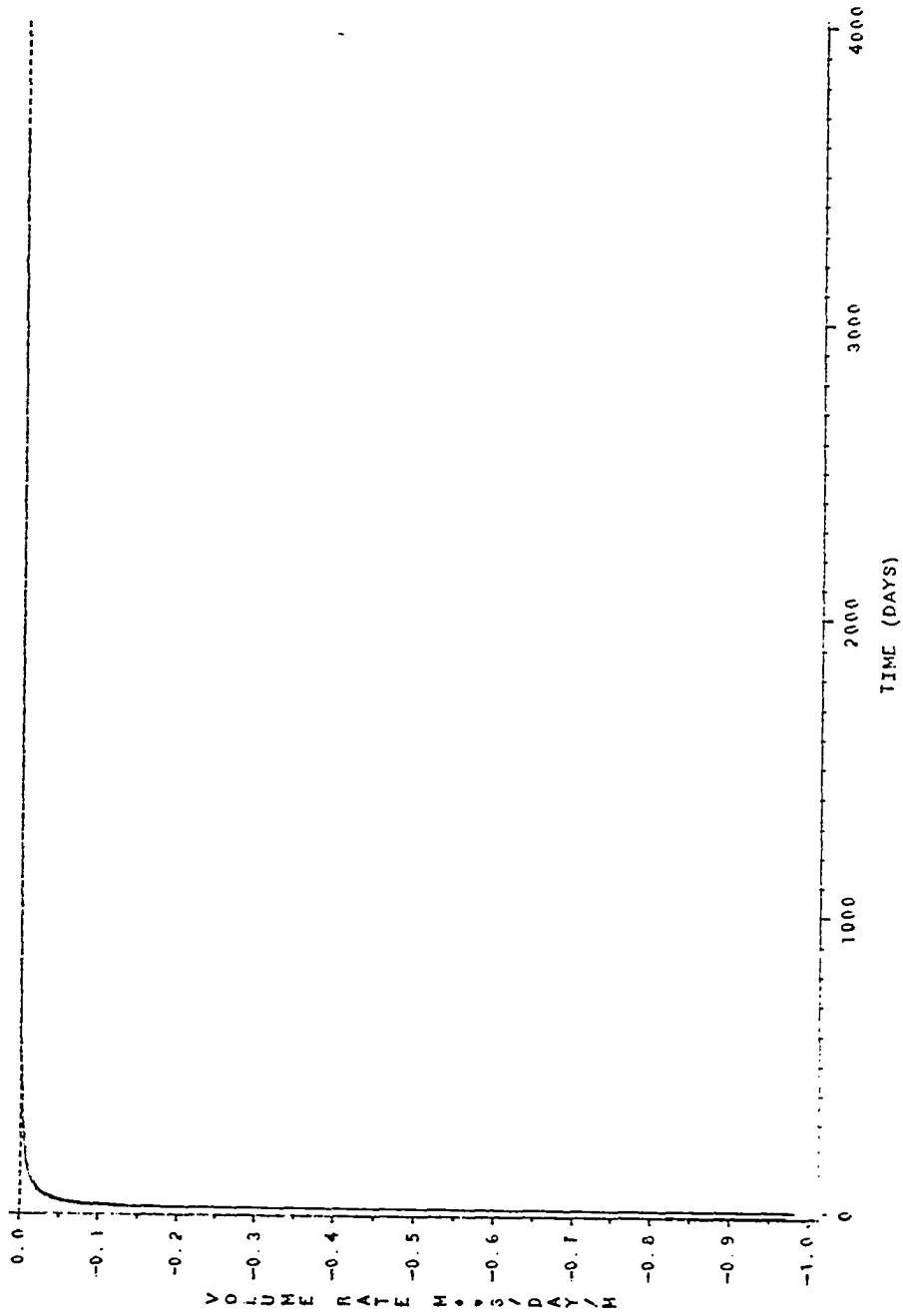
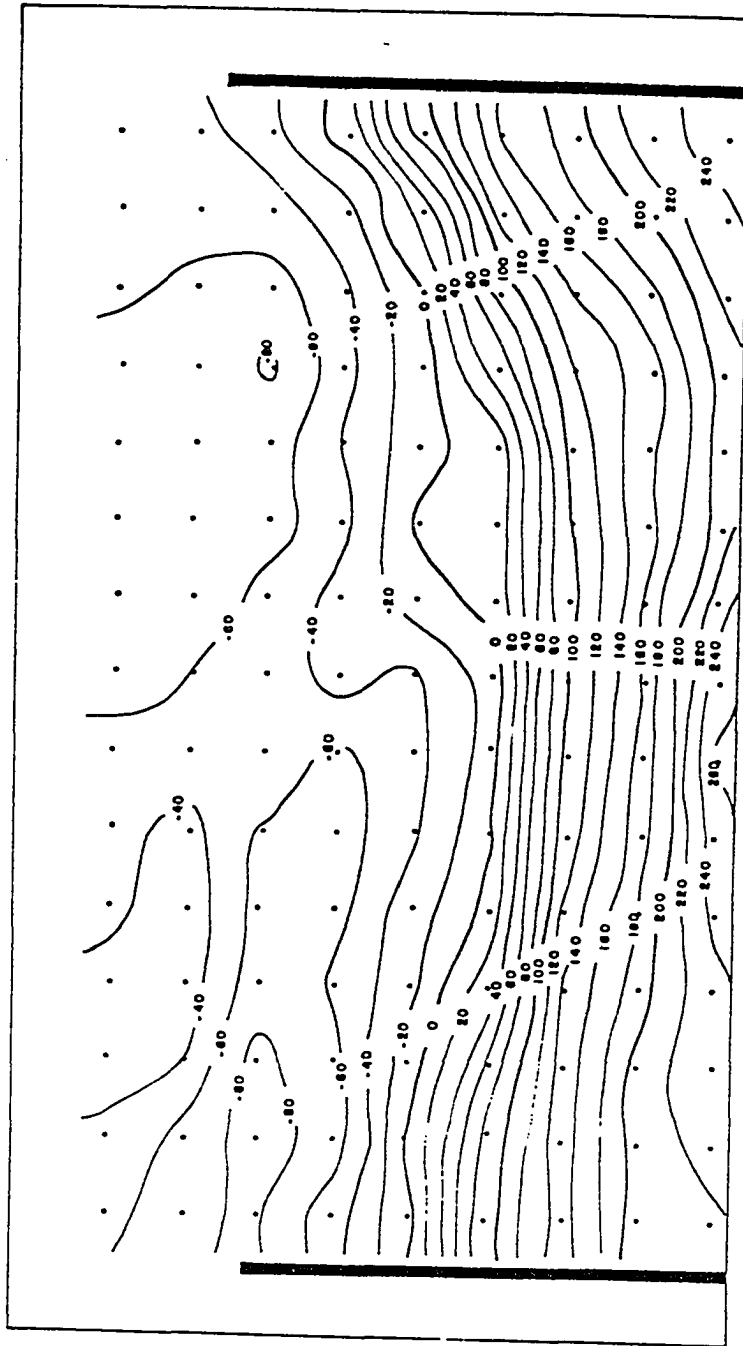


Figure 33. Post-fill bathymetry approximately 1 year after the fill

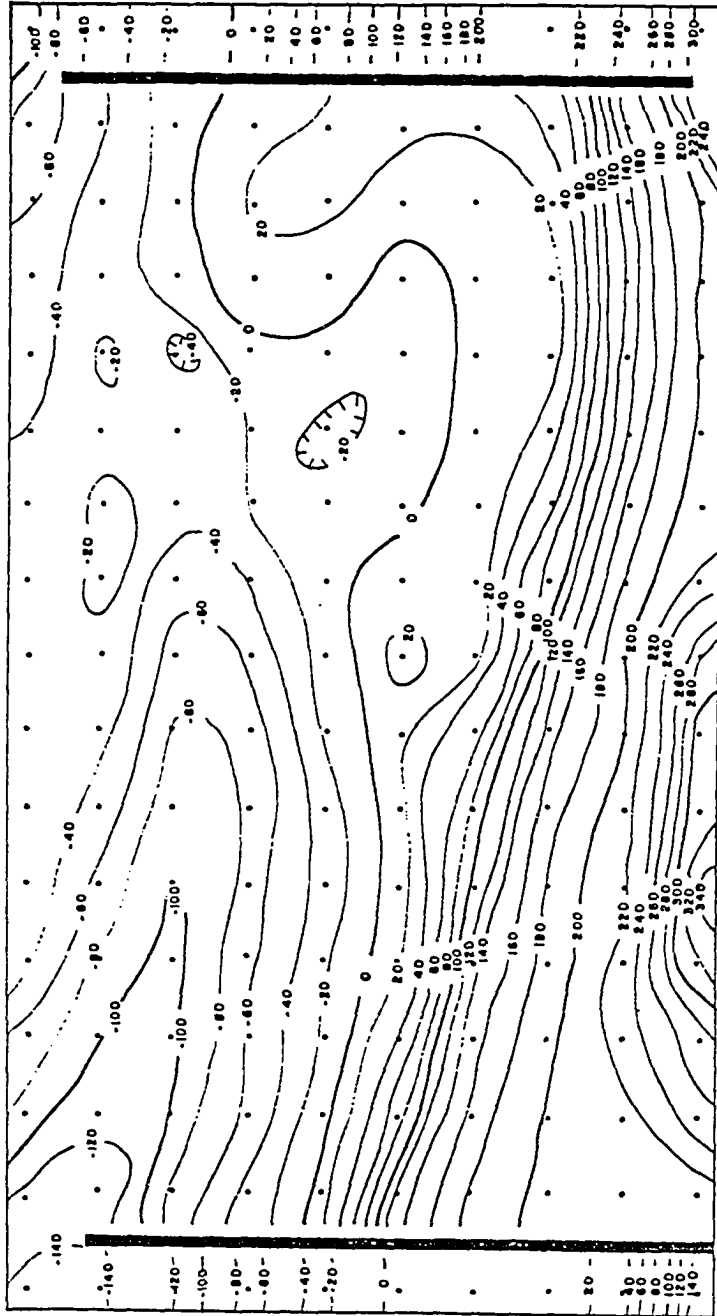


9 - 27 - 85

ELEVATIONS IN CENTIMETERS



Figure 34. Pre-fill bathymetry approximately 1 month before the fill



7 - 6 - 84

ELEVATIONS IN CENTIMETERS



sufficient to cause a significant shoreline change. It will also be seen in the next section that most of the offshore loss takes place a little farther offshore from the shoreline after the 1 to 2 months.

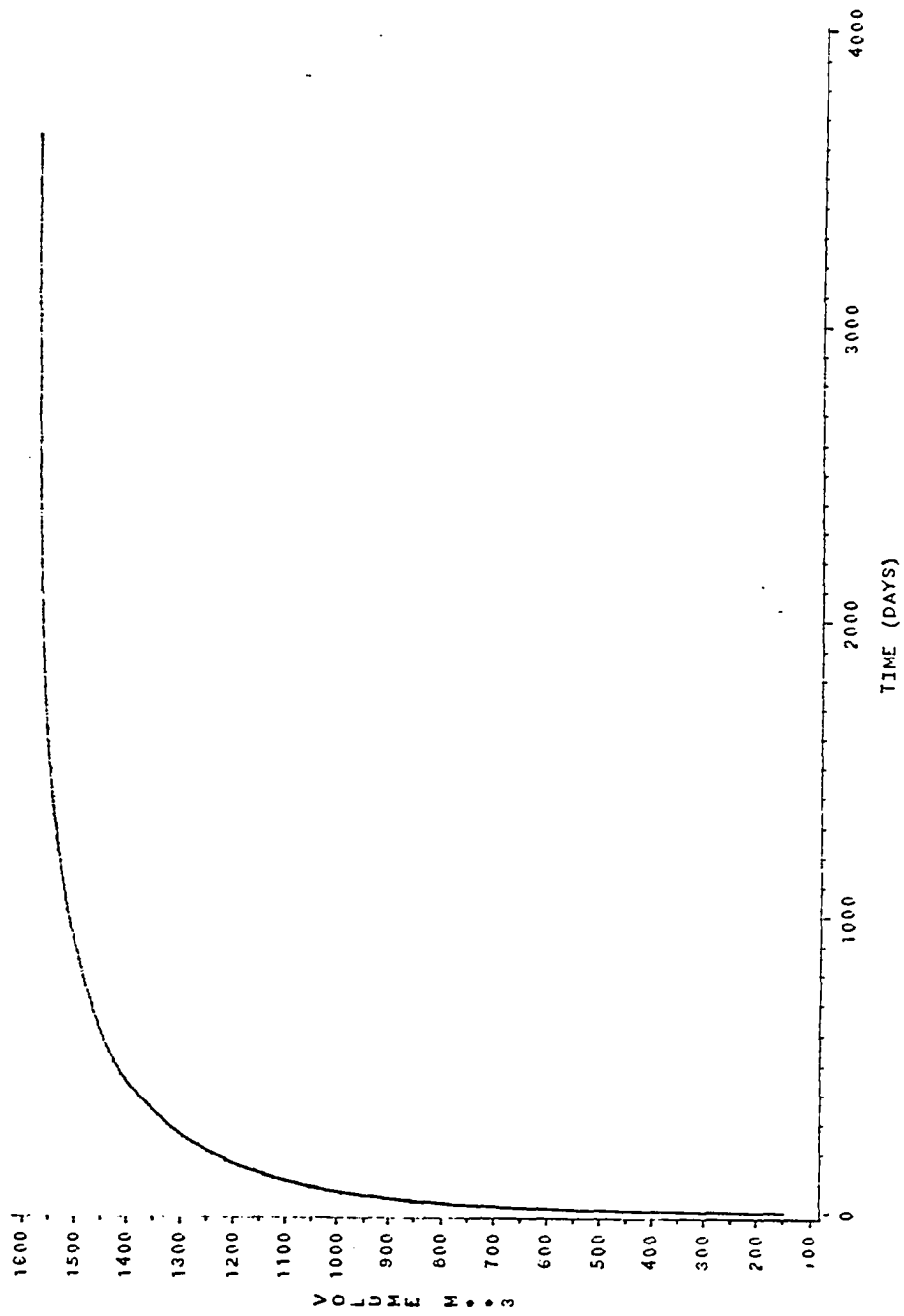
Figure 35 shows the cumulative volume of sediment lost offshore calculated from the increase of the average water depth shown in Figure 31 across the 152 m width of the compartment. It is seen that the volume of sediment lost offshore increases rapidly for 2 to 3 years and that the compartment does not lose any significant amount of sediment due to the asymmetry of the waves in the submerged area after 6 to 7 years.

When Figure 35 is compared to the measured volume of sediment loss within the groin compartment (Fig. 10), about 35 percent of the loss for the 1 year period after the fill, which is approximately 3,800 m³ (fill and native material), can be attributed to offshore loss and the sediment is thus entrained into Belt 2 by the asymmetry of the waves. However, as time elapses and the submerged area reaches equilibrium, the affect of offshore loss to the total loss would diminish. Only about 5 percent of the total measured loss of about 1,900 m³ could be attributed to offshore loss due to wave asymmetry for the 10 month period following the initial 1 year period.

Ludwick (1987) estimated that the effective life of the fill, defined as the time when 15 percent of the original fill volume remains in the system, was approximately 8.8 years. It is suggested here that the submerged area will lose most of its fill material and thus reach an equilibrium approximately 2 to 3 years before the entire beach loses most of its fill material, providing sediment is not supplied from the backshore to the submerged area.

Figure 35. Cummulative volume loss from the compartment after the fill
calculated from the characterisitic irregular waves

TOTAL VOLUME LOST OFFSHORE BETWEEN GROINS



However, in nature, the sediment in the backshore would be transferred to the submerged area even though the amount seems to be minimal after the initial rapid recession of the shoreline. The sediment carried by the rip currents along the groin walls would also be redistributed in part into the submerged area within the compartment. Therefore the actual time for the submerged area to reach equilibrium would be longer than the time calculated above.

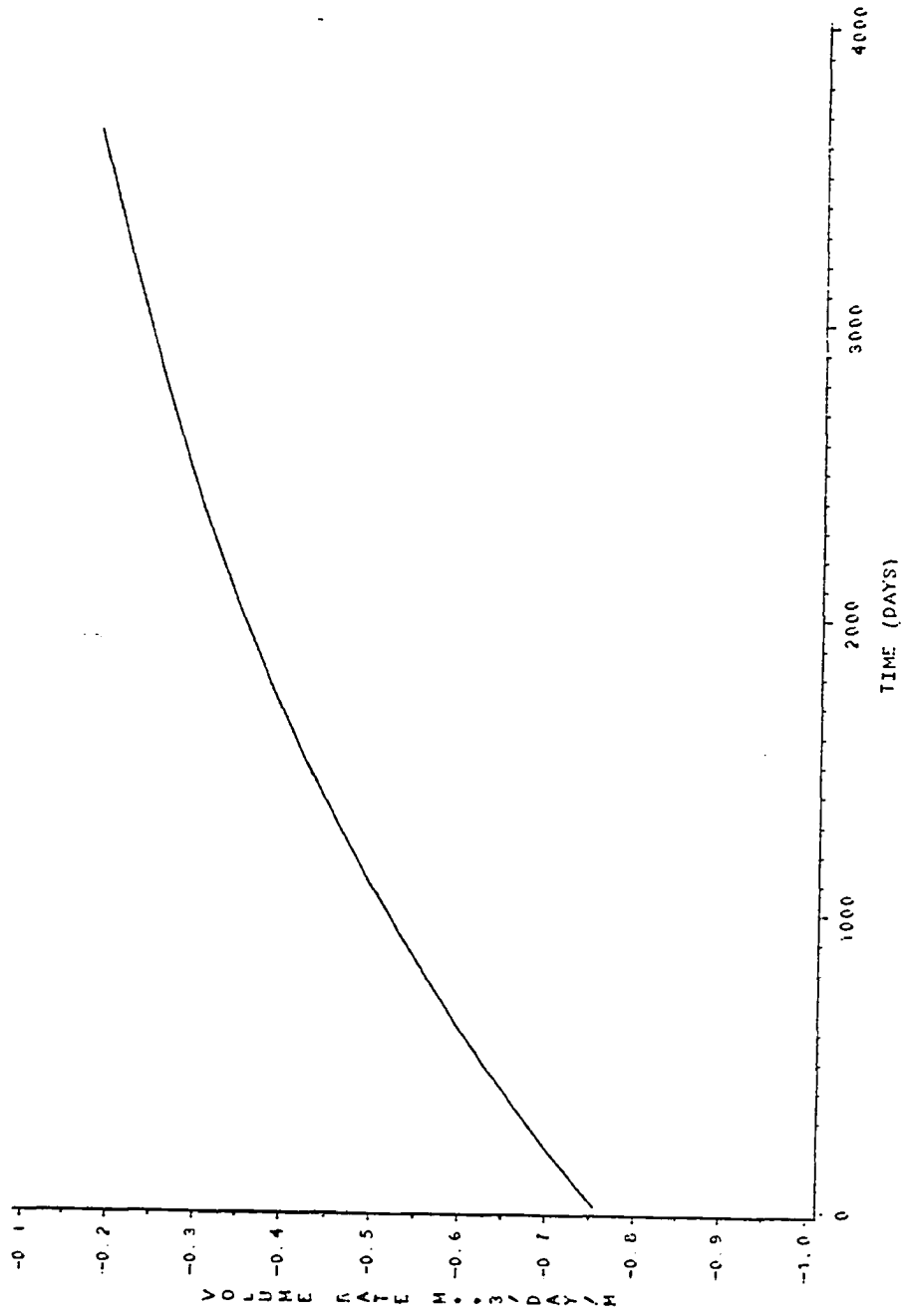
When the rate of offshore loss is calculated using the model of Ludwick (1987), which accounts for both of the losses by the rip currents and by the wave asymmetry, it is shown that a considerable amount of sediment is lost offshore even after 6 to 7 years (Fig. 36). It can also be deduced from Figures 35 and 36 that most of the offshore losses after 1 to 2 years are caused by the rip currents if Figure 35 is a reasonable estimation of offshore loss of sediment by wave asymmetry despite the assumptions made in the calculation.

- Evolution of bathymetry after the fill

Assuming that the bathymetry before the fill was in a quasi-steady state, the most prominent pre-fill morphologic feature at the study area was the existence of a bar and trough system extending from the end of the western groin eastward to the middle of the groin compartment. Direction of the axis of the trough was approximately 280 degrees CTN (Clockwise from True North). Another feature contrasting to the bar and trough system was the development of shallow area near the end of the eastern groin (Figs. 4 and 34).

Figure 36. Total offshore loss of sediment calculated by the model of Ludwick (1987)

RATE OF OFFSHORE SEDIMENT LOSS WITH TIME
(TOTAL VOLUME MODEL, LUDWICK, 1967)



At the study area, strong tidal currents flow almost parallel to the shoreline at the end of the groins. When a strong current flows at the open end of a compartmentalized basin, a gyre-type circulation is expected within the compartment (Askren, 1979; Gatski et. al., 1982). Ludwick (1987) found some evidence of a counter-flowing current by analysing near-bottom current measurements in the study area. The result of drogue tracking at the study area also shows the possibility of weak counter-flowing currents within the compartment (Figs 14 and 15). Therefore a precise understanding of the development of morphologic features is only possible when the flow pattern within the compartment is known in great detail.

However, even though an elaborate study of the circulation pattern between the groins was not conducted in the present investigation, the gross morphologic features can be understood by examining the change of neutral depth due to the interaction of waves and currents in the area. It was seen in the previous section that the direction and amount of sediment transport and the magnitude of the neutral depth were greatly affected by the interaction of steady currents and waves. Since the groin compartment at the study area was filled to a depth shallower than the neutral depth, it is implied by the results of the present study that the compartment will lose sediment in a seawards direction until the water depth reaches the neutral depth corresponding to local flow conditions.

With the same assumptions for waves and sediment that were made in the previous calculations, the resulting change in neutral depth with change in the angle of the steady current with respect to positive x-direction (westward at the study area) is

shown in Figure 37. The speed of the steady current was chosen to be 25 *cm/sec* which is approximately the average speed of the tidal current during the flood. The wave-current friction factor f_{cw} was calculated by the same method described in the previous section.

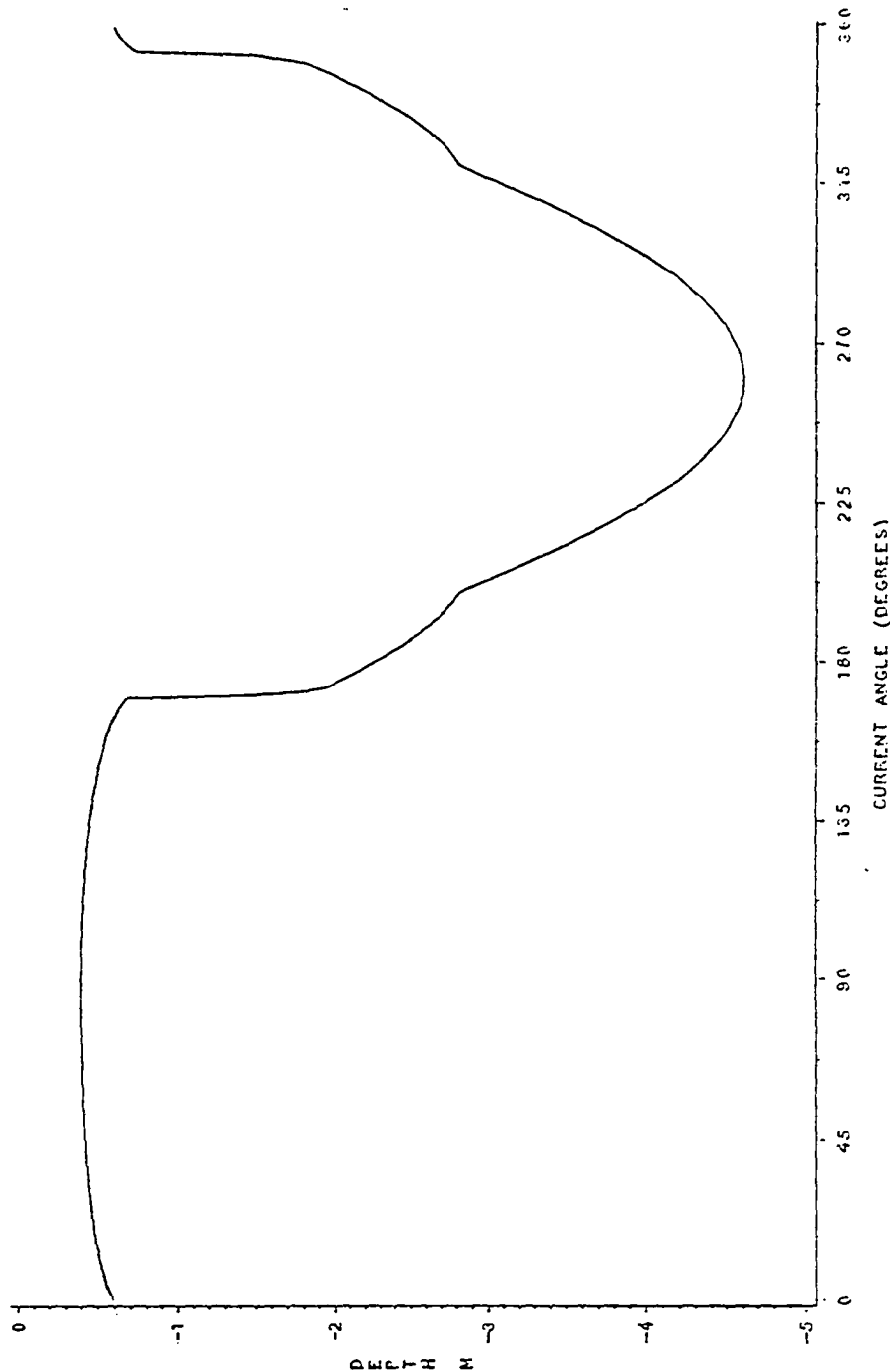
In Figure 37, when the angle is less than 170 degrees, it is seen that the neutral depth is shallower than the neutral depth due to waves alone which was approximately 0.7 *m* and that the neutral depth does not change very much with change in the angle. When the angle is greater than 170 degrees, the neutral depth increases abruptly due to the enhanced offshore component of sediment transport that occurs due to the superposition of the steady current. As the angle becomes greater than 260 degrees the neutral depth decreases.

It is expected from Figure 37 that, on a submerged beach which is in a state of equilibrium, at any place where the current is interacting at an angle of less than 170 degrees the water depth will be shallower than the water depth where the current is not interacting. Where the current is interacting at an angle greater than 170 degrees the water depth would be much deeper than the water depth of places where the current is interacting at an angle of less than 170 degrees or only the waves are acting.

At the study site, the tidal currents are flood dominant in duration and strength. The measured current strengths for average flood and ebb flows near the bottom were 27 *cm/sec* and 18 *cm/sec* respectively when corrected to mean range. The durations of flood and ebb were 7 and 5.4 hours, respectively (Ludwick, 1987). Therefore, in the vicinity of the compartment, bottom topography is most likely to be affected by the

Figure 37. Change of neutral depth due to the wave-current interaction
(Current speed = 25 *cm/sec*)

CHANGE OF NEUTRAL DEPTH BY WAVE CURRENT INTERACTION
($T_1=3.15$ SEC. $T_2=5$ SEC. $H_1=10$ CM. $H_2=10$ CM. $\text{ALPHA}=10$ DEG. $\text{CURR}=25$ CM/S)



flood current.

Drogue tracking experiments done at the water surface and 50 *cm* below the surface before the fill show that flood current flowing westward bends towards shore at the end of the eastern groin. Flood currents which penetrate into the groin compartment then bend offshore approximately at the halfway point between the two groins (Fig. 14). On the other hand the main ebb current does not seem to penetrate into the groin compartment (Fig. 15).

Assuming that the gradient of sediment transport rate in the longshore direction ($\partial q_s/\partial x$) is negligible. The change of local elevation with time ($\partial\eta/\partial t$) can be calculated by the gradient of sediment transport rate in the onshore-offshore direction ($\partial q_s/\partial y$) as

$$\frac{\partial q_s}{\partial y} = \frac{\partial\eta}{\partial t} \quad (52)$$

Since the direction of sediment transport after the fill is always offshore at the study site, the first order approximation of equation (52) can be obtained numerically by

$$\frac{(q_s)_j^n - (q_s)_{j-1}^n}{\Delta y} \approx \frac{\eta_j^{n+1} - \eta_j^n}{\Delta t} \quad (53)$$

where j, n : indices for space and time respectively

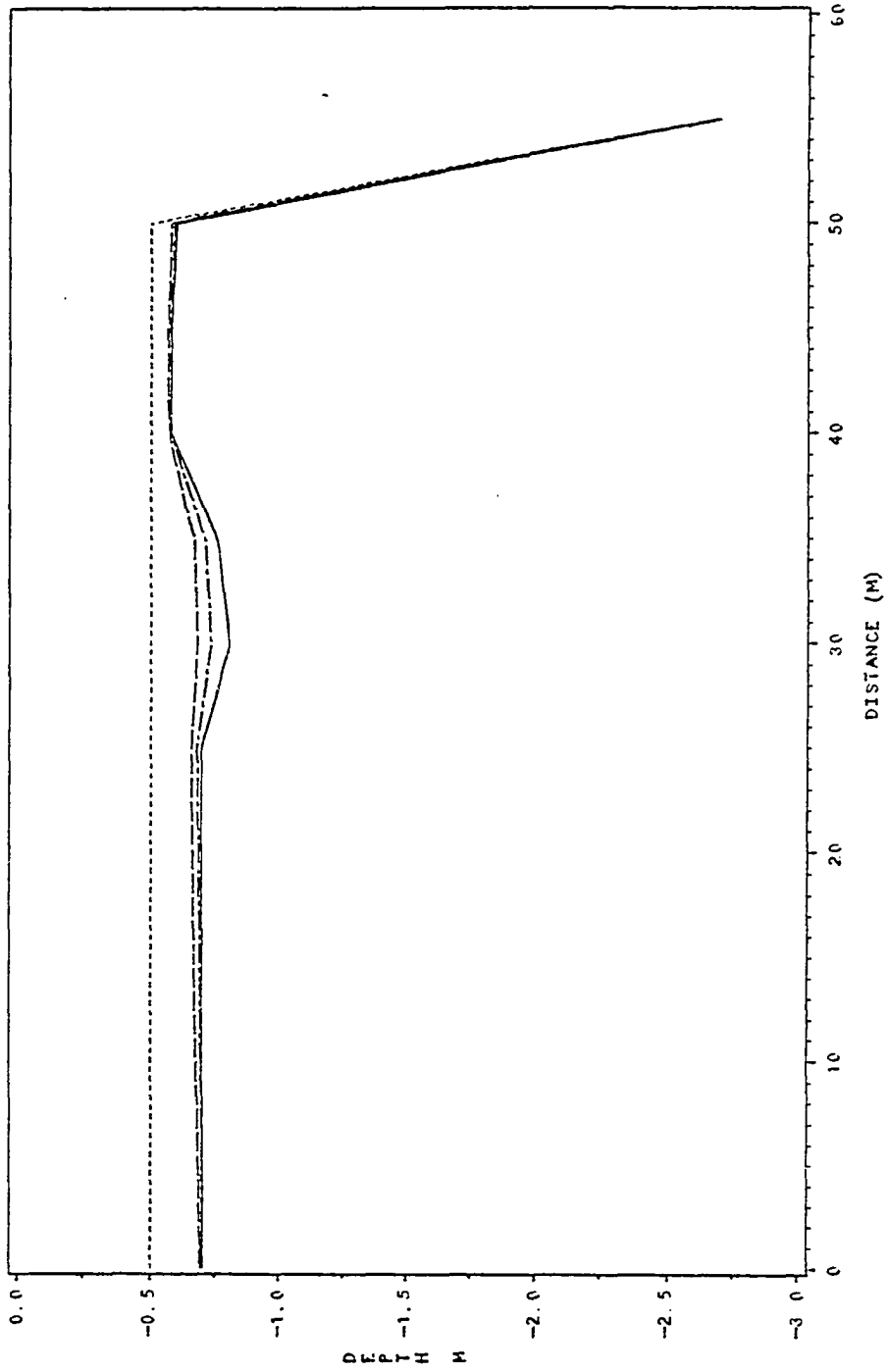
Δy : distance between j and $j-1$

Δt : duration between n and $n+1$

Figure 38 shows the change of bottom profile calculated by equation (53) for a 1-year period after the bottom was filled up to the water depth of 0.5 *m*. The assumptions made in the calculation are: 1) the area from the shoreline to 30 *m* offshore is only affected by waves; 2) between 30 *m* and 35 *m* a steady current of 25 *cm/sec*

Figure 38. Numerical calculation of the evolution of bottom profile for 1 year after the fill (west)

PROFILE CHANGE FOR 1 YEAR (WEST)
(.....: 0 MO - - - - : 3 MO - : 6 MO - - - - : 1 YR)



interacts with the waves at an angle of 350 degrees with respect to positive x-axis; 3) beyond 35 *m* from the shoreline the angle of the steady current is 0 degrees; 4) no sediment is supplied from the beach area landwards of the shoreline; 5) Belt 2 processes continuously carry-off the sediment entrained and thus the water depth is kept constant beyond 55 *m* from the shoreline. The calculation was performed using the time interval (Δt) of 0.1 *day* and the space interval (Δy) of 5 *m*.

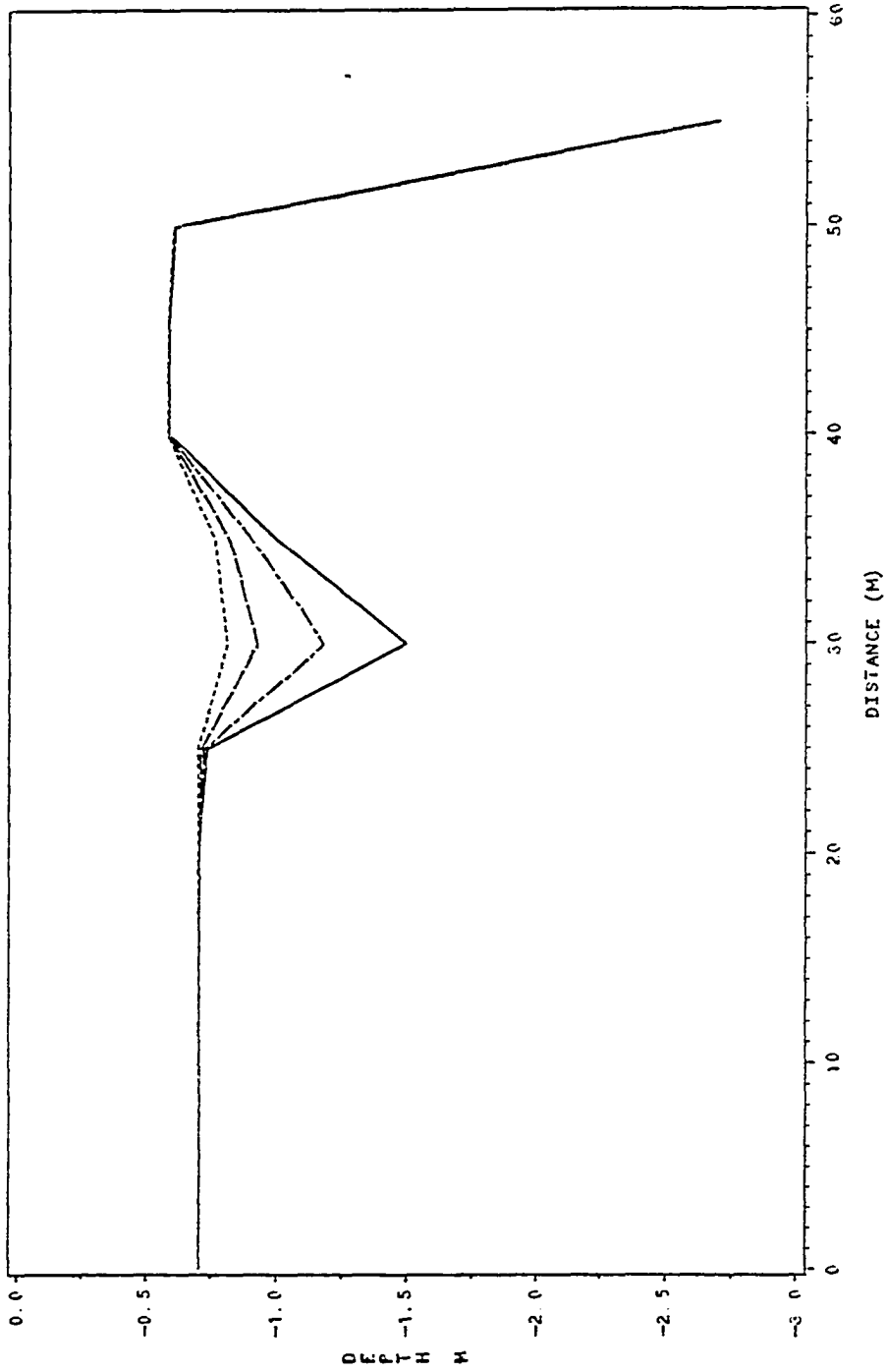
While equation (53) is only a first order approximation, it is seen in Figure 38 that a trough and bar system begins to develop after 3 months. It is also seen that most of the significant erosion occurred during the first 3 months near the shoreline which might account for the initial rapid retreat of the shoreline after the fill at the study area. The figure also shows that deepening of the water depth generally takes place in the offshore region away from the shoreline especially where the trough is developing after the initial rapid erosion of the bottom. Therefore, the shoreline would stay stable after an initial rapid retreat until the longshore gradient of sediment transport by Belt 1 processes becomes significant at the study area.

After the initial 1-year period, the overall area does not show a significant change in water depth except for the trough region (Fig. 39). Figure 39 shows that the trough develops continuously until it reaches the neutral depth of about 1.75 *m* for the case of the current interacting at an angle of 350 degrees (Fig. 37).

Assuming that the numerical calculation shown above approximates the wave and current conditions of a cross-shore beach profile in the western half of the groin compartment, the development of the trough and bar system is consistent with the calcula-

Figure 39. Numerical calculation of the evolution of bottom profile for 10 years after the fill (west)

PROFILE CHANGE FOR 10 YEARS (WEST)
(.....: 1 YR - - - - : 2 YR - : 5 YR - - - - : 10 YR)



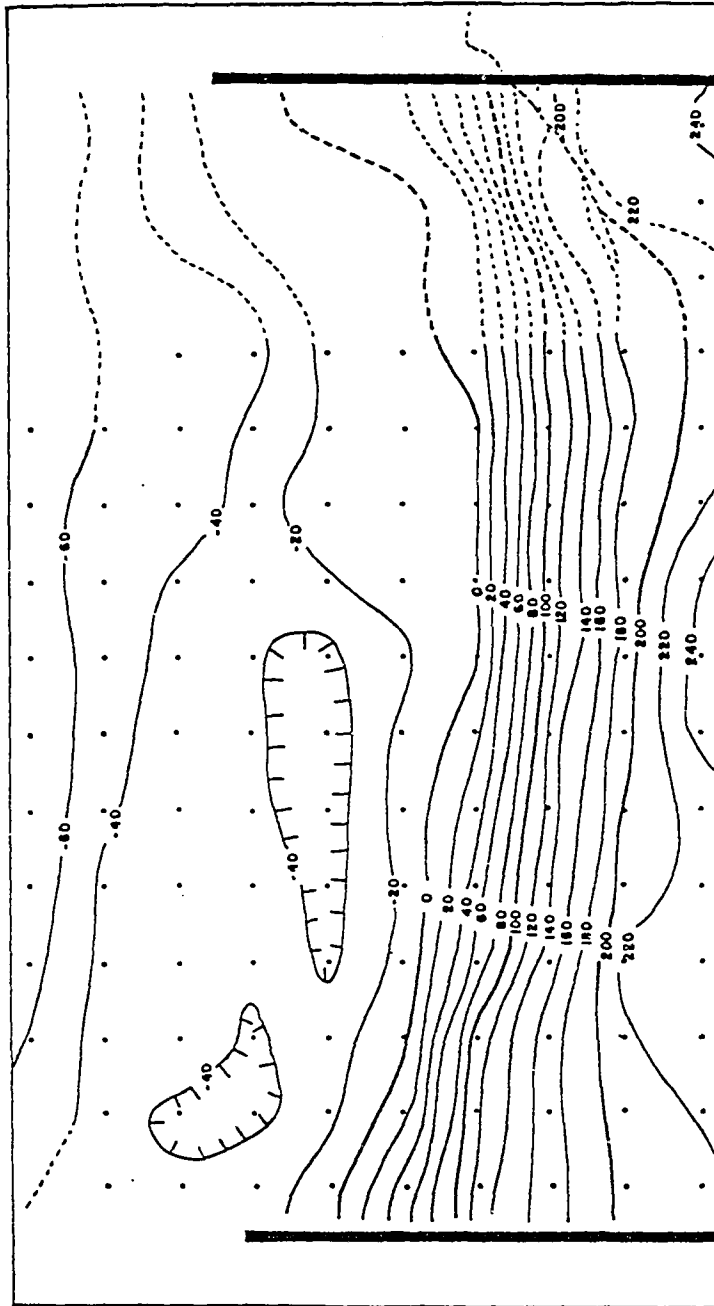
tion shown in Figure 38. A bathymetric survey done approximately 3 months after the fill shows that a trough and bar system, the axis of which approximately follows the direction of the deflected flood current, has already begun to develop (Fig. 40).

On the other hand, in the eastern half of the compartment, the flow direction of the flood current before the fill changed at the end of the eastern groin so as to make the current angle approximately 10 degrees penetrating into the compartment. With the same assumptions as those made for the above numerical calculation, except that the current angle was taken to be 10 degrees in the area between 30 *m* and 35 *m*, Figure 41 shows the development of a shallow area, which was the one of the prominent features of the pre-fill bathymetry, where the current was assumed to be flowing at an angle of 10 degrees. It is also seen that the water depth does not show a significant change after the initial rapid change for the 1 year period (Fig. 42).

In the eastern half of the compartment, the bathymetric surveys done after the fill show no evidence of development of the trough and bar system. However, the shallow area near the end of the eastern groin, which was shown in the pre-fill bathymetric surveys and in the numerical calculation, also was not developing for the time being. Instead, the bathymetric survey done approximately 1 year after the fill shows that a deep area was developing near the seaward end of the eastern half region (Fig. 33). The fact that the shallow area has not developed yet suggests that the flow conditions, possibly the direction of the steady current, in the eastern half region may have been altered from the pre-fill conditions due to the fill.

The gyre-type circulation within the compartment may also affect topographic

Figure 40. Post-fill bathymetry approximately 3 months after the fill



1 - 2 - 85

ELEVATIONS IN CENTIMETERS



Figure 41. Numerical calculation of the evolution of bottom profile for 1 year after the fill (east)

PROFILE CHANGE FOR 1 YEAR (EAST)
(.....: 0 MO - - - - : 3 MO - : 6 MO - - - - : 1 YR)

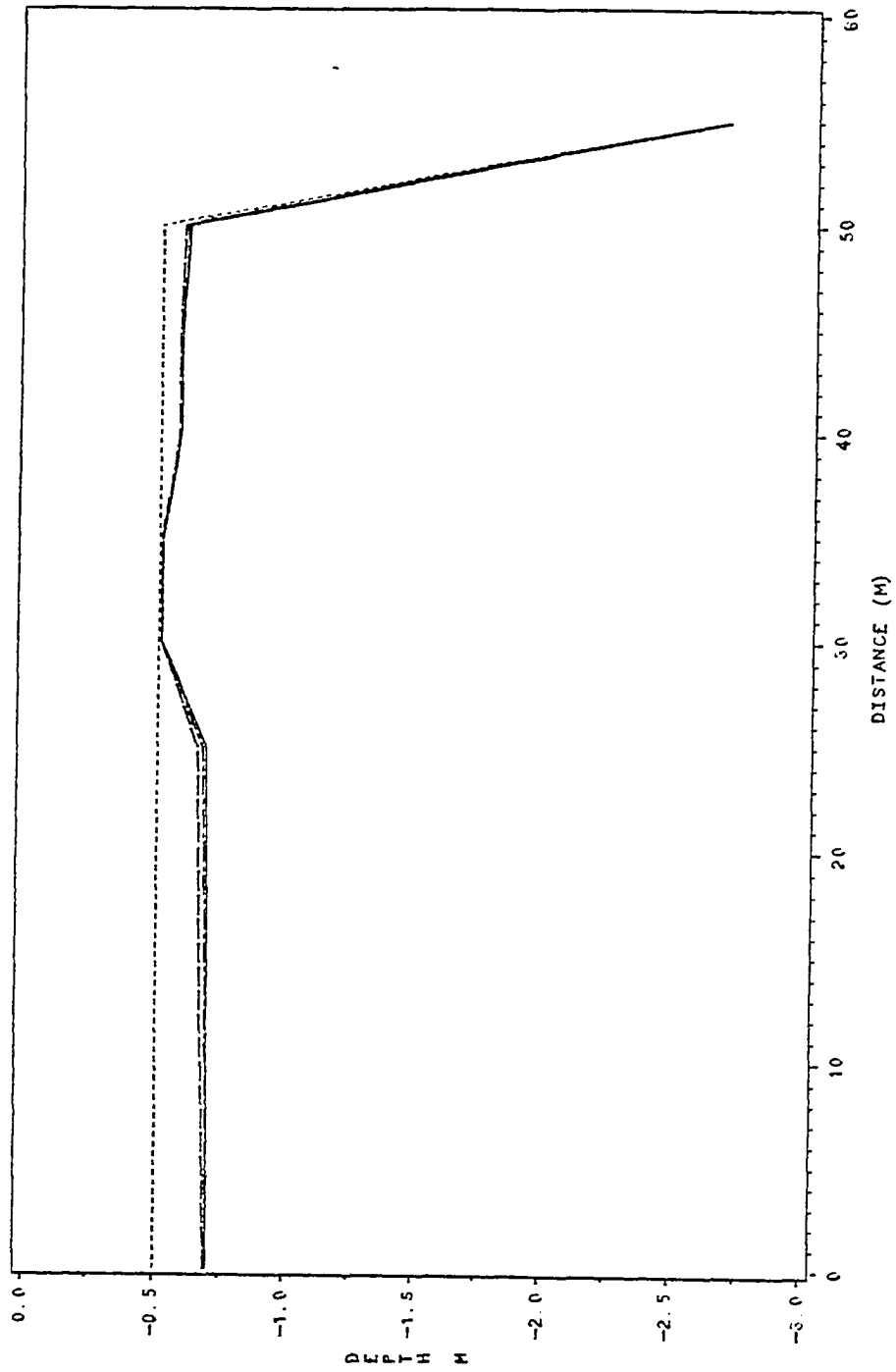
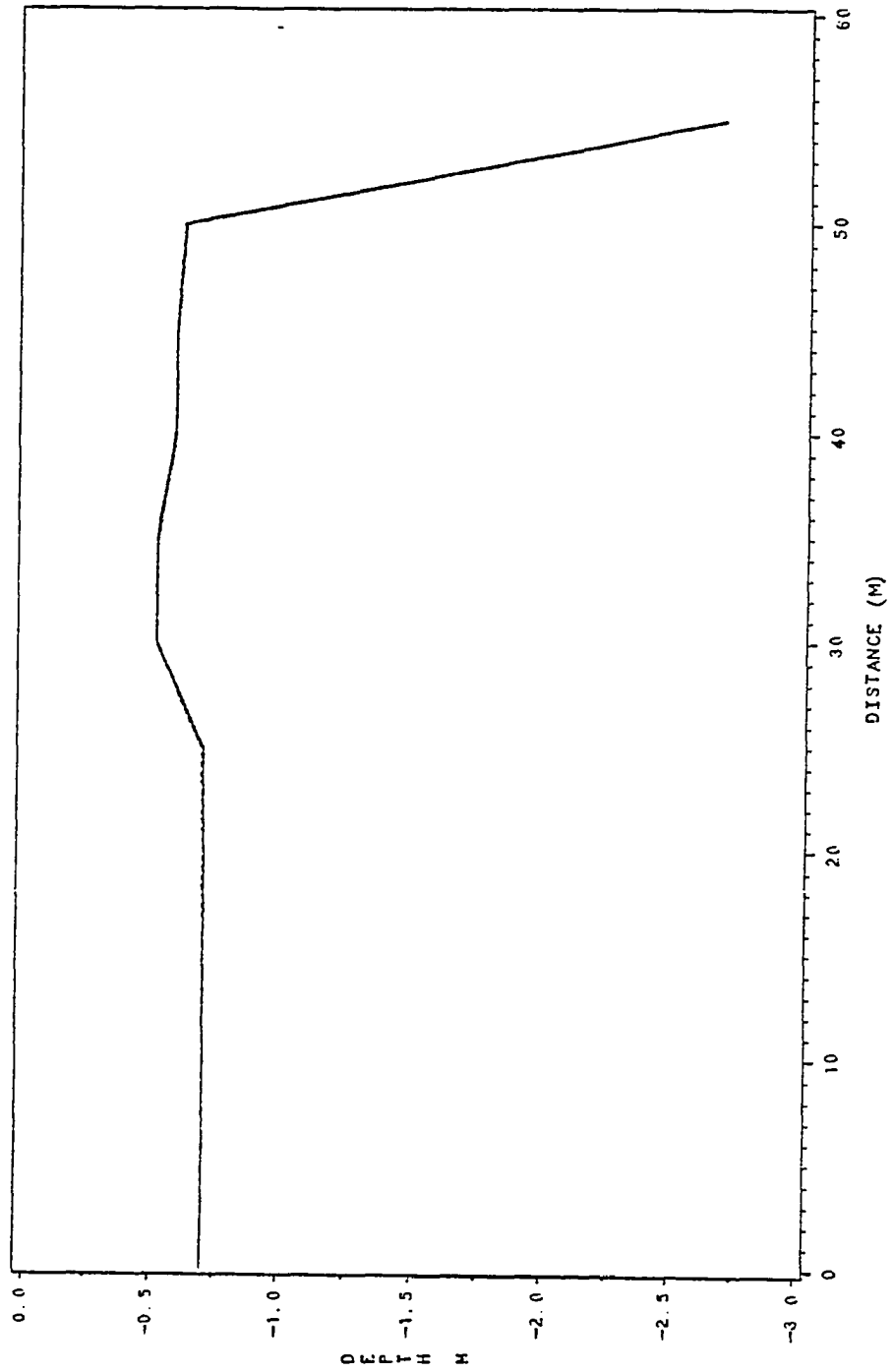


Figure 42. Numerical calculation of the evolution of bottom profile for 10 years after the fill (east)

PROFILE CHANGE FOR 10 YEARS (EAST)
(.....: 1 YR - - - - : 2 YR - : 5 YR - - - - : 10 YR)

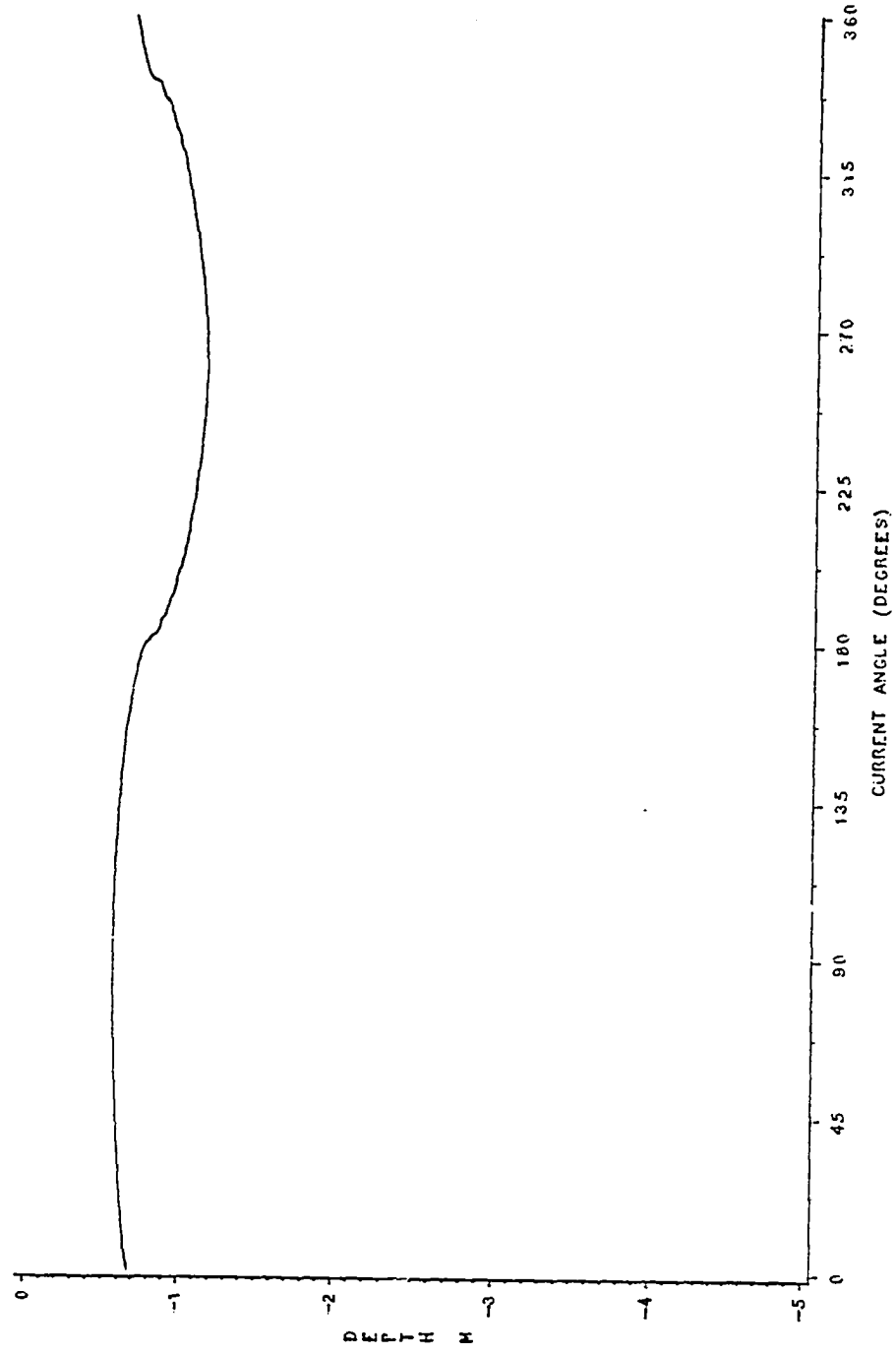


change between the two groins. However, the strength of the gyre currents are almost certainly much smaller than the strength of the tidal currents flowing near the end of the groins. Figure 43 shows the change of neutral depth when a steady current of 5 *cm/sec* was interacting with the same waves used in previous calculations. It is seen that the neutral depth does not show a significant change compared to the case of strong steady current (Fig. 37). Therefore a pronounced changes in bathymetry due to the gyre-type circulation within the compartment are not expected. However, if rip currents of the same order of magnitude are flowing mostly along the western groin wall, which makes the current angle approximately 270 degrees, these currents may partly explain the fact that the western part of the compartment was generally deeper than the eastern part before the fill (Figs. 4 and 34).

Figure 43. Change of neutral depth due to the wave-current interaction
(current speed = 5 *cm/sec*)

CHANGE OF NEUTRAL DEPTH BY WAVE CURRENT INTERACTION

($T_1=3.75$ SEC. $T_2=5$ SEC. $H_1=10$ CM. $H_2=10$ CM. $\text{ALPHA}=10$ DEG. $\text{CURR}=5$ CM/S)



SUMMARY AND CONCLUSIONS

Cross-shore sediment transport by waves and currents determines the gain or loss of sediment to a beach in those areas where the local gradient of sediment transport in the longshore direction is negligible. The sediment transport rate on a submerged sloping bed can be effectively calculated by evaluating the apparent shear stress which includes the drag force and the tangential component of gravity force acting on the sediment. By using the apparent shear stress the threshold shear stress required to initiate the motion of the sediment as bedload on a sloping bed can be calculated using Shields' criterion established for a horizontal bed.

A net cross-shore transport of sediment may result from the asymmetry in wave-induced near-bottom velocities. The asymmetries studied in the present work include the magnitude asymmetry, the ratio of the onshore peak velocities to the offshore peak velocities, and the duration asymmetry. This latter is the ratio of the duration of onshore velocities to the duration of offshore velocities. All these asymmetries are greatly enhanced by the nonlinear interaction of the waves in shallow water. The sign of the asymmetries is found to change with changing water depth. Generally, in very shallow water, the near-bottom velocities show stronger peak velocities in the offshore direction than in the onshore direction and the duration of the velocities in the offshore direction is shorter than that in the onshore direction.

Since sediment transport occurs when the shear stress acting on the sediment exceeds the threshold shear stress for the sediment, peak velocities are more important in the calculation of sediment transport than the entire distribution of the velocities act-

ing on the bottom. The importance of peak velocities is augmented by the fact that the rate of sediment transport is a function of the sixth power of velocities. An example of a numerical calculation of sediment transport rate using the model of Madsen and Grant (1976) shows that the direction of net sediment transport generally follows the direction of stronger peak velocities if the velocities are sufficient to move the sediment in an area.

The numerical calculation of sediment transport rate under the nonlinearly interacting waves shows the existence of a neutral depth at which no net sediment transport is expected. At depths less than the neutral depth the direction of net sediment transport is found to be offshore; the direction of net sediment transport is onshore where the depth is greater than the neutral depth. Given this convergence towards neutral depth, the submerged beach adjusts itself to local wave conditions to attain a dynamic equilibrium. The amount of sediment transport showed an exponential decrease with increasing water depth. When a steady current is superimposed on the waves the nonlinear interaction of waves and currents greatly affects the amount and direction of net sediment transport and thus the neutral depth is also changed from that of waves acting alone.

Along the northern shore of Willoughby Spit, a series of groins were built to protect the beach from erosion. The wave-induced near-bottom current in the area is strong enough to move sediment even though the waves are mostly of very low amplitude and non-breaking except for a break in the narrow swash zone. Before beach nourishment, the area showed a significant time rate of change in neither the nearshore

bottom morphology nor the position and shape of the shoreline. After the beach was filled, the shoreline initially underwent a rapid retreat for approximately 2 months followed by a period of stabilization. The water depth between the groins and offshore increased rapidly for the initial 1 to 1.5 years after the fill, almost reaching pre-fill water depths even though the position of the shoreline was farther offshore than the position of the pre-fill shoreline. The characteristic topography of the bar and trough system at the western part of the groin compartment began to develop within approximately 2 to 3 months after the fill.

Measurements of near bottom currents in the study area shows that the peak wave-induced currents between the two groins were mostly stronger in the offshore direction than in the onshore direction. Numerical calculations of sediment transport rate using the characteristic wave conditions of the area with some assumptions showed that the neutral depth of the study area is approximately 0.7 m. The calculations also suggested that approximately 35 percent of the sediment loss for the 1-year period after the fill could be attributed to the asymmetry of the wave-induced near-bottom current. The affect of wave asymmetry on the loss of sediment reduced to about 5 percent for the 10 month period following the initial 1-year period. The early rapid retreat of the shoreline and the deepening of water seem to be the result of the sediment loss offshore due to the wave asymmetry. The rate of sediment transport due to wave asymmetry becomes extremely small as the water depth increases.

Beyond the ends of the groins, strong tidal currents flow almost parallel to the shoreline at the site of the study area. The flood current is more effective in sediment

transport near the end of the groins than the ebb current. It is concluded that the trough and bar system that has developed in the western part of the outer compartment is the result of interaction between the incident waves and the flood current and its deflected path within the compartment. A possible gyre-type circulation is also expected within the compartment, and a redistribution of sediment may occur there due to the interaction of the waves and that circulation pattern.

The reasonable agreement found between field measurements and the results of the numerical calculations of wave asymmetry and sediment transport rate suggests that the model of Madsen and Grant (1976) can also predict the sediment transport under irregular waves such as were solved for by Biésel (1952) which are most likely to occur in shallow nearshore areas. However, equation (38), which allows the calculation of the average sediment transport rate in one direction during the half period of the waves, does not seem to be appropriate to use to calculate the sediment transport rate under irregular wave conditions. When maximum shear stress was calculated in terms of the root mean square value of peak velocities of the irregular waves in one direction, the resultant average sediment transport rate appeared to be approximately one order of magnitude lower than that calculated using equation (46).

The model of Wells (1967) which predicted the direction of sediment transport under irregular waves considering the entire distribution of velocities does not seem to be successful for bedload sediment transport.

FURTHER SUGGESTIONS

The threshold shear stress for grains on sloping beds analysed in the present study is fundamentally based on the results of experiments done by Shields (1936) on a horizontal bed under unidirectional steady current. However, grain behavior on a sloping bed under unsteady flow would be materially different from that on a horizontal bed. Therefore a criterion for the initiation of motion of sediment on a sloping bed should be established by new laboratory experiments.

Since the sediment transport rate is greatly affected by flow conditions, the exact nature of the nonlinear interaction of waves needs be studied both in the laboratory and in the field.

The theoretical works on the interaction between linear waves and currents need be extended to the interaction between irregular waves and currents theoretically and experimentally.

For a successful prediction of sediment transport in a subaqueous beach area, long term continuous measurement of waves and currents is necessary.

Longshore sediment transport, which is of great importance in many nearshore areas, is ignored in the present study. For a study of total sediment budget on a beach, the longshore sediment transport should also be considered.

Flow pattern near coastal structures are complex, a precise study of flow pattern is necessary for the understanding of sediment transport near the coastal structure. Wave deformation due to refraction, reflection, and diffraction by the coastal structures are also important.

REFERENCES

- About Seida, M. M., 1965. Bed load function due to wave action. Univ. Calif. Hydraul. Lab., Rep. HEL-2-11. 78 pp.
- Askren, D. R., 1979. Numerical simulation of sedimentation and circulation in rectangular marina basins. NOAA Tech. Rep., NOS 77, 114 pp.
- Aubrey, D. G., 1978. Statistical and dynamical prediction of changes in natural sand beaches. Ph.D. Diss., Univ. Calif. San Diego.
- Bagnold, R. A., 1946. Motion of waves in shallow water. Interaction between waves and sand bottoms. Proc. Roy. Soc. Ser. A, 187, 1-15.
- Bagnold, R. A., 1956. The flow of cohesionless grains in fluids. Phil. Trans. Roy. Soc. London, A249, 235-297.
- Bagnold, R. A., 1963. Mechanics of marine sedimentation. in *The Sea* (Hill, M. N. ed.), Wiley-Interscience, New York, 3, 507-528.
- Bailard, J. A., 1981. An energetics total load sediment transport model for a plane sloping beach. Jour. Geophys. Res., 86, 10938-10954.
- Bailard, J. A., 1982. Modeling on-offshore sediment transport in the surfzone. Proc. 18th Conf. Coast. Eng., 1419-1438.
- Bailard, J. A. and Inman, D. L., 1981. An energetics bedload model for a plane sloping beach. Jour. Geophys. Res., 86, C3, 2035-2043.
- Bakker, W. T., 1968. The dynamics of a coast with a groyne system. Proc. 11th Conf. Coast. Eng., A.S.C.E., 1, 492-517.
- Bakker, W. T., Breteler, E. H. J. K. and Roos, A., 1970. The dynamics of a coast with a groyne system. Proc. 12th Conf. Coast. Eng., A.S.C.E., 2, 1001-1020.
- Balsillie, J. H. and Bruno, R. O., 1972. Groins: An annotated bibliography. CERC Misc. Paper 1-72. U.S. Army Corps of Eng., 249 pp.
- Biéssel, F., 1952. Équations générales au second ordre de la houle ir régulière. Houille Blanche, 3, 372-376.
- Bowen, A. J. and Doering, J. C., 1984. Nearshore sediment transport: Estimates from detailed measurements of the nearshore velocity field. Proc. 19th Conf. Coast. Eng., A.S.C.E., 1703-1714.

- Bowen, A. J. and Huntley, D. A., 1984. Waves, long waves and nearshore morphology. *Mar. Geol.*, 60, 1-13.
- Brooks, N. H., 1963. Boundary shear stress in curved trapezoidal channels: A discussion. *J. Hydraul. Div., A.S.C.E.*, 189, 327-333.
- Brown, C. B., 1950. Sediment transportation. In *Engineering Hydraulics* (Rouse, H. ed.), John Wiley and Sons, N.Y., 1039 pp.
- Brown, E. I., Daley, E. L., Young, G. R., Bowman, F. O., Hale, R. K., Gelineau, V. and Saville, T., 1938. Beach erosion at Willoughby Spit, Va. House of Representatives 75th Congress 3rd Session Document No. 482, 28pp
- Bruun, P., 1972. The history and philosophy of coastal protection. *Proc. 13th Coast. Eng. Conf.*, 33-74.
- Byrne, R. J. and Anderson, G. L., 1977. Shoreline erosion in Tidewater Virginia. *Spec. Rep. Appl. Mar. Sci. and Ocean Eng.*, No. 111, Virginia Inst. Mar. Sci., 102 pp.
- Cornforth, D. H., 1973. Prediction of drained strength of sands from relative density measurements. *Am. Soc. Test. Mat. Spec. Tech. Pub. 523*, 281-303.
- Cornaglia, P., 1889. Delle Spiagge. *Accad. Naz. Lincei Atti. Cl. Sci. Fis., Mat. e Nat. Mem. 5, ser. 4*, 284-304. (Translated by Felder, W. N. in *Beach Processes and Coastal Hydrodynamics*, Fisher, J. S. and Dolan, R. eds., 1977, Dowden, Hutchinson & Ross).
- Christoffersen, J. B. and Jonsson, I. G., 1985. Bed friction and dissipation in a combined current and wave motion. *Ocean Eng.*, 12, 387-423.
- Curren, C. R. and Chatham, C. E., 1977. Imperial Beach, California, design of structures for beach erosion control. U.S. Army Corp of Eng., Waterways Exp. Stat. Tech. Rept. H-77-15.
- Dean, R. G., 1973. Heuristic models of sand transport in the surf zone. *Proc. Conf. Eng. Dynm. in the Surf Zone*, Sydney, Australia, 7 pp.
- Dean, R. G. and Dalrymple, R. A., 1984. *Water wave mechanics for engineers and scientists*. Prentice-Hall, NJ., 353 pp.
- Einstein, H. A., 1950. The bed-load function for sediment transport at in open channel flows. U.S. Dept. Agr. Soil Cons. Serv., Tech. Bull. 1026, 68 pp.
- Einstein, H. a., 1971. A basic description of sediment transport of sediment transport on beaches. *Hydr. Eng. Lab., Univ. Cal. Berkeley, HEL 2-34*. 36 pp.

- Fleischer, P., McRee, G. J. and Brady, J. J., 1977. Beach dynamics and erosion control, Ocean View section, Norfolk Virginia. Tech. Rep. No. 50, Inst. Ocean. Old Dominion Univ., 185 pp.
- Fredsoe, J., 1974. The development of oblique dunes in erodible channels. *J. Fluid Mech.*, 64, 1-16.
- Gatski, T. B., Grosch, C. E. and Rose, M. E., 1982. A numerical study of the two-dimensional Navier-Stokes equations in vorticity-velocity variables. *Journ. Comp. Phys.*, 48, 1-22.
- Grant, W. D. and Madsen, O. S., 1978. Bottom friction under waves in the presence of a weak current. NOAA Tech. Memo. ERL MESA-29, 131 pp.
- Grant, W. D. and Madsen, O. S., 1979. Combined wave and current interaction with a rough bottom. *J. Geophys. Res.*, 84, 1797-1808.
- Greenwood, B. and Sherman, D. J., 1984. Waves, currents, sediment flux and morphological response in a barred nearshore system. *Mar. Geol.*, 60, 31-61.
- Hallermeier, R. J., 1982. Oscillatory bedload transport: Data review and simple formulation. *Cont. Shelf Res.*, 1, 159-190.
- Hardisty, J., 1983. An assessment and calibration of formulations for Bagnold's bedload equation. *Jour. Sed. Petrol.*, 53, 1007-1010.
- Hardisty, J., Collier, J. and Hamilton, D., 1984. A calibration of the Bagnold beach equation. *Mar. Geol.*, 61, 95-101.
- Harris, D. L., 1981. Tides and tidal datums in the United States. CERC Spec. Rep., No. 7, U.S. Army Corp of Engineers, 382 pp.
- Hashimoto, H. and Uda, T., 1979. Analysis of beach profile changes at Ajigaura by empirical eigenfunctions. *Coast. Eng. Japan*, 22, 47-57.
- Hattori, M., 1980. Onshore-offshore transport and beach profile change. *Coast. Eng.* 1980, 1175-1193.
- Hattori, M., 1982. Field study on onshore-offshore sediment transport. *Coastal Eng.* 1982, 923-940.
- Hattori, M. and Kawamata, R., 1980. Onshore-offshore transport and beach profile change. *Proc. 17th Conf. Coast. Eng.*, 1175-1194.

- Hicks, S. D., 1973. Trends and variability of yearly mean sea level 1893 -1971. NOAA Tech. Memo. NOS 12.
- Holman, R. A. and Bowen, A. J., 1982. Bars, bumps, and holes: Models for the generation of complex beach topography. *Jour. Geophys. Res.*, 87, 457-468.
- Horikawa, K. and Watanabe, A., 1967. A study on sand movement due to wave action. *Coast. Eng. Japan*, 10, 39-57.
- Horikawa, K., Watanabe, A. and Katori, S., 1982. Sediment transport under sheet flow condition. *Proc. 18th Conf. Coast. Eng.*, 1335-1352.
- Hulsbergen, C. H., Bakker, W. T. and van Bochove, G., 1976. Experimental verification of groyne theory. *Coast. Eng.* 1976,1439-1458.
- Huntley, D. A. and Bowen, A. J., 1975. Comparison of the hydrodynamics of steep and shallow beaches. In *Nearshore Sediment Dynamics and Sedimentation* (Hails, J. and Carr, A. eds.), John Wiley, 69-109.
- Inman, D. L. and Bagnold, R. A., 1963. Littoral processes. in *The Sea* (Hill, M. N. ed.), Wiley-Interscience, New York, 3, 529-533.
- Inman, D. L. and Bowen, A. J., 1963. Flume experiments on sand transport by waves and currents. *Proc. 8th Conf. Coast. Eng.*, 137-150.
- Jonsson, I. G., 1966. Wave boundary layers and friction factors. *Proc. 10th Coast. Eng. Conf.*, 127-148.
- Kachel, N. B. and Sternberg, R. W., 1971. Transport of bed-load as ripples during an ebb current. *Mar. Geol.*, 10, 229-244.
- Kalkanis, G., 1964. Transportation of bed material due to wave action. U.S. Army Corp of Engineers, CERC, Tech. Memo No. 2, 38 pp.
- Kemp, P. H., 1962. A model study of the behaviour of beaches and groynes. *Proc. Inst. Civil Eng. London*, 22, 191-210.
- King, C. A. and Williams, W. W., 1949. The formation and movement of sand bars by wave action. *Geography Jour.*, 70-85.
- Kinsman, B., 1965. *Wind Waves*, Prentice-Hall, Englewood Cliffs, NJ, 676 pp.
- Kobayashi, N., 1982. Sediment transport on a gentle slop due to waves. *Proc. ASCE Jour. Waterw. Port Coast. Ocean Div.*, 108 (WW3), 254-271.

- Kolp, O., 1970. Coloured-sand tests with luminescent sands in groin fields. *Petermanns geographische Mittheilungen*, 114, 81-102.
- Komar, P. D., 1978. Relative quantities of suspension versus bedload transport on beaches. *Jour. Sed. Petrol.*, 48, 921-932.
- Komar, P. D. and Miller, M. C., 1975. Reply: On the comparison between the threshold of sediment motion under waves and unidirectional currents with a discussion of the particle evaluation of the threshold. *Jour. Sed. Petrol.*, 45, 362-367.
- Lane, E. W., 1955. Design of stable channels. *Trans A.S.C.E.*, 120, 1234-1279.
- Longuet-Higgins, M. S. and Stewart, R. W., 1960. Changes in the form of short gravity waves on long waves and tidal currents. *Jour. Fluid Mech.*, 8, 565-583.
- Longuet-Higgins, M. S. and Stewart, R. W., 1964. Radiation stresses in water waves: a physical discussion, with applications. *Deep Sea Res.*, 11, 529-562.
- Ludwick, J. C., 1987. Mechanisms of sand loss from an estuarine groin system following an artificial sand fill. Dept. Ocean. Old Dominion Univ., Tech. Rept. 87-2, 89 pp.
- Ludwick, J. C., Kang, H. J. and Reynolds, R. N., 1987. Loss of filled sand from an estuarine groin system. *Coastal Sediment* 88, 2, 1158-1173.
- Lundberg, D. L., 1987. Groin-associated rip currents measured using a new digital current meter. Ph.D. Diss., Dept. Oceanogr., Old Dominion Univ., in prep.
- Madsen, O. S. and Grant, W. D., 1975. The threshold of sediment movement under oscillating waves: a discussion. *Jour. Sed. Petrol.*, 45, 360-361.
- Madsen, O. S. and Grant, W. D., 1976. Sediment transport in the coastal environment. Ralph M. Parsons Lab. for Water Resources and Hydro., Rep. 209, 105 pp.
- Madsen, O. S. and Grant, W. D., 1977. Quantitative description of sediment transport by waves. *Proc. 15th Conf. Coast. Eng.*, 2, 1093-1112.
- Manohar, M., 1955. Mechanics of bottom sediment movement due to wave action. U.S. Army Corp of Engineers, Beach Erosion Board, Tech. Memo 75, 121 pp.
- Manze, P. A., 1977. Incipient transport of fine grains and flakes by fluids: extended Shields diagram. *Proc. A.S.C.E., J. Hydraul. Div.*, 103, 601-615.

- Melchor, J. R., 1970. The legend of Willoughby Spit, fact or fiction. Unpub. Rep., Dept. Geol., College of William and Mary, 18 pp.
- Morison, J. R., O'Brien, M. P., Johnson, J. W. and Schaaf, S. A., 1950. Forces exerted by surface waves on piles. *Pet. Trans.*, 189, 149-157; 193-212.
- Nagai, S. and Kubo, H., 1958. Motion of sand particles between groins. *Jour. Waterways and Harbour Div., A.S.C.E.*, 84, 1876, 1-28.
- Nielson, P., 1979. Some basic concepts of wave sediment transport. *Inst. Hydrodyn. Hydraul. Eng., Tech. Univ. Denmark, Ser. Paper 20*, 160 pp.
- Nielsen, P., Svendsen, I. A. and Staub, C., 1978. Onshore-offshore sediment movement on a beach. *Proc. 16th Conf. Coast. Eng.*, 2, 1475-1492.
- NWRF (Navy Weather Research Facility), 1964. Climatology and low-level air pollution potential from ships in the Hampton Roads. NWRF 39-0664-093, 72 pp.
- Pattiaratchi, C. B. and Collins, M. B., 1985. Sand transport under the combined influence of waves and tidal currents: an assessment of available formulae. *Mar. Geol.*, 67, 83-100.
- Pelnard-Considere, R., 1956. Essai de théorie de l'évolution des formes de rivages en plages de sable et de galets. 4th Journées de l'Hydraulique, Les Energies de la Mer, Question III. Rapport No. 1.
- Phillips, O. M., 1977. *The Dynamics of The Upper Ocean* (2nd ed.), Cambridge Univ. Press, Cambridge, 336 pp.
- Quick, M. C. and Har, B. C., 1985. Criteria for onshore-offshore sediment movement on beaches. *Proc. Canad. Coast. Conf., St. John's, Newfoundland*, 257-269.
- Rance, P. J. and Warren, N. F., 1968. The threshold of movement of coarse material in oscillatory flow. *Proc. 11th Conf. Coast. Eng.*, 487-491.
- Rasmussen, P. and Fredsøe, J., 1981. Measurements of sediment transport in combined waves and current. *Inst. Hydrodyn. and Hydraul. Eng., Prog. Rept. 53*, 27-30.
- Reynolds, R. N., 1987. The role of longshore sediment transport in the loss of fill material from an estuarine groin field. M.S. Thesis, Dept. Oceanogr., Old Dominion Univ., in prep.
- Seibolt, E., 1963. Geological investigations of nearshore sand transport. In *Progress in Oceanography* (Sears ed.), Pergamon Press, New York, 3-70.

- Seymour, R. J. and Castel D., 1987. Modeling cross-shore transport. in *Nearshore Sediment Transport* (Seymour, R. J. ed.), Plenum Press. in press.
- Seymour, R. J. and King, D. B., 1982. Field comparisons of cross-shore transport models. *Jour. Waterway, Port, Coastal and Ocean Div., ASCE*, 108,WW2, 163-179.
- Shepard, F. P., 1950. Beach cycles in Southern California. *Beach Erosion Board Tech. Mem. No. 20*.
- Shibayama, T. and Horikawa, K., 1980. Bed load measurement and prediction of two-dimensional beach transformation due to waves. *Coast. Eng. Japan*, 23, 179-190.
- Shields, I. A., 1936. Anwendung der aehnlichkeitsmechanik und der turbulenz forschung auf die geschiebebewegung. *Mitt. Preuss. Versuchsanstalt Wasserbau Schiffbau. Berlin*, 26.
- Short, A. D., 1978. Wave power and beach stages: a global model. *Proc. 16th Coast. Eng. Conf.*, 11, 1145-1162.
- Simmons, D. B. and Albertson, M. L., 1960. Uniform water conveyance channels in alluvial material. *Proc. A.S.C.E., J. Hydraul. Div.*, 86, 33-99.
- Simmons, D. B. and Senturk, F., 1977. *Sediment transport technology*. Water Res. Pub. Fort Collins, 807 pp.
- Sleath, J. F., 1978. Measurements of bed load in oscillatory flow. *Proc. ASCE Jour. Waterw. Port Coast. Ocean Eng. Div.*, 104 (WW3), 291-307.
- Sleath, J. F., 1984. *Sea Bed Mechanics*. Wiley-Interscience, New York, 334 pp.
- Smith, J. D., 1977. Modeling of sediment transport on continental shelves. In *The Sea* (McCave, I. N., O'Brien, J. J. and Steele, J. H. eds.), Wiley, N.Y., 6, 538-578.
- Sternberg, R. W., 1972. Predicting initial motion and bed-load transport of sediment particles in the shallow marine environment. In *Shelf Sediment Transport: Process and Pattern* (Swift, D. J. P., Duane, D. B. and Pilkey, O. H. eds.), Dowden, Hutchinson & Ross, 61-82.
- Sunamura, T. and Horikawa, K., 1974. Two-dimensional beach transformation due to waves. *Proc. 14th Conf. Coast. Eng.*, 920-938.
- Tanaka, H. and Shuto, N., 1981. Friction coefficient for a wave-current coexistent system. *Coast. Eng. Japan*, 24, 105-128.

- Tomlinson, J. H., 1980. Groynes in coastal engineering. hydraulic Res. Station, Wallingford, England, Rep. No. IT 199, 21 pp.
- USACE (United States Army Corps of Engineers), 1982. Willoughby Spit and vicinity, Norfolk, Virginia, hurricane protection and beach erosion control study. Feasibility Rep. and Final Impact Statement, Parts 1 and 2, Supporting Documentation.
- Vincent, G. E., 1958. Contribution to the study of sediment transport on a horizontal bed due to wave action. Proc. 6th Conf. Coast. Eng., A.S.C.E., 326-354.
- Vincent, C. E., Young, R. A. and Swift, D. J. P., 1981. Bed-load transport under waves and currents. Mar. Geol., 39, M71-M80.
- Vincent, C. E., Young, R. A. and Swift, D. J. P., 1983. Sediment transport on the Long Island shoreface, North American Atlantic Shelf: role of waves and currents in shoreface maintenance. Cont. Shelf Res., 2, 163-182.
- Wells, D. R., 1967. Beach equilibrium and second-order wave theory. Jour. Geophys. Res., 72, 497-504.
- Wright, L. D., Nielsen, P., Short, A. D. and Green, M. O., 1982. Morphodynamics of a macrotidal beach. Mar. Geol., 50, 97-128.
- Yalin, M. S., 1977. Mechanics of sediment transport (2nd ed.), Pergamon Press, Oxford. 298 pp.
- Young, R. A., Vincent, C. E., Clark, T. L. and Swift, D. J. P., 1980. Near bottom sediment transport mechanics on the inner shelf: Time scales, processes and response from model and field studies. Trans. EOS, 61, p. 999 (abstracts).

APPENDIX

$$u = \sum_{i=1}^N (A_i \cos \theta_i + B_i \cos 2\theta_i) + \sum_{i=1}^N \sum_{j=1}^{i-1} \left\{ S_{ij} \cos(\theta_i + \theta_j) + D_{ij} \cos(\theta_i - \theta_j) \right\}$$

$$\theta_i = (k_i x - \sigma_i t), \quad k_i = \frac{2\pi}{L_i}, \quad \sigma_i = \frac{2\pi}{T_i}$$

$$A_i = a_i \sigma_i \frac{\cosh k_i (h-y)}{\sinh k_i h}$$

$$B_i = \frac{3}{4} a_i^2 \frac{k_i \sigma_i \cosh 2k_i (h-y)}{\sinh^4 k_i h}$$

$$S_{ij} = \frac{a_i a_j}{2 \sinh k_i h \sinh k_j h} (k_i + k_j) E_{ij} \cosh [(k_i + k_j)(h-y)]$$

$$D_{ij} = \frac{-a_i a_j}{2 \sinh k_i h \sinh k_j h} (k_i - k_j) F_{ij} \cosh [(k_i - k_j)(h-y)]$$

$$E_{ij} = \frac{(\sigma_i + \sigma_j)(\sigma_i^2 + \sigma_i \sigma_j + \sigma_j^2) - C_{g,ij}^2 (k_i \sigma_i - k_j \sigma_j)(k_i - k_j)}{(\sigma_i + \sigma_j)^2 \left[1 - \left(\frac{D'_{g,ij}}{D_{g,ij}} \right)^2 \right]} \frac{\cosh (k_i - k_j) h}{\cosh (k_i + k_j) h}$$

$$F_{ij} = \frac{(\sigma_i - \sigma_j)(\sigma_i^2 - \sigma_i \sigma_j + \sigma_j^2) - D_{g,ij}^2 (k_i \sigma_i - k_j \sigma_j)(k_i + k_j)}{(\sigma_i - \sigma_j)^2 \left[1 - \left(\frac{C'_{g,ij}}{C_{g,ij}} \right)^2 \right]} \frac{\cosh (k_i + k_j) h}{\cosh (k_i - k_j) h}$$

$$C'_{g,ij} = \left[\frac{g}{k_i - k_j} \tanh (k_i - k_j) h \right]^{1/2}, \quad C_{g,ij} = \frac{\sigma_i - \sigma_j}{k_i - k_j}$$

$$D'_{g,ij} = \left[\frac{g}{k_i + k_j} \tanh (k_i + k_j) h \right]^{1/2}, \quad D_{g,ij} = \frac{\sigma_i + \sigma_j}{k_i + k_j}$$

AUTOBIOGRAPHICAL STATEMENT

Kang, Hyo Jin was born in Pusan, Korea on 2 March, 1951. He received a B.S. in Oceanography from Seoul National University, Seoul, Korea in February 1973 and an M.S. in Oceanography (Geological) from the same university in February 1981.

He served in the Korean Army from 1974 to 1976 and worked for a private company for 2 years after military service. He served as an editorial secretary for the Journal of the Oceanological Society of Korea between 1981 and 1982 while he was working as a research assistant for the Department of Oceanography, Seoul National University.

He is a member of the national honor society Phi Kappa Phi and of the Oceanological Society of Korea and the American Geophysical Union.

THESIS AND PUBLICATIONS

- Chough, S. K. and Kang, H. J., 1980. Geology of Gamagyang Bay, Southern coast of Korea: 26th Int. Geol. Congr., Paris. (abstract)
- Kang, H. J., 1981. Late Quaternary sedimentary processes in the Gamagyang Bay, southern coast of Korea. M.S. Thesis, Seoul National Univ., Seoul, Korea, 102 pp.
- Chough, S. K., Kang, H. J., Bahk, K. S., Kim, J. H. and Park, J. K., 1981. Submarine debris flow deposits in the Ogcheon Basin (? Late Proterozoic-Cretaceous), Korean Peninsula: preliminary results. Proc. CCOP, 18th session, Seoul Korea.
- Kang, H. J. and Chough, S. K., 1982. Gamagyang Bay, southern coast of Korea: sedimentation on a tide-dominated rocky embayment. Mar. Geol., 48, 197-214.

Chough, S. K., Kim, K. and Kang, H. J., 1982. Deposition of fine-grained sediments in tide-dominated embayment, Gamagyang Bay, southern coast of Kore. Korea Ocean Res. and Devel. Inst. Bull., BSPE 00028-51-3, 37-74.

Ludwick, J. C. and Kang, H. J., 1984. Currents and sediment transport in a groin field at Willoughby Spit, Virginia. in A field trip guide book for the 11th annual shelf and shore workshop (Gingerich, K. J. and Byrnes, M. R. eds.), Dept. Ocean., Old Dominion Univ., Norfolk, Virginia, 32-37.

Ludwick, J. C., Kang, H. J. and Reynolds, N. R., 1987. Loss of filled sand from an estuarine groin system. Coastal Sediment 88, 2, 1158-1173.